Density functional approach to neutron star astrophysics

David Blaschke (HZDR/CASUS, IFT UWr)

CASUS
CENTER FOR ADVANCED SYSTEMS UNDERSTANDING

www.casus.science

HZDR HELMHOLTZ ZENTRUM DRESDEN ROSSENDORF · TECHNISCHE UNIVERSITÄT DRESDEN · CBG · UFZ HELMHOLTZ Centre for Environmental Research · Uniwersytet Wrocławski · Federal Ministry of Education and Research · STAATSMINISTERIUM FÜR WISSENSCHAFT KULTUR UND TOURISMUS · Freistaat SACHSEN

QCD Phase Diagram

Landscape of our investigations

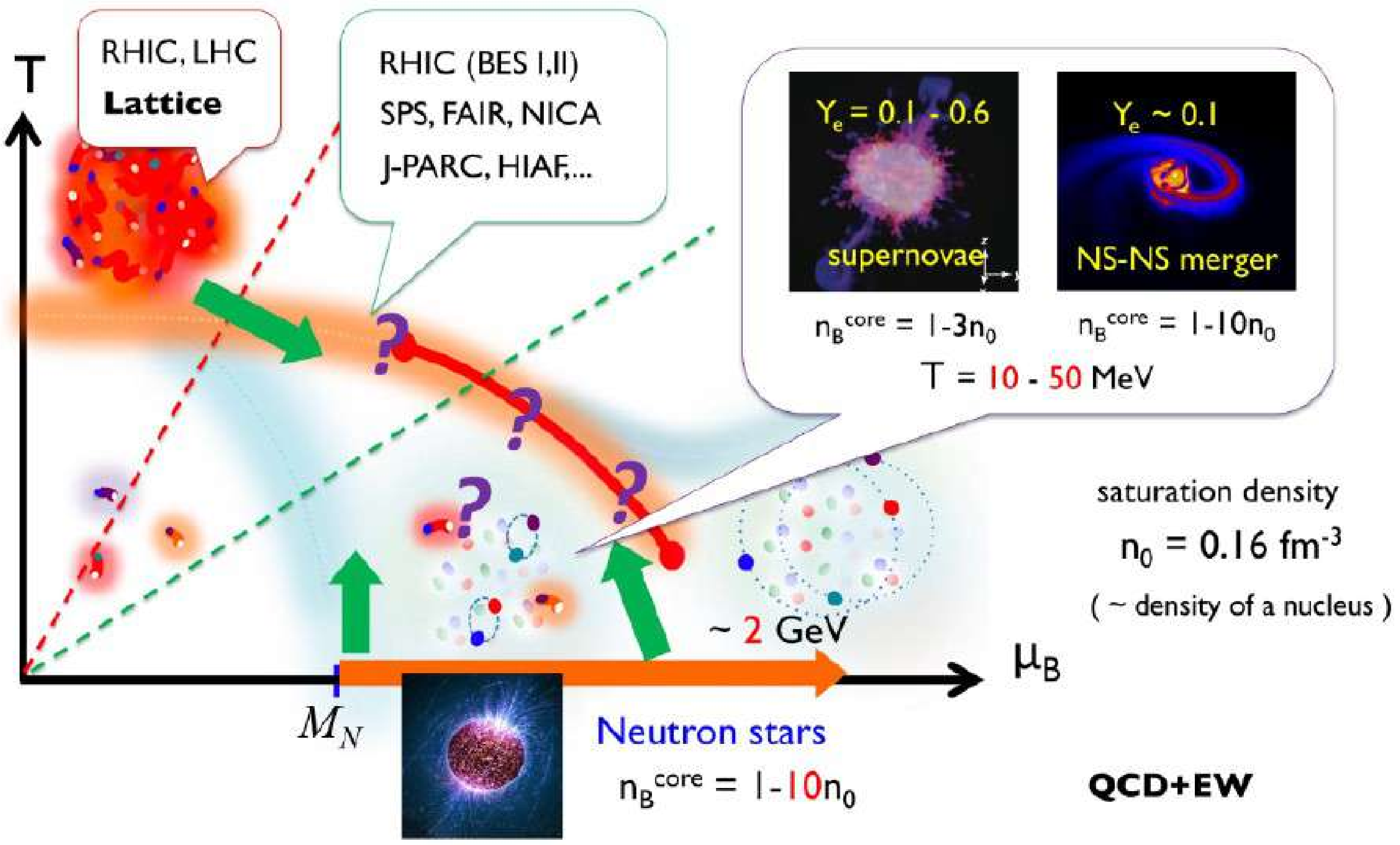

Figure from T. Kojo arXiv:1912.05326 [nucl-th]

QCD Phase Diagram

Landscape of our investigations

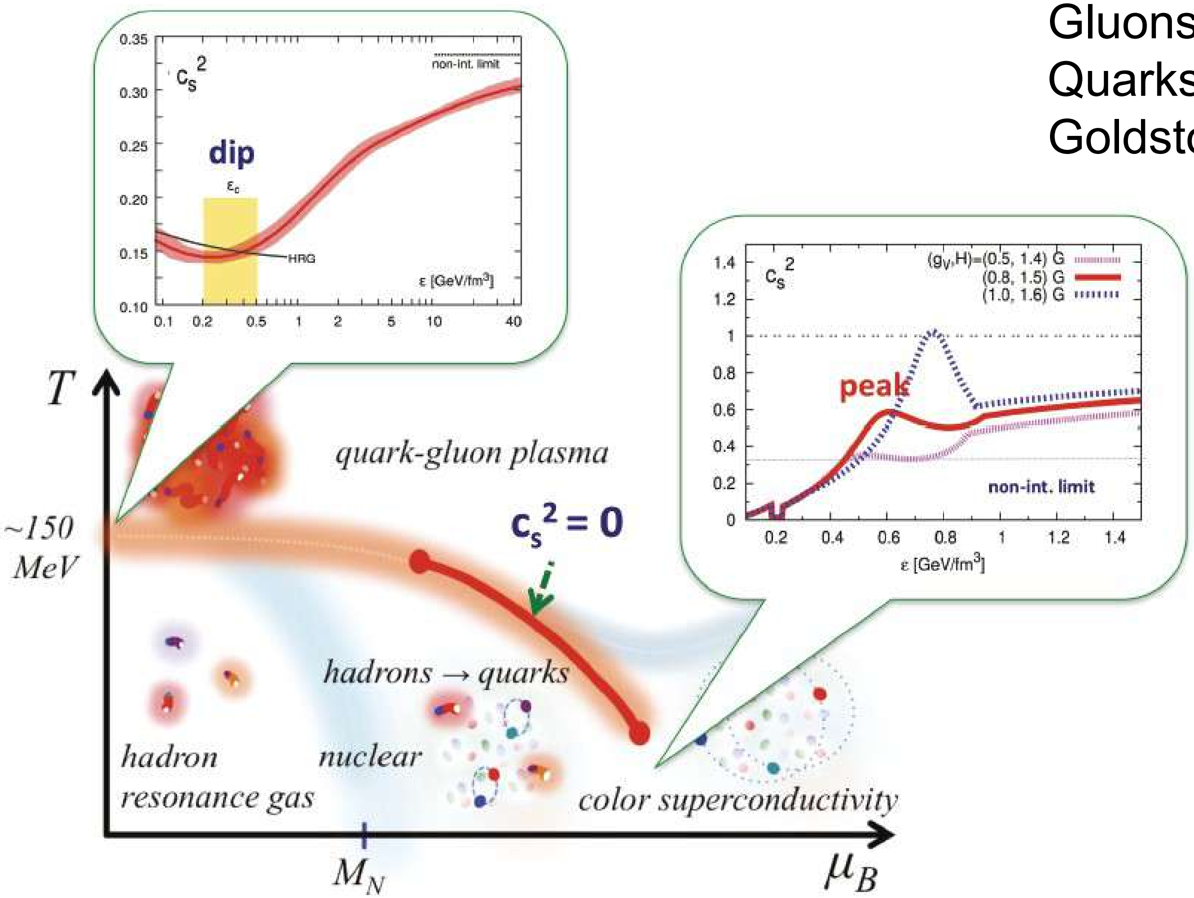

Gluons ↔ Vector mesons
Quarks ↔ Baryons
Goldstones ↔ Pseudoscalar mesons

Quark-Hadron Duality?

Mutual influence of Order parameters for ChiSB and CSC

From: T. Kojo, "QCD equations of state in quark-hadron continuity", Universe 4 (2018) 42

T. Schaefer & F. Wilczek, Phys. Rev. Lett. 82 (1999) 3956
C. Wetterich, Phys. Lett. B 462 (1999) 164
T. Hatsuda, M. Tachibana, T. Yamamoto & G. Baym, Phys. Rev. Lett. 97 (2006) 122001

Contents

Density functional approach to nuclear matter

- Paradigma: Walecka model for symmetric nuclear matter and neutron star matter
- DD2 approach to relativistic mean field theory with density-dependent couplings
- Hyperon puzzle, sexaquark dilemma and the „Berlin Wall“ constraint for neutron stars

Relativistic density functionals for quark matter with confinement

- Density functional for warm, dense quark matter; chiral symmetry breaking and color superconductivity
- Quark confinement as density functional →effective Nambu model with density-dependent couplings
- Phase transition construction and hybrid neutron star properties

Towards a unified approach to quark-nuclear matter

- Generalized Φ-derivable approach with clusters; cluster virial expansion
- Hadrons (mesons, baryons, multiquark states) as clusters in quark matter; Beth-Uhlenbeck approach

Walecka model for dense nuclear matter

CASUS CENTER FOR ADVANCED SYSTEMS UNDERSTANDING

Meson exchange model

example: scalar (σ) meson

$$(-\triangle + m_\sigma^2)\sigma(\vec{r}) = -g_\sigma \delta(\vec{r})$$

$$\Rightarrow \quad \sigma(r) = -\frac{g_\sigma}{4\pi}\frac{e^{-m_\sigma r}}{r}$$

$$V_{NN}^{(\sigma)}(r) = g_\sigma \sigma(r) = -\frac{g_\sigma^2}{4\pi}\frac{e^{-m_\sigma r}}{r}$$

Meson	I^π	T	S	M[MeV]
$\pi^0, \pi^\pm$	0^-	1	0	140
σ	0^+	0	0	≈ 500
$K^0, K^\pm$	0^-	1/2	± 1	495
η	0^-	0	0	550
$\rho^0, \rho^\pm$	1^-	1	0	770
ω	1^-	0	0	780
δ	0^+	1	0	900

Feynman diagrams for π^- exchange

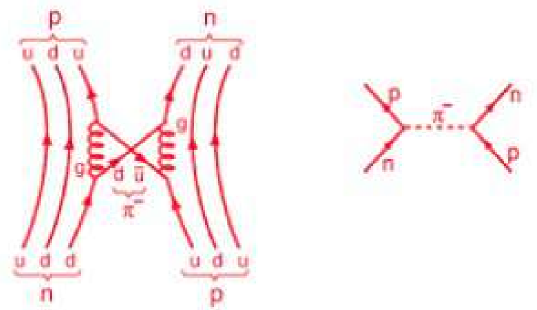

NN- Potential

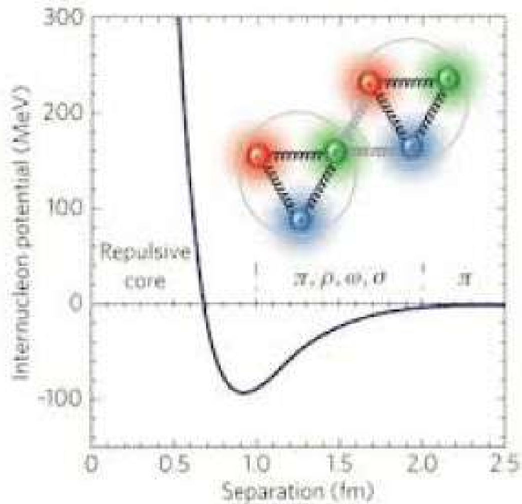

Walecka model for dense nuclear matter (II)

Field theoretical formulation: Lagrangian and Path Integral for Partition Function

$$\mathcal{Z}_{gk}(T,V,\{\mu_i\}) = \int [d\overline{\Psi}][d\Psi] \exp\left\{ \int_0^{\beta=1/T} d\tau \int_V d^3\vec{x} \; \left(\mathcal{L}_0 + \mathcal{L}_I + \mu_p \Psi_p^+ \Psi_p + \mu_n \Psi_n^+ \Psi_n\right) \right\}$$

$$\mathcal{L}_0(\tau,\vec{x}) \quad = \quad \overline{\Psi}(\tau,\vec{x})\left(i\gamma_\mu \partial_\mu - m_N\right)\Psi(\tau,\vec{x}) \,, \qquad \mathcal{L}_I(\tau,\vec{x}) = j_{\omega_\mu}(\tau,\vec{x})\frac{G_\omega}{2} j_{\omega_\mu}(\tau,\vec{x}) - j_\sigma(\tau,\vec{x})\frac{G_\sigma}{2} j_\sigma(\tau,\vec{x})$$

$$j_\sigma(\tau,\vec{x}) = \overline{\Psi}(\tau,\vec{x})\Psi(\tau,\vec{x})$$
$$j_{\omega_\mu}(\tau,\vec{x}) = \overline{\Psi}(\tau,\vec{x})\gamma_\mu\Psi(\tau,\vec{x})$$

$$\Psi = \begin{pmatrix} \psi_n \\ \psi_p \end{pmatrix}; \quad \psi_n = \begin{pmatrix} u_{n,\uparrow} \\ u_{n,\downarrow} \\ v_{n,\uparrow} \\ v_{n,\downarrow} \end{pmatrix} \begin{matrix} \Big\} \text{Neutron} \\ \Big\} \text{Antineutron} \end{matrix}$$

$\mu_n = \mu_p \quad \rightarrow \quad$ symmetric nuclear matter

$\mu_n \neq 0;\ \mu_p = 0 \quad \rightarrow \quad$ pure neutron matter

$\mu_n = \mu_p + \mu_{e^-} \quad \rightarrow \quad$ neutron star matter (β-equilibrium)

Walecka model for dense nuclear matter (III)

Evaluation of the Path Integral: Hubbard-Stratonovich trick

$$\exp\left(-\left(\overline{\Psi}\Psi\right)\frac{G_\sigma}{2}\left(\overline{\Psi}\Psi\right)\right) = \left(\det G_\sigma^{-1}\right)^{\frac{1}{2}}\int[d\sigma]\exp\left(\frac{\sigma^2}{2G_\sigma}+\sigma\overline{\Psi}\Psi\right)$$

Effective action quadratic $\Longrightarrow$ Gaussian Path Integral

$$\mathcal{S} \equiv \int_0^\beta d\tau\int d^3\vec{x}\left\{\overline{\Psi}(\vec{x},\tau)\left(-\gamma_0\frac{\partial}{\partial\tau}+i\vec{\gamma}\vec{\nabla}-m_N+\gamma_0\mu+\sigma-\gamma_\mu\omega_\mu\right)\Psi(\vec{x},\tau)+\frac{\sigma^2}{2G_\sigma}-\frac{\omega_\mu^2}{2G_{\omega_\mu}}\right\}$$

Fourier representation: $\Psi(\vec{x},\tau)=\sqrt{\frac{T}{V}}\sum_n\sum_{\vec{p}}e^{i(\vec{p}\vec{x}+\omega_n\tau)}\Psi_n(\vec{p})$, with $\omega_n\equiv\pi T(2n+1)$

$$\begin{aligned}
& \int_0^\beta d\tau\int d^3\vec{x}\,\overline{\Psi}(\vec{x},\tau)\left(-\gamma_0\frac{\partial}{\partial\tau}+i\vec{\gamma}\vec{\nabla}-m_N+\gamma_0\mu+\sigma-\gamma_0\omega_0\right)\Psi(\vec{x},\tau)\\
= \quad & \frac{1}{\beta V}\int_0^\beta d\tau\int d^3\vec{x}\sum_{n,n'}\sum_{\vec{p},\vec{p}'}\overline{\Psi}_{n'}(\vec{p}')\left(-i\gamma_0\omega_n-\vec{\gamma}\vec{p}-m_N^*+\gamma_0\mu^*\right)\Psi_n(\vec{p})\,e^{i\{(\vec{p}-\vec{p}')\vec{x}+(\omega_n-\omega_{n'})\tau\}}\\
= \quad & \beta\sum_n\sum_{\vec{p}}\overline{\Psi}_n(\vec{p})(-\gamma_\mu p_\mu-m_N^*)\Psi_n(\vec{p})=\sum_n\sum_{\vec{p}}\overline{\Psi}_n(\vec{p})G^{-1}[\sigma,\omega_0]\Psi_n(\vec{p})
\end{aligned}$$

Effective mass $m_N^*=m_N-\sigma$, chemical potential $\mu^*=\mu-\omega_0$ and quasiparticle propagator

$$G^{-1}[\sigma,\omega] \quad = \quad -\beta(\gamma_\mu p_\mu+m_N^*) \quad , \quad p_0=i\omega_n-\mu^*$$

Walecka model for dense nuclear matter (IV)

Evaluate fermionic path integral and mean field approximation

$$
\begin{aligned}
\mathcal{Z}_{gk}(T,V,\{\mu_i\}) &= \mathcal{N}\prod_{n,\vec{p}}\int [d\overline{\Psi}_n(\vec{p})][d\Psi_n(\vec{p})][d\sigma][d\omega_0]\mathrm{e}^{\left\{\frac{\sigma^2-\omega_0^2}{2G_{\omega_0}}+\sum_{n,\vec{p}}\overline{\Psi}_n(\vec{p})G^{-1}[\sigma,\omega_0]\Psi_n(\vec{p})\right\}} \\
&= \int [d\sigma][d\omega_0]\exp\left\{Tr\ \ln G^{-1}[\sigma,\omega_0]+\frac{\sigma^2}{2G_\sigma}-\frac{\omega_0^2}{2G_{\omega_0}}\right\} \\
&= \exp\left\{Tr\ \ln G^{-1}[\overline{\sigma},\overline{\omega}_0]+\frac{\overline{\sigma}^2}{2G_\sigma}-\frac{\overline{\omega}_0^2}{2G_{\omega_0}}\right\}
\end{aligned}
$$

Stationarity condition: $\partial \ln Z_{gk}/\partial\overline{\sigma} = \partial \ln Z_{gk}/\partial\overline{\omega}_0 = 0$ corresponds to "gap equations":

$$
\overline{\sigma} = -G_\sigma\, Tr\, G[\overline{\sigma},\overline{\omega}_0] = G_\sigma n_s\ , \quad \overline{\omega}_0 = -G_\omega\, Tr\,\gamma_0 G[\overline{\sigma},\overline{\omega}_0] = G_\omega n\ .
$$

Thermodynamics: $\Omega(T,V,\mu) = -T\ln\mathcal{Z}_{gk} = -pV$

$$
p(\mu,T) = \frac{1}{2}G_\omega n^2 - \frac{1}{2}G_\sigma n_s^2 + 4T\int\frac{d^3\vec{p}}{(2\pi)^3}\left[\ln\left(1+e^{-\beta(E^*-\mu^*)}\right)+\ln\left(1+e^{-\beta(E^*+\mu^*)}\right)\right]
$$

$$
n = 4\int\frac{d^3\vec{p}}{(2\pi)^3}\left[f_-(E^*)-f_+(E^*)\right]\ ,\ n_s = 4\int\frac{d^3\vec{p}}{(2\pi)^3}\frac{m_N^*}{E^*}\left[f_-(E^*)+f_+(E^*)\right]\ ,\ f_\pm(E^*) = \frac{1}{e^{\beta(E^*\pm\mu^*)}+1}
$$

Quasiparticle properties $E^* = \sqrt{\vec{p}^2+m_N^{*\,2}}$, $m_N^* = m_n - G_\sigma n_s$, $\mu^* = \mu - G_\omega n$.

Walecka model for dense nuclear matter (V)

Evaluate Traces: $Tr\ln G^{-1} = tr_p tr_D \ln G^{-1} = tr_p \ln \det_D G^{-1} = \sum_n \sum_{\vec{p}} \ln \det_D G^{-1}$

Scalar mean field

$$\begin{aligned}
\overline{\sigma} &= -G_{\overline{\sigma}}\, Tr\, G[\overline{\sigma}, \overline{\omega}_0] \\
&= -2G_\sigma T \sum_n \int \frac{d^3\vec{p}}{(2\pi)^3} tr_D \left[\gamma_\mu p_\mu - (m - \overline{\sigma}) + i\gamma_0(\mu - \overline{\omega})\right]^{-1} \\
&= 2G_\sigma T \sum_n \int \frac{d^3\vec{p}}{(2\pi)^3} \left(\frac{m^*}{\vec{p}^2 + m^{*2} + (\omega_n + i\mu^*)^2} \right) \\
&= G_\sigma \int \frac{d^3\vec{p}}{(2\pi)^3} \frac{m^*}{E^*} \left(\frac{1}{e^{\beta(E^* - \mu^*)} + 1} + \frac{1}{e^{\beta(E^* + \mu^*)} + 1} \right) \\
&\equiv G_\sigma n_s
\end{aligned}$$

Vector mean field

$$\begin{aligned}
\overline{\omega}_0 &= -G_{\overline{\omega}_0}\, Tr\, \gamma_0 G[\overline{\sigma}, \overline{\omega}_0] \\
&= G_\omega \int \frac{d^3\vec{p}}{(2\pi)^3} \left(\frac{1}{e^{\beta(E^* - \mu^*)} + 1} - \frac{1}{e^{\beta(E^* + \mu^*)} + 1} \right) \\
&\equiv G_\omega n
\end{aligned}$$

Walecka model for dense nuclear matter (VI)

Numerical Results

Effective mass

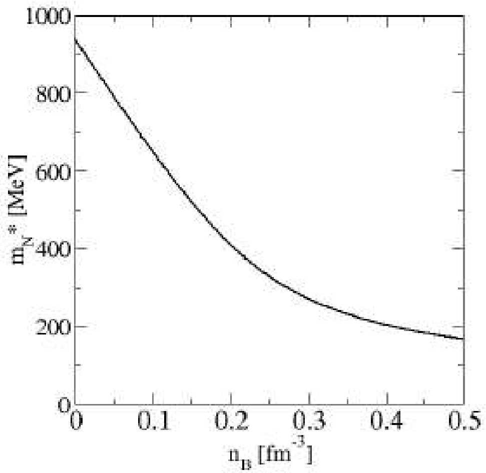

Energy per nucleon

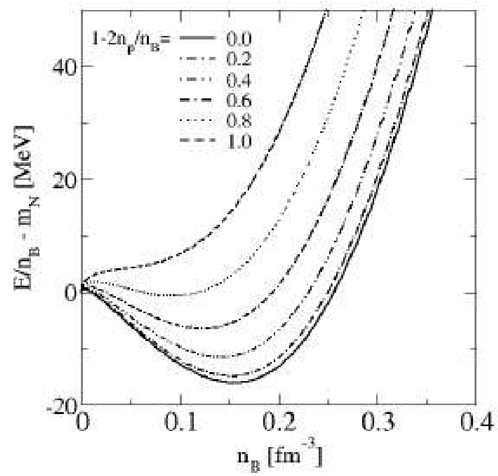

Pressure

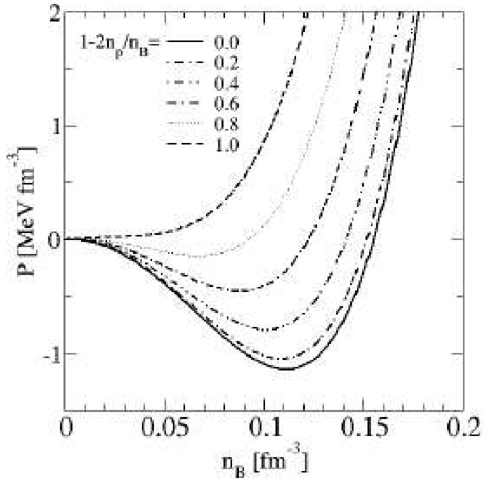

Symmetric nuclear matter ($n_p/n_B = 0.5$) saturates with a binding energy per nucleon of $E_B/A = 16$MeV at $n_B = n_p + n_n = 0.16$ fm^{-3}.
Increasing the asymmetry towards pure neutron matter ($n_p = 0$) makes the system unbound.

Problem: Too high incompressibility and too low m_N^* at saturation.

Solutions:
A) nonlinear generalisation of the potential energy $V_\sigma = G_\sigma n_s^2/2 + bn_s^3 + cn_s^4$
B) density-dependent couplings: $G_j \longrightarrow \Gamma_j(n) = G_j f_j(n)$, $j = \sigma, \omega$
DD2 class of density functionals: $f_j(n) = a_j[1 + b_j(n/n_0 + d_j)^2]/[1 + c_j(n/n_0 + d_j)^2]$.

For more details, e.g., J. Kapusta: Finite temperature field theory, CUP (1989)

“Berlin Wall” constraint for neutron stars?

Mass-radius diagram for purely hadronic EOS

Neutron star phenomenology from TOV eqns.

There is a 1:1 correspondence EOS $\leftrightarrow$ M(R)

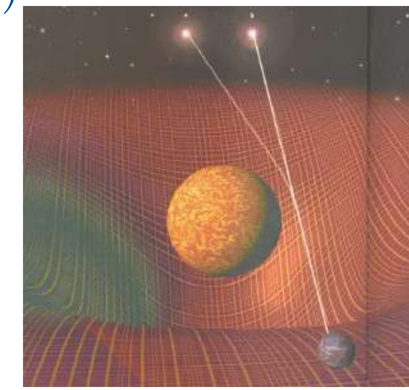

Tolman-Oppenheimer-Volkoff (TOV) equations

Einstein equations

$$G_{\mu\nu} = 8\pi G\, T_{\mu\nu}$$

Non-rotating, spherical masses $\rightarrow$ Schwarzschild Metrics

$$ds^2 = -(1 - \frac{2M}{r})dt^2 + (1 - \frac{2M}{r})^{-1}dr^2 + r^2 d\Omega^2$$

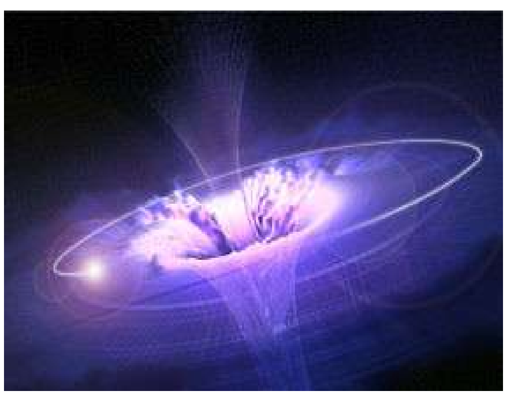

Tolman-Oppenheimer-Volkoff eqs.*) for structure and stability of spherical compact stars

$$\frac{dP(r)}{dr} = -G\frac{m(r)\varepsilon(r)}{r^2}\left(1 + \frac{P(r)}{\varepsilon(r)}\right)\left(1 + \frac{4\pi r^3 P(r)}{m(r)}\right)\left(1 - \frac{2Gm(r)}{r}\right)^{-1}$$

Newtonian case GR corrections from EoS and metrics

*)R.C. Tolman, Phys. Rev. 55 (1939) 364; J.R. Oppenheimer, G.M. Volkoff, ibid., 374

Neutron star phenomenology from TOV eqns.

There is a 1:1 correspondence EOS P(ε)↔M(R)

Tolman-Oppenheimer-Volkoff (TOV) equations - solutions

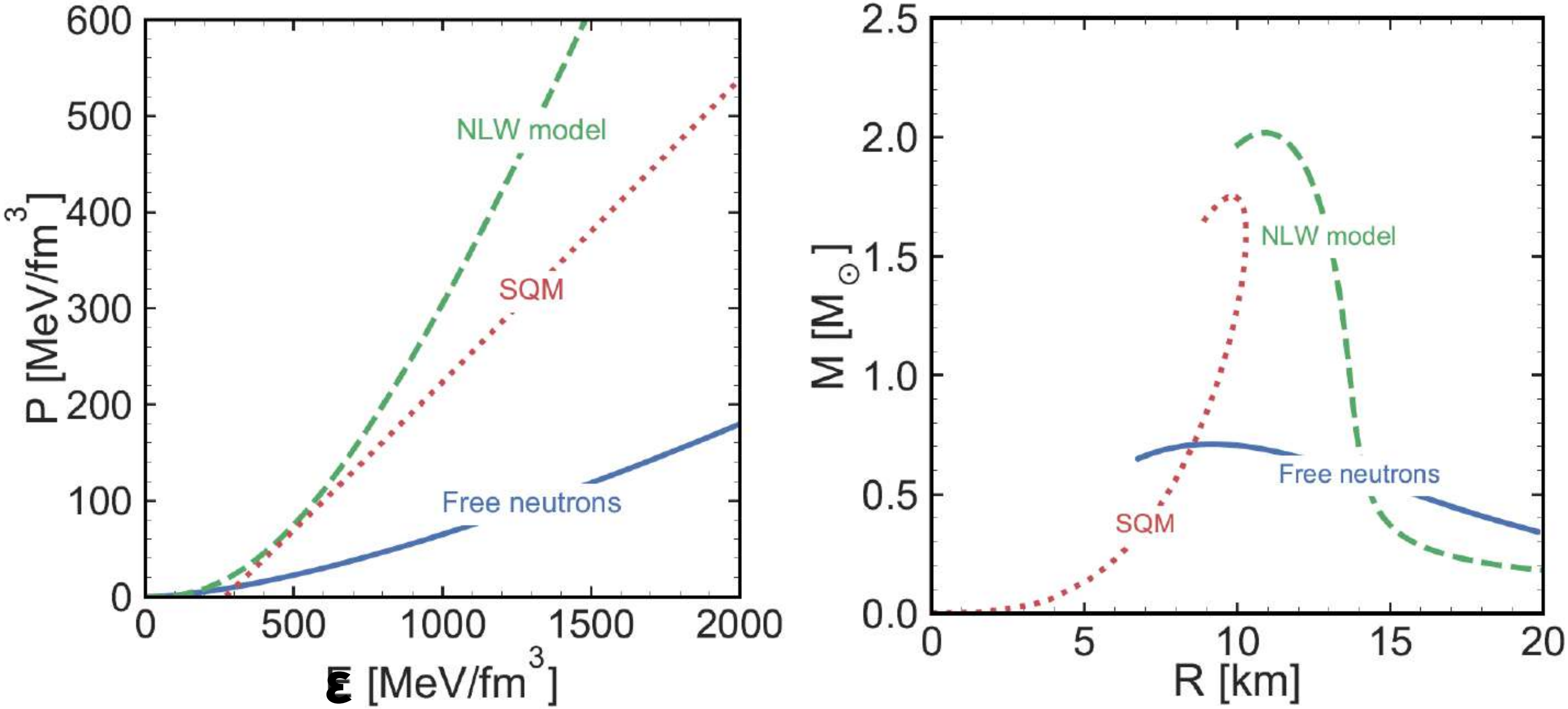

Stiffer equation of state → larger radius and larger maximum mass

“Berlin wall” constraint for neutron stars

Realistic hadronic EOS (with strange baryons)

Tension with modern multi-messenger observations by LVC and NICER

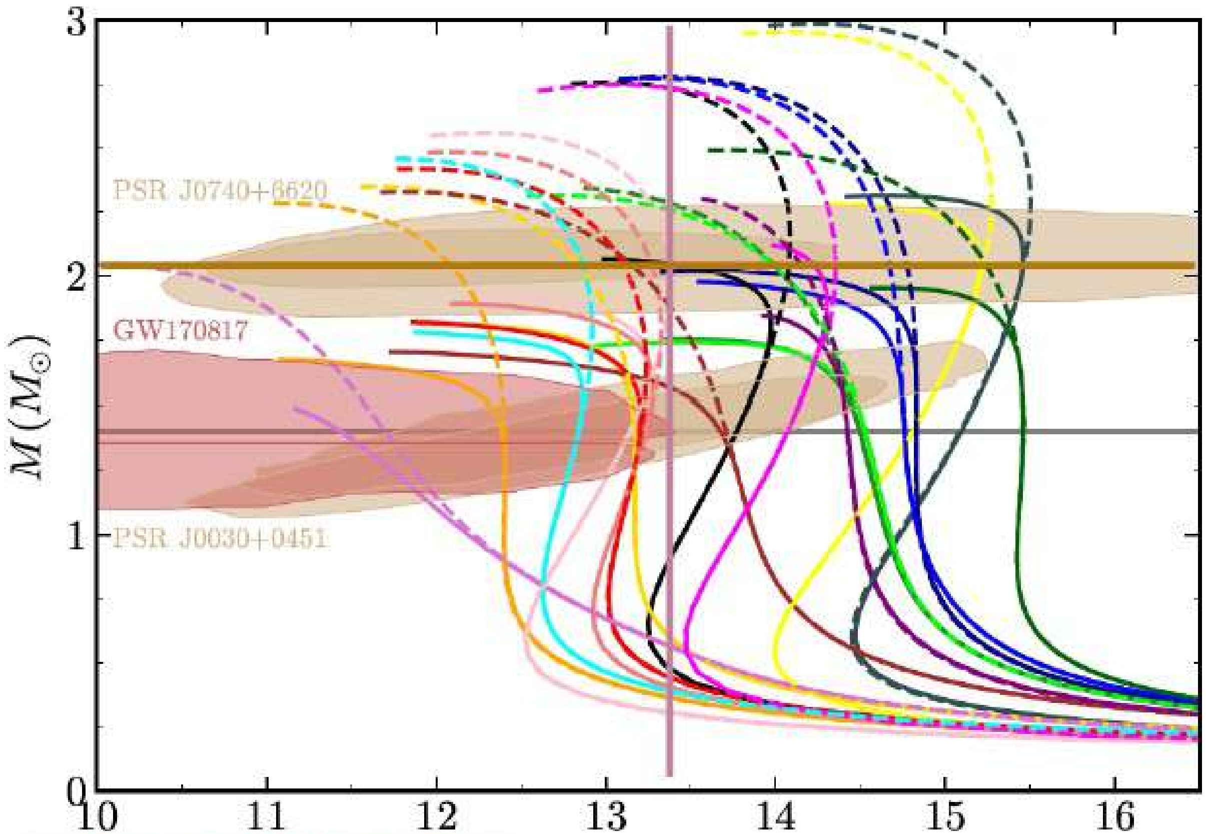

Sun, Miao, Sun, Li, ApJ 942 (2023) 55; arXiv:2205.10631 [astro-ph.HE]

Examples for hadronic EoS without (dashed lines) and with (solid lines) strange baryons. EoS which fulfill the observational constraints should be left of the vertical line at 1.4 Msun and should cross the horizontal line for the minimal maximum mass at 2.01 Msun. There is no EoS of this sample which fulfills both constraints !!

From Tab. 2 select EoS which fulfill (w. Y) 70 < Λ_1.4 < 580 and check their M_max

EoS	M_max	EoS	M_max
NL3ωρ	1.974	DD2	1.935
DDLZ1	1.989	PKDD	1.781
DD-ME2	1.971	HC	1.828
OMEG	1.862		

"Berlin Wall" constraint for neutron stars?

Mass-radius diagram for purely hadronic EOS

Appearance of hyperons softens the EOS → Limitation for the maximum mass

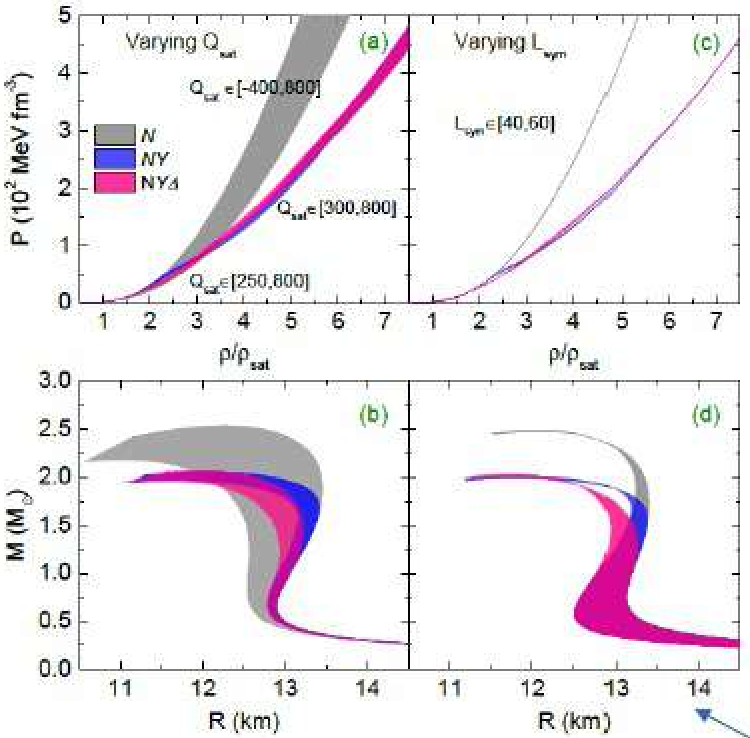

FIG. 4. EoS models and MR relations for N, NY, and $NY\Delta$ compositions of stellar matter. The bands are generated by varying the parameters Q_{sat} [MeV] (a, b) and L_{sym} [MeV] (c, d). The ranges of Q_{sat} and L_{sym} allowed by χEFT and maximum mass constraints are indicated in the figures.

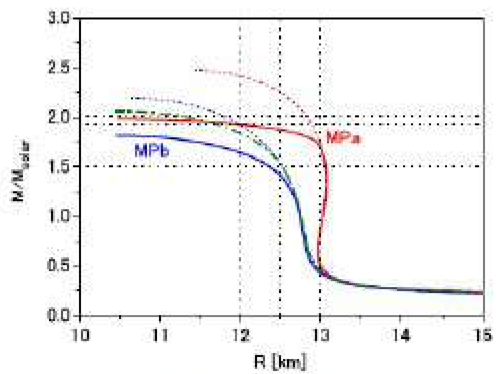

FIG. 7. Neutron-star masses as a function of the radius R. Solid (dashed) curves are with (without) hyperon (Λ and Σ^-) mixing for ESC+MPa and ESC+MPb. The dot-dashed curve for MPb is with Λ mixing only. Also see the caption of Fig. 3.

Yamamoto et al., Phys.Rev.C 96 (2017) 06580; arXiv:1708.06163 [nucl-th]

Yamamoto et al., Eur. Phys. J. A 52 (2016) 19; arXiv:1510.06099 [nucl-th]

Ji & Sedrakian, Phys. Rev. C 100 (2019) 015809; arXiv:1903.06057 [astro-ph.HE]

Examples for realistic hadronic EoS which suggest a Berlin Wall is inferior to the line M = 2.0 M_sun

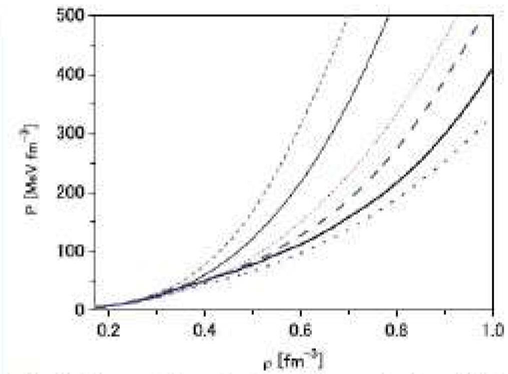

Fig. 8. Pressure P as a function of baryon density ρ. Thick (thin) curves are with (without) hyperon mixing. Solid, dashed and dotted curves are for MPa, MPa$^+$ and MPb.

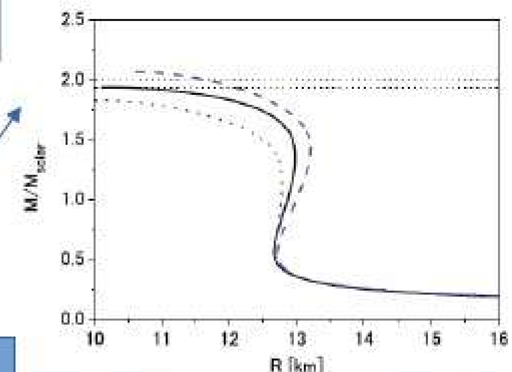

Fig. 9. Neutron-star masses as a function of the radius R. Solid, dashed and dotted curves are for MPa, MPa$^+$ and MPb. Two dotted lines show the observed mass $(1.97 \pm 0.04)M_\odot$ of J1614-2230.

“Berlin wall” constraint for neutron stars

Realistic hadronic EOS (with strange baryons)

CASUS CENTER FOR ADVANCED SYSTEMS UNDERSTANDING

Y. Yamamoto, H. Togashi, T. Tamagawa, T. Furumoto, N. Yasutake, T. Rijken, PRC 96 (2017)

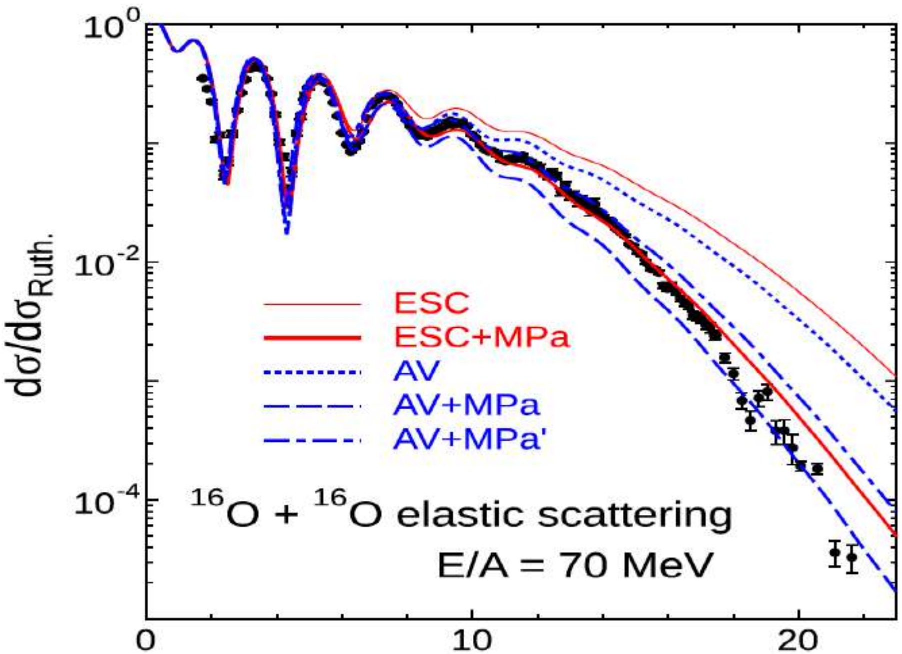

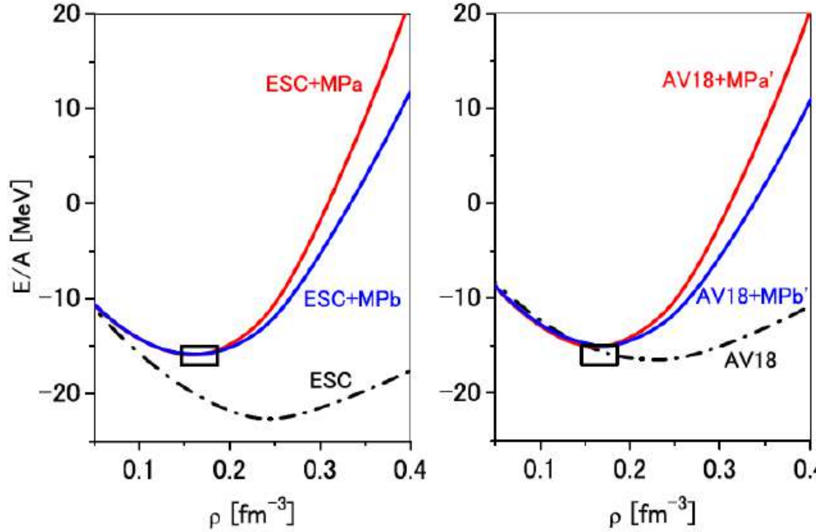

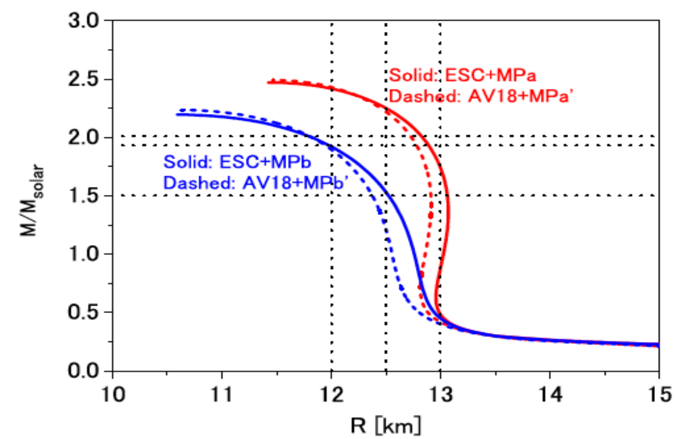

Short-range multipomeron exchange potential (MPP) added to AV18 potential gives significant improvement of large-angle scattering cross section (s.a.) and the Nuclear saturation properties, when compared to APR.
→ Neutron star radii R(M< 2 M_sun) > 12 km !!

Breaking the “Berlin wall” constraint

With Bayesian analyses and hybrid EOS

Neutron star EoS constraint from pQCD

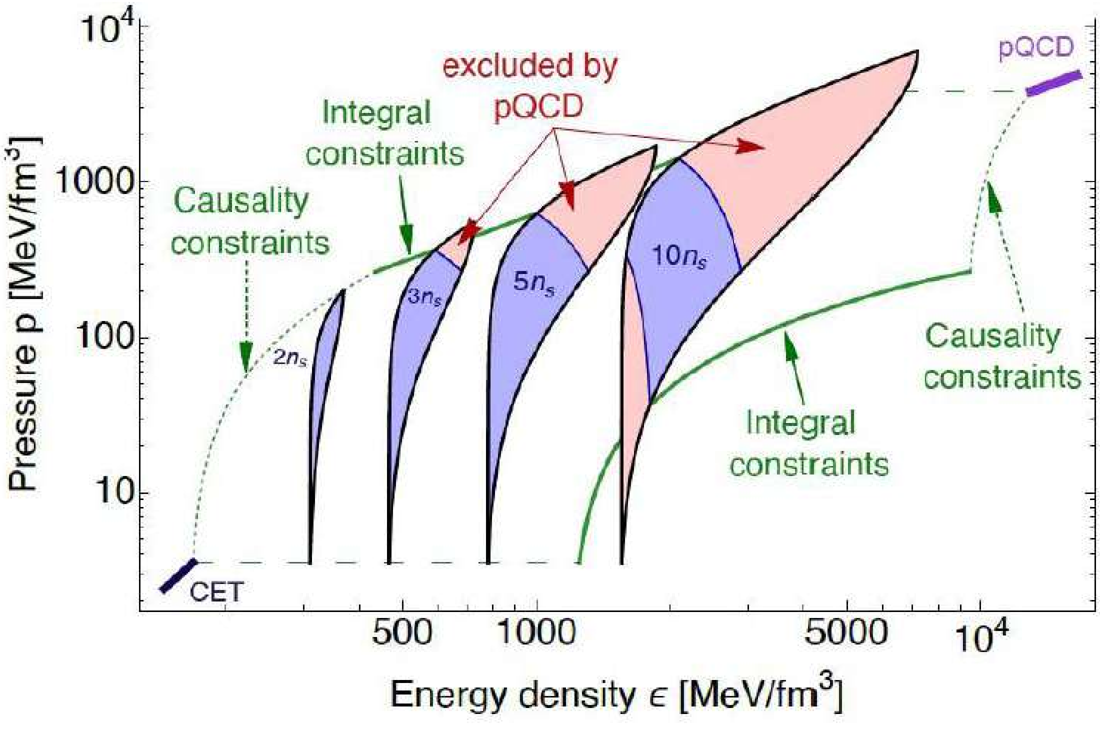

O. Komoltsev and A. Kurkela, Phys. Rev. D 128 (2022) 202701

Consistency check for neutron star EoS from the CompOSE library

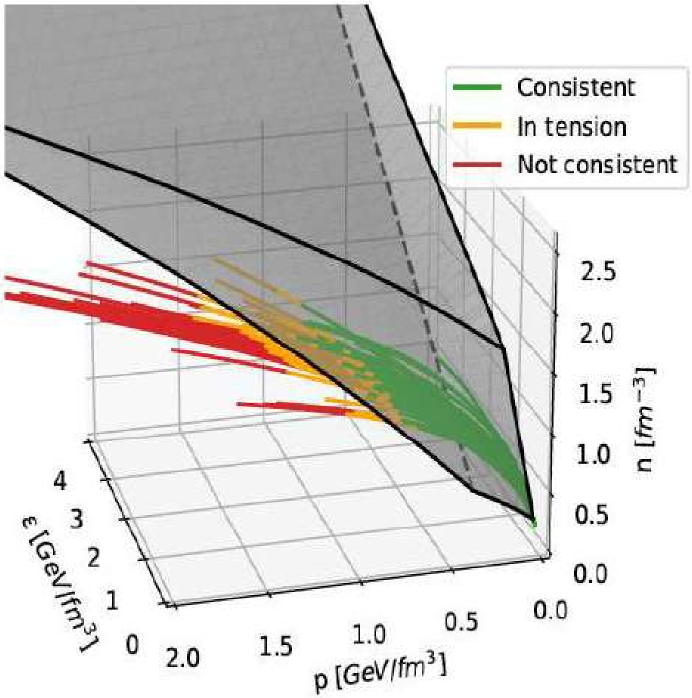

Result: Not all EoS fulfill the consistency check with pQCD asymptotics! pQCD important for NS!

Breaking the "Berlin wall" constraint

With Bayesian analyses and hybrid EOS

M(R) curves generated by causality, thermodynamic stability and pQCD limit

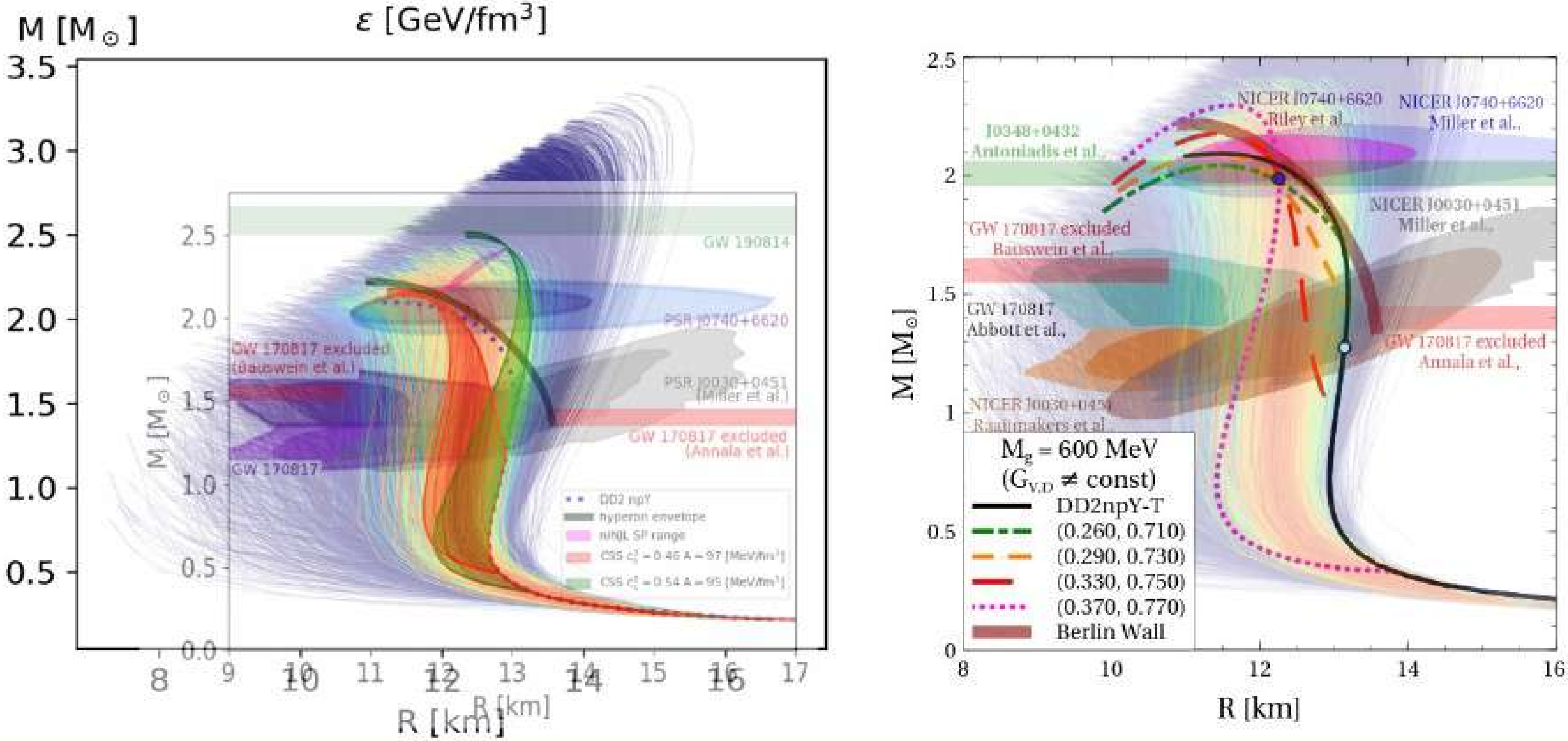

The conjectured "Berlin Wall" overlaid to the Fig. 2 from Gorda, Komoltsev & Kurkela [2204.11877 [nucl-th]] and hybrid EoS with quark matter described by a CSS model (left) and a confining relativistic density functional (right).

Relativistic density functionals for QCD

String-flip model for quark matter

Röpke, Blaschke, Schulz, PRD34 (1986) 3499

$$\mathcal{Z} = \int \mathcal{D}\bar{q}\mathcal{D}q \exp\left\{ \int_0^\beta d\tau \int_V d^3x \left[\mathcal{L}_{\rm eff} + \bar{q}\gamma_0\hat{\mu}q\right] \right\} , \quad q = \begin{pmatrix} q_u \\ q_d \end{pmatrix} , \quad \hat{\mu} = {\rm diag}(\mu_u, \mu_d)$$

$$\mathcal{L}_{\rm eff} = \mathcal{L}_{\rm free} - \boxed{U(\bar{q}q, \bar{q}\gamma_0 q)} , \quad \mathcal{L}_{\rm free} = \bar{q}\left(-\gamma_0\frac{\partial}{\partial\tau} + i\vec{\gamma}\cdot\vec{\nabla} - \hat{m}\right)q , \ \hat{m} = {\rm diag}(m_u, m_d)$$

General nonlinear functional of quark density bilinears: scalar, vector, isovector, diquark ...
Expansion around the expectation values:

$$U(\bar{q}q, \bar{q}\gamma_0 q) = U(n_{\rm s}, n_{\rm v}) + (\bar{q}q - n_{\rm s})\Sigma_{\rm s} + (\bar{q}\gamma_0 q - n_{\rm v})\Sigma_{\rm v} + \dots ,$$

$$\langle\bar{q}q\rangle = n_{\rm s} = \sum_{f=u,d} n_{{\rm s},f} = -\sum_{f=u,d}\frac{T}{V}\frac{\partial}{\partial m_f}\ln\mathcal{Z} , \quad \Sigma_{\rm s} = \left.\frac{\partial U(\bar{q}q, \bar{q}\gamma_0 q)}{\partial(\bar{q}q)}\right|_{\bar{q}q = n_{\rm s}} = \frac{\partial U(n_{\rm s}, n_{\rm v})}{\partial n_{\rm s}} ,$$

$$\langle\bar{q}\gamma_0 q\rangle = n_{\rm v} = \sum_{f=u,d} n_{{\rm v},f} = \sum_{f=u,d}\frac{T}{V}\frac{\partial}{\partial \mu_f}\ln\mathcal{Z} , \quad \Sigma_{\rm v} = \left.\frac{\partial U(\bar{q}q, \bar{q}\gamma_0 q)}{\partial(\bar{q}\gamma_0 q)}\right|_{\bar{q}\gamma_0 q = n_{\rm v}} = \frac{\partial U(n_{\rm s}, n_{\rm v})}{\partial n_{\rm v}}$$

$$\boxed{\mathcal{Z} = \int \mathcal{D}\bar{q}\mathcal{D}q \exp\left\{\mathcal{S}_{\rm quasi}[\bar{q}, q] - \beta V \Theta[n_{\rm s}, n_{\rm v}]\right\} , \quad \Theta[n_{\rm s}, n_{\rm v}] = U(n_{\rm s}, n_{\rm v}) - \Sigma_{\rm s} n_{\rm s} - \Sigma_{\rm v} n_{\rm v}}$$

$$\mathcal{S}_{\rm quasi}[\bar{q}, q] = \beta\sum_n\sum_{\vec{p}} \bar{q}\, G^{-1}(\omega_n, \vec{p})\, q , \quad G^{-1}(\omega_n, \vec{p}) = \gamma_0(-i\omega_n + \hat{\mu}^*) - \vec{\gamma}\cdot\vec{p} - \hat{m}^*$$

Relativistic density functionals for QCD

$$\mathcal{Z} = \int \mathcal{D}\bar{q}\mathcal{D}q \exp\{\mathcal{S}_{\rm quasi}[\bar{q},q] - \beta V \Theta[n_{\rm s}, n_{\rm v}]\}~, \quad \Theta[n_{\rm s}, n_{\rm v}] = U(n_{\rm s}, n_{\rm v}) - \Sigma_{\rm s} n_{\rm s} - \Sigma_{\rm v} n_{\rm v}$$

$$\mathcal{Z}_{\rm quasi} = \int \mathcal{D}\bar{q}\mathcal{D}q \exp\{\mathcal{S}_{\rm quasi}[\bar{q},q]\} = \det[\beta G^{-1}]~,$$

$$\ln\det A = {\rm Tr}\ln A$$

$$P_{\rm quasi} = \frac{T}{V}\ln \mathcal{Z}_{\rm quasi} = \frac{T}{V}{\rm Tr}\ln[\beta G^{-1}]$$

"no sea" approximation ...

$$= 2N_c \sum_{f=u,d} \int \frac{d^3p}{(2\pi)^3} \left\{T\ln\left[1+{\rm e}^{-\beta(E_f^*-\mu_f^*)}\right] + T\ln\left[1+{\rm e}^{-\beta(E_f^*+\mu_f^*)}\right]\right\}$$

$$P_{\rm quasi} = \sum_{f=u,d} \int \frac{dp}{\pi^2}\frac{p^4}{E_f^*}\left[f(E_f^*-\mu_f^*) + f(E_f^*+\mu_f^*)\right]$$

$$E_f^* = \sqrt{p^2 + {m_f^*}^2}$$

$$f(E) = 1/[1+\exp(\beta E)]$$

$$P = \sum_{f=u,d} \int_0^{p_{{\rm F},f}} \frac{dp}{\pi^2}\frac{p^4}{E_f^*} - \Theta[n_{\rm s}, n_{\rm v}]~, \quad p_{{\rm F},f} = \sqrt{{\mu_f^*}^2 - {m_f^*}^2}$$

$$\hat{m}^* = \hat{m} + \Sigma_{\rm s}$$
$$\hat{\mu}^* = \hat{\mu} - \Sigma_{\rm v}$$

Selfconsistent densities

$$n_{\rm s} = -\sum_{f=u,d}\frac{\partial P}{\partial m_f} = \frac{3}{\pi^2}\sum_{f=u,d}\int_0^{p_{{\rm F},f}} dp\, p^2 \frac{m_f^*}{E_f^*}~, \quad n_{\rm v} = \sum_{f=u,d}\frac{\partial P}{\partial \mu_f} = \frac{3}{\pi^2}\sum_{f=u,d}\int_0^{p_{{\rm F},f}} dp\, p^2 = \frac{p_{{\rm F},u}^3 + p_{{\rm F},d}^3}{\pi^2}~.$$

Relativistic density functionals for QCD

String-flip model for quark matter

Density functional for the SFM

$$U(n_s, n_v) = D(n_v) n_s^{2/3} + a n_v^2 + \frac{b n_v^4}{1 + c n_v^2},$$

Quark selfenergies

$$\Sigma_s = \frac{2}{3} D(n_v) n_s^{-1/3},$$ Quark "confinement"

$$\Sigma_v = 2 a n_v + \frac{4 b n_v^3}{1 + c n_v^2} - \frac{2 b c n_v^5}{(1 + c n_v^2)^2} + \frac{\partial D(n_v)}{\partial n_v} n_s^{2/3}$$

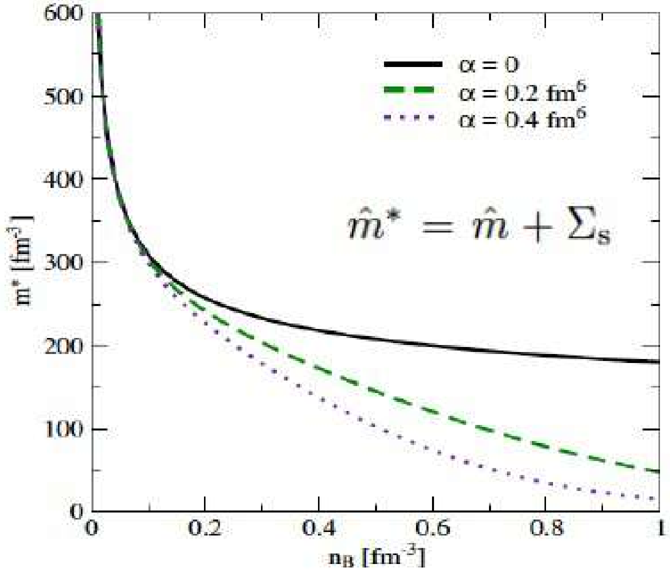

String tension & confinement due to dual Meissner effect (dual superconductor model)

$$D(n_v) = D_0 \Phi(n_v)$$

Effective screening of the string tension in dense matter by a reduction of the available volume $\alpha = v|v|/2$

$$\Phi(n_B) = \begin{cases} 1, & \text{if } n_B < n_0 \\ e^{-\alpha(n_B - n_0)^2}, & \text{if } n_B > n_0 \end{cases}$$

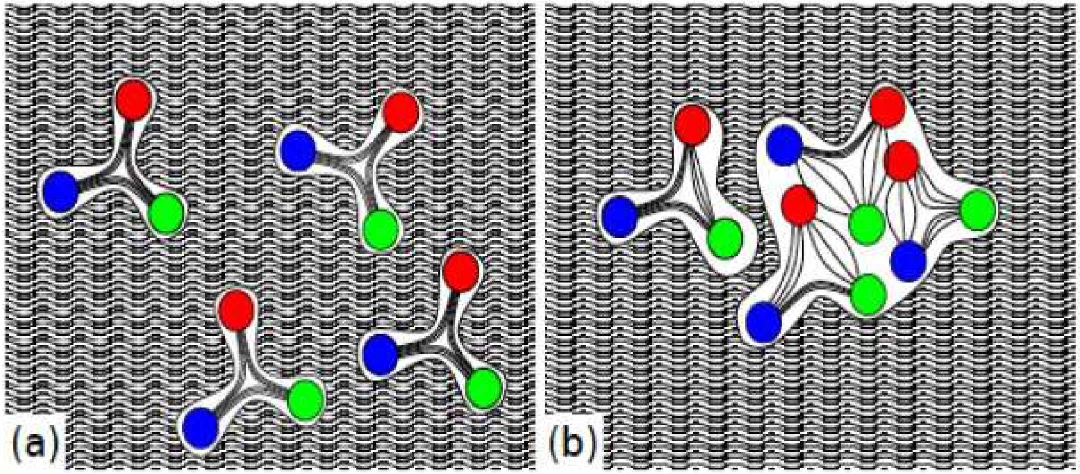

Relativistic density functionals for QCD

String-flip model for quark matter

Results for 1st order phase transition by Maxwell construction with DD2p40

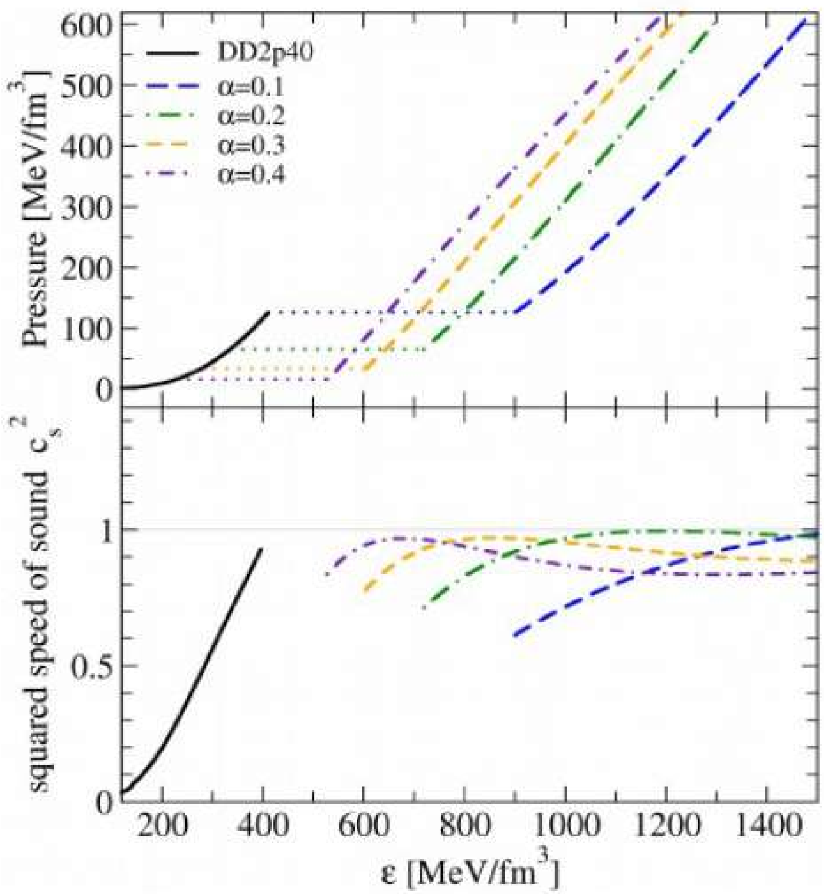

third family ↔ mass twin stars

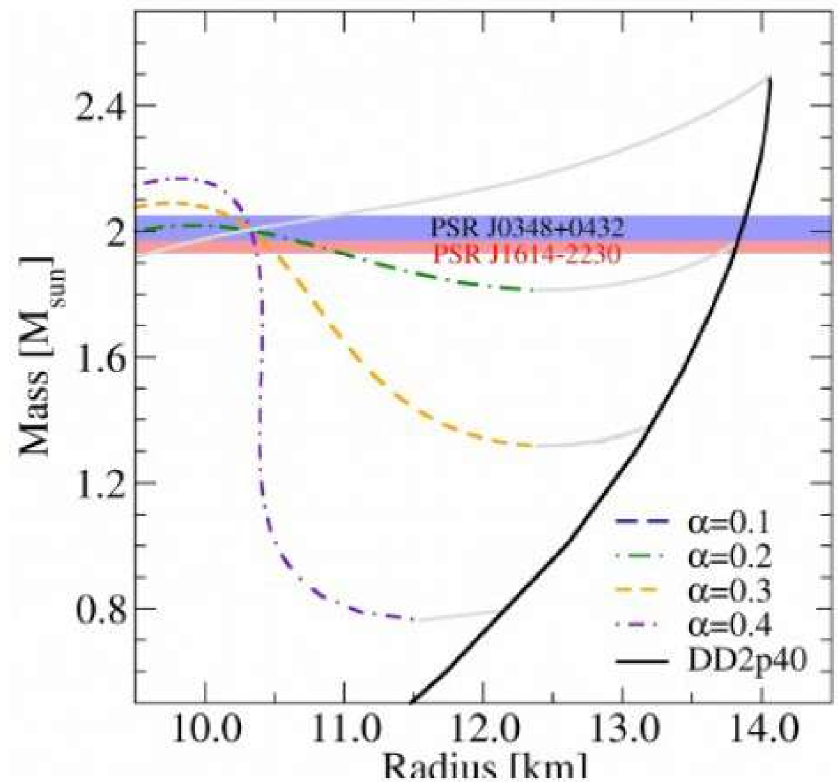

Kaltenborn, Bastian, Blaschke, arXiv:1701.04400 → Phys. Rev. D 96, 056024 (2017)

Deconfinement as supernova engine

Of massive blue supergiant star explosions

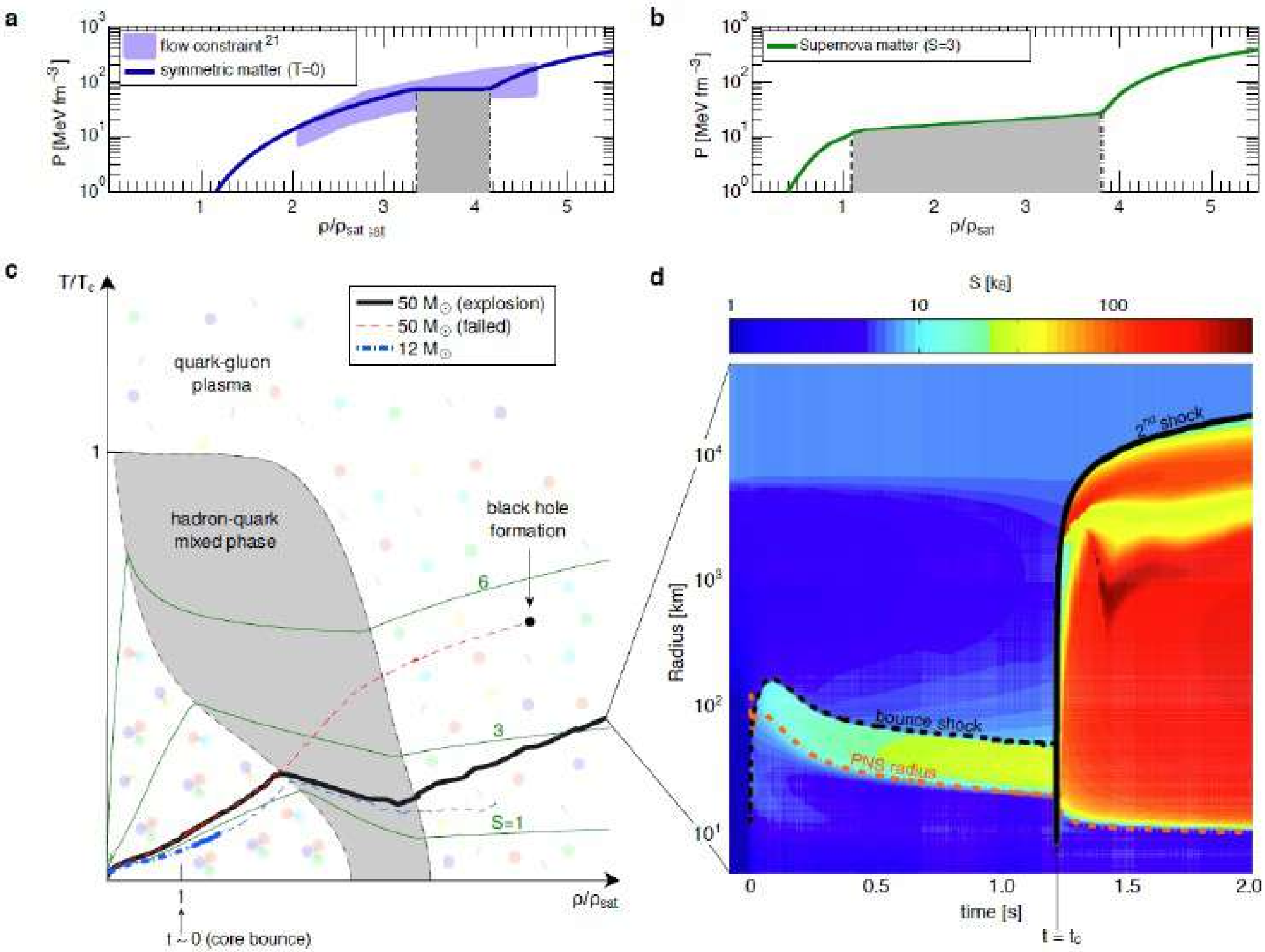

Progenitor:
M = 50 M_O

T. Fischer et al., Nature Astronomy 2, 960 (2018)

Ultra-heavy Nucleus-Nucleus Collisions !

CASUS
CENTER FOR ADVANCED
SYSTEMS UNDERSTANDING

Population of the QCD phase diagram in a merger

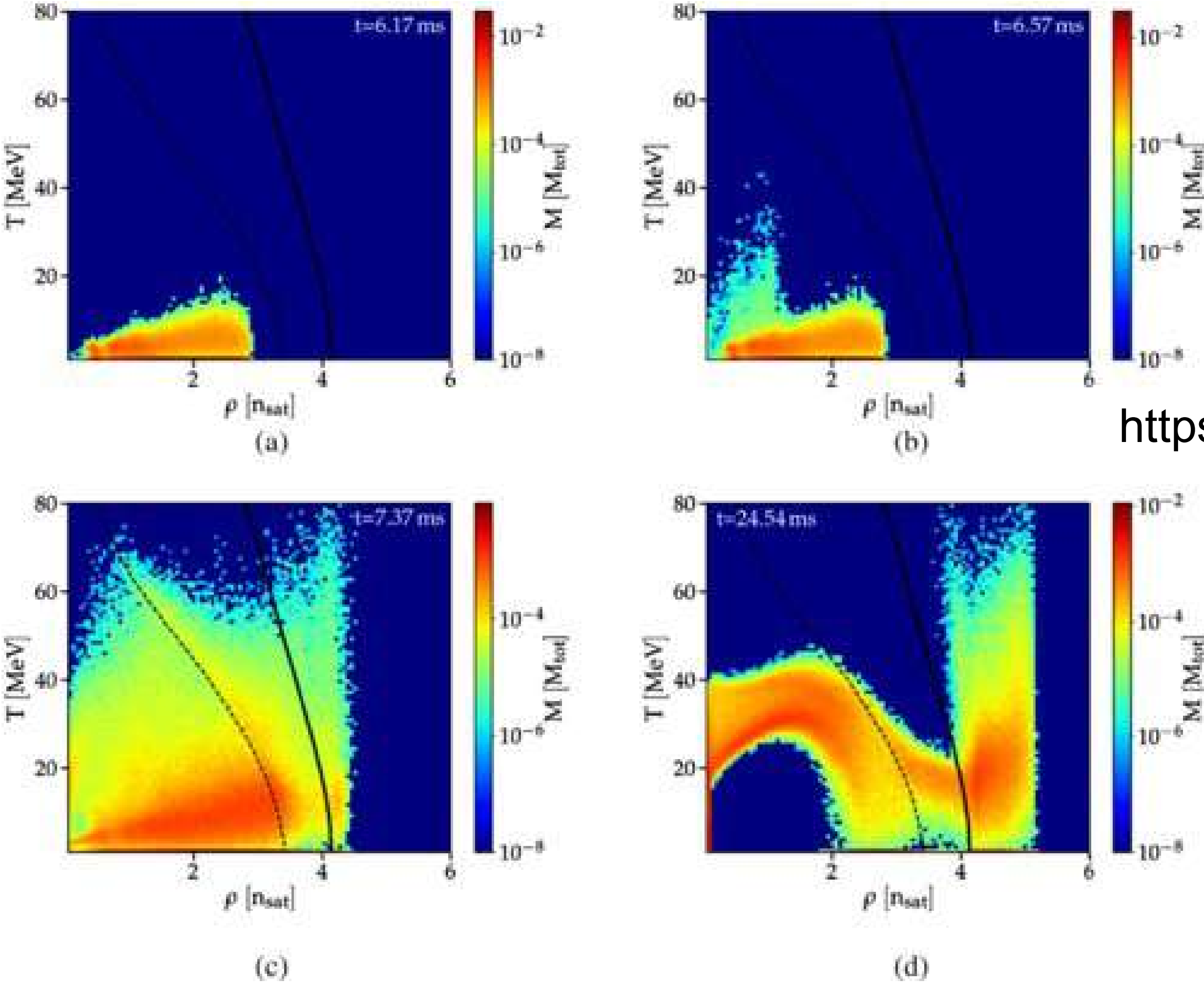

1.35 M_sun + 1.35 M_sun

EoS for supernova and merger simulations:

CompOSE

With deconfinement:

https://compose.obspm.fr/eos/166

S. Blacker, A. Bauswein, et al., Phys. Rev. D 102 (2020) 123023

Binary neutron star merger simulation

S. Blacker, A. Bauswein et al., Phys. Rev. D 102 (2020) 123023

Population of the QCD phase diagram with mixed phase; time = 6 … 25 ms

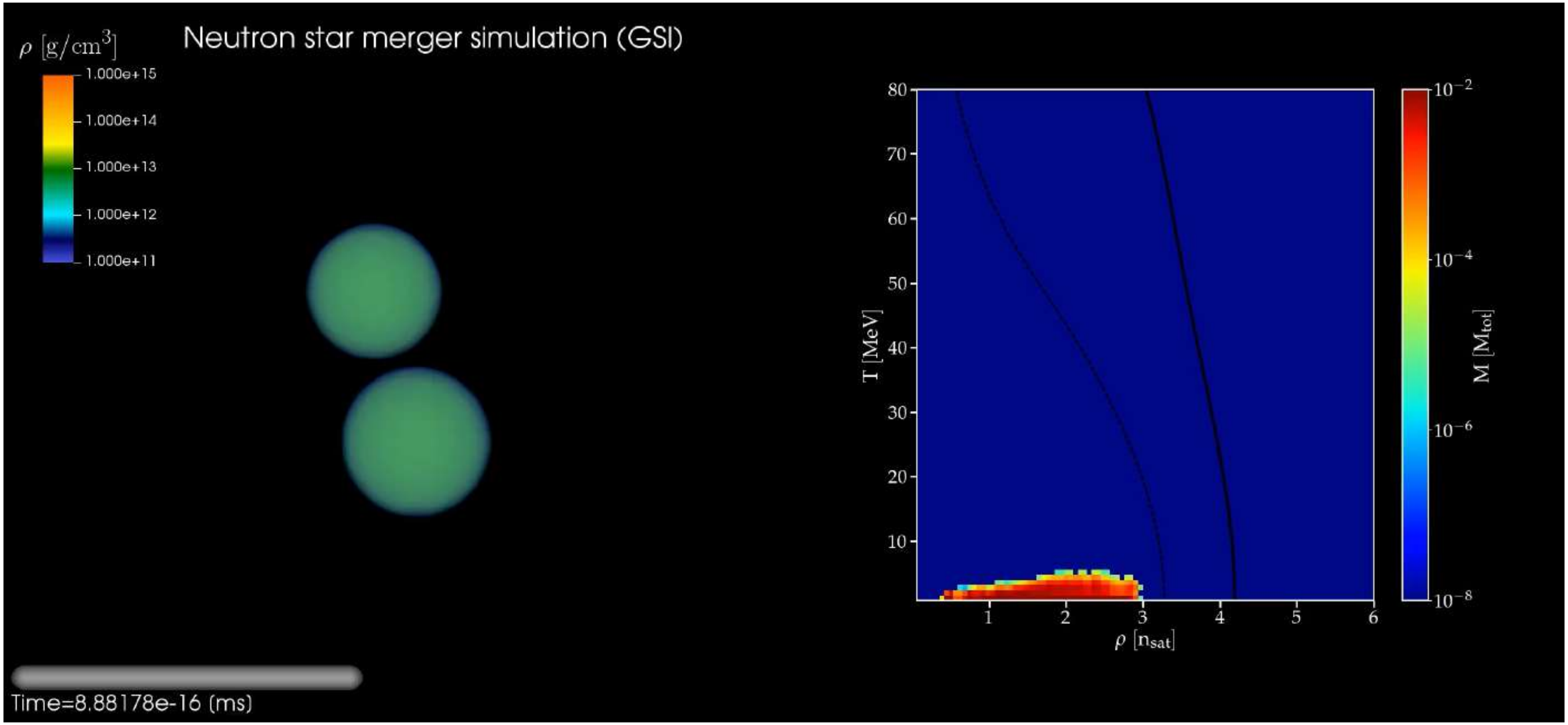

Ultra-heavy Nucleus-Nucleus Collisions !

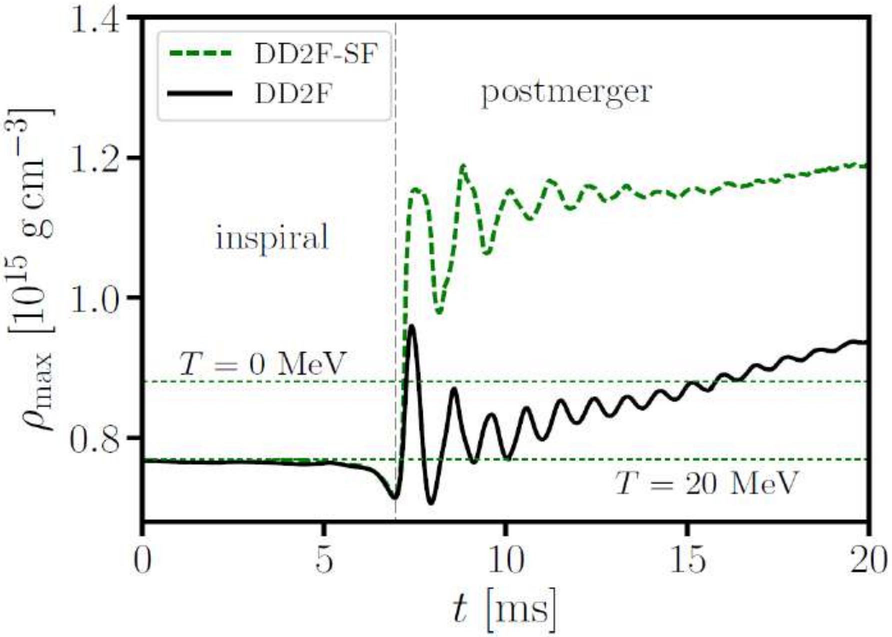

A. Bauswein et al.,
Strong phase transition in postmerger GW,
PRL 122 (2019) 061102; [arxiv:1809.01116]

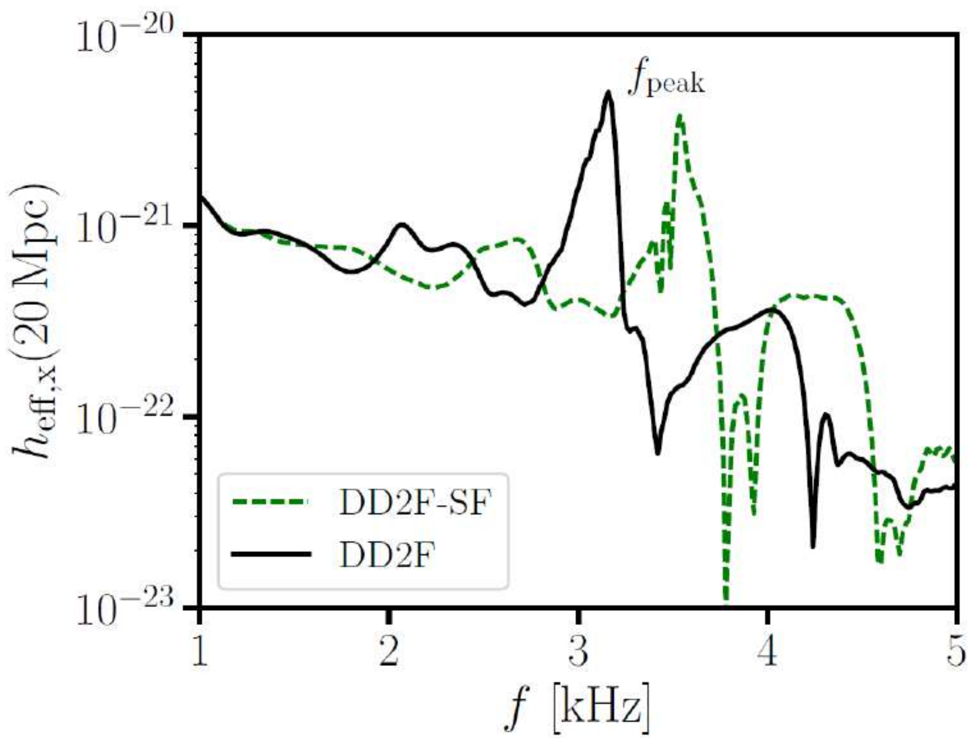

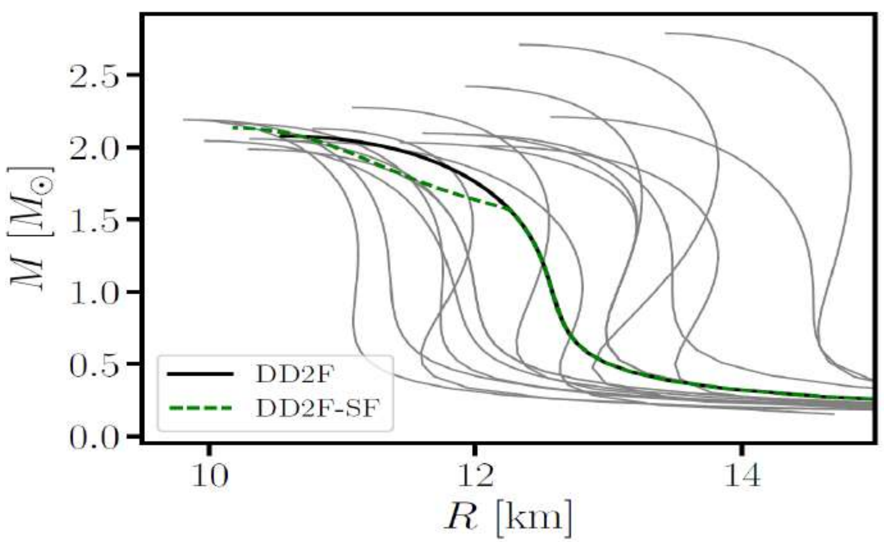

Hybrid star formation during NS merger
→ higher densities and compacter star
→ higher peak frequency of the GW

Ultra-heavy Nucleus-Nucleus Collisions !

Signal of a deconfinement transition

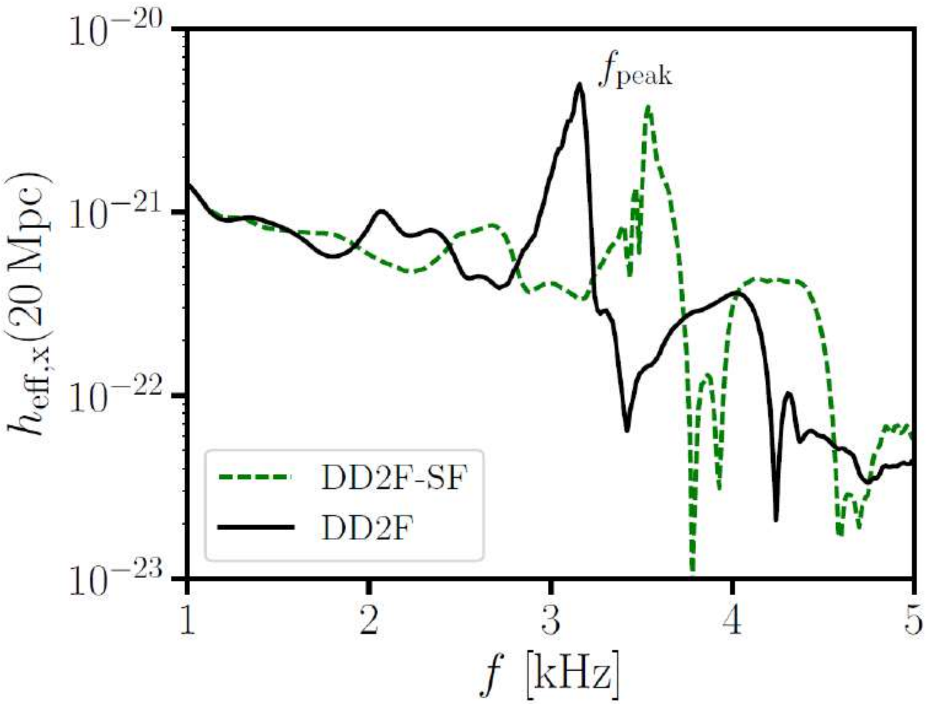

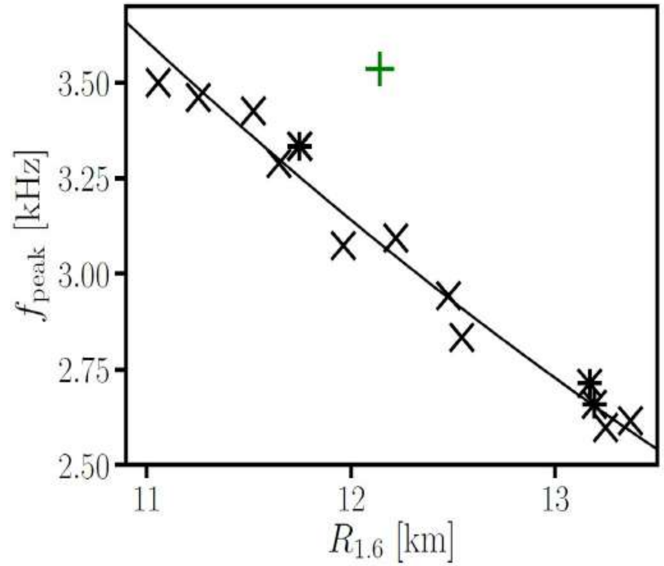

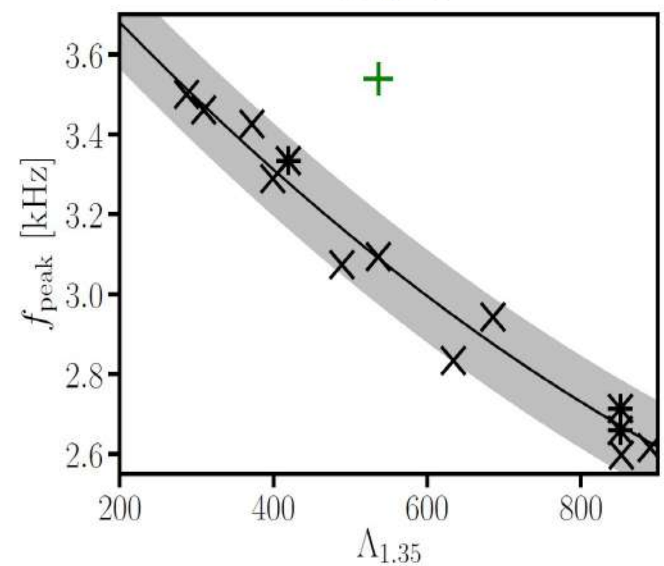

Strong deviation from $\mathbf{f_{peak} - R_{1.6}}$ relation signals **strong phase transition in** NS merger**!**

Complementarity of $\mathbf{f_{peak}}$ from postmerger with tidal deformability $\mathbf{\Lambda_{1.35}}$ from inspiral phase.

A. Bauswein et al., PRL 122 (2019) 061102; [arxiv:1809.01116]

Ultra-heavy Nucleus-Nucleus Collisions !

Signal of a deconfinement transition

Strong PT in postmerger GW signal, S. Blacker et al., arxiv:2006.03789, PRD102 (2020) 123023

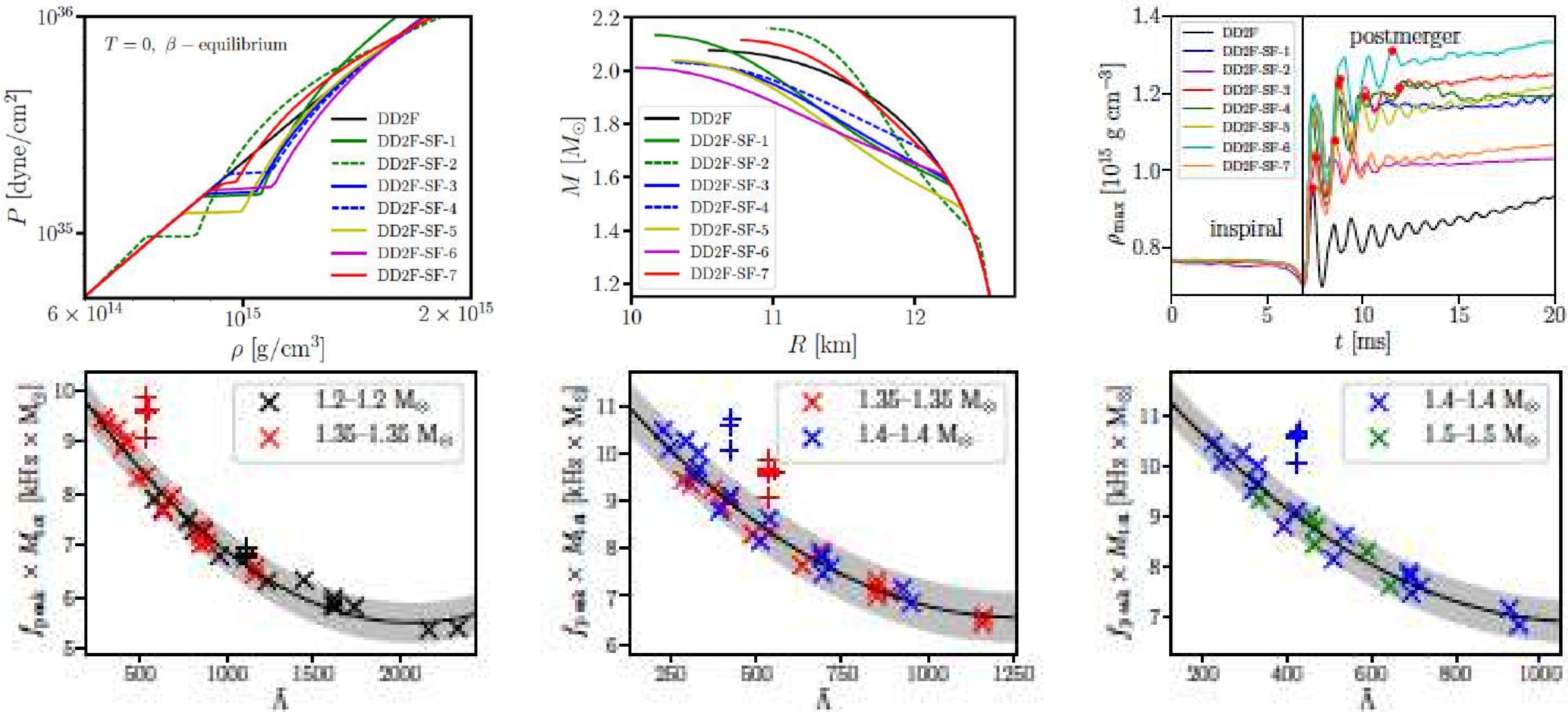

Dominant postmerger frequency f_{peak} vs. tidal deformability $\Lambda_{1.35}$ from inspiral phase:
Results from hybrid models appear as **outliers** of the grey band (maximal deviation of purely hadronic models from a least squares fit) = signalling a **strong phase transition in** NS **!**

Ultra-heavy Nucleus-Nucleus Collisions !

Signal of a deconfinement transition

Merger of hybrid stars with early phase transition: Bauswein & Blacker, EPJ ST 229 (2020)

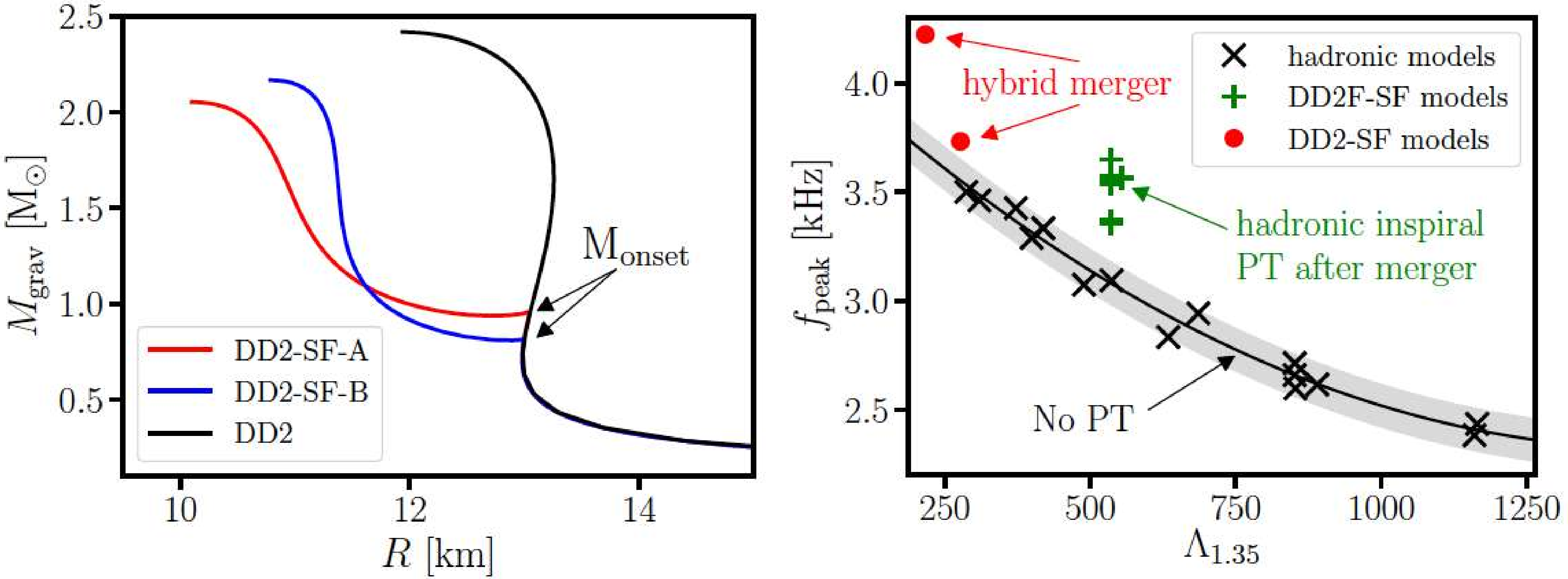

The combination of stiff hadronic EoS (DD2) and string-flip (SF) model allows for early onset of deconfinement in low-mass neutron stars and even third-family solutions (mass twins).
For these cases, the event GW170817 could have been a **merger of two hybrid stars**!
Also in these cases (red dots in above figure) a **significant deviation** from the grey band of Purely hadronic star mergers without a phase transition is obtained!

Relativistic density functional for quark matter

With chiral symmetry, color SC & confinement

Lagrangian $\mathcal{L} = \overline{q}(i\not\partial - \hat{m})q - \mathcal{U} + \mathcal{L}_V + \mathcal{L}_I + \mathcal{L}_D$

- **Scalar & pseudoscalar interaction channels**

$$\mathcal{U} = G_0 \left[(1+\alpha)\langle\overline{q}q\rangle_0^2 - (\overline{q}q)^2 - (\overline{q}i\vec{\tau}\gamma_5 q)^2\right]^{\frac{1}{3}}$$

  (motivated by String Flip Model, χ-dynamics, quark "confinement")

- **Vector-isoscalar interaction channel**

$$\mathcal{L}_V = -G_V(\overline{q}\gamma_\mu q)^2$$

  (motivated by gluon exchange, stiff EoS needed to reach $2M_\odot$)

- **Vector-isovector interaction channel**

$$\mathcal{L}_I = -G_I(\overline{q}\gamma_\mu \vec{\tau} q)^2$$

  (motivated by gluon exchange, isospin sensitive interaction)

- **Diquark interaction channel**

$$\mathcal{L}_D = G_D \sum_{A=2,5,7} (\overline{q}i\gamma_5\tau_2\lambda_A q^c)(\overline{q}^c i\gamma_5\tau_2\lambda_A q)$$

  (motivated by Cooper theorem, color superconductivity)

Relativistic density functional for quark matter

What is new?

O. Ivanytskyi & D.B., Phys. Rev. D 105 (2022) 114042

Interaction $\mathcal{U} = D_0 \left[(1+\alpha)\langle\overline{q}q\rangle_0^2 - (\overline{q}q)^2 - (\overline{q}i\vec{\tau}\gamma_5 q)^2\right]^{\varkappa}$

- **Parameters**

  D_0 - dimensionfull coupling, controls interaction strength

  α - dimensionless constant, controls vacuum quark mass

  $\langle\overline{q}q\rangle_0$ - χ-condensate in vacuum (introduced for the sake of convenience)

$\varkappa = 1/3$ $\Downarrow$ motivated by String Flip model

$\varkappa = 1$ $\Downarrow$ Nambu–Jona-Lasinio model

$$\mathcal{U}_{SFM} \propto \langle q^+q\rangle^{2/3}$$

$$\Sigma_{SFM} = \frac{\partial\mathcal{U}_{SFM}}{\partial\langle q^+q\rangle} \propto \langle q^+q\rangle^{-1/3} \propto separation$$

- **Dimensionality**

$$[\mathcal{U}] = energy^4 \quad [\overline{q}q] = energy^3 \quad \Rightarrow \quad [D_0]_{\varkappa=1/3} = energy^2 = [string\ \ tension]$$

self energy = string tension × separation $\Rightarrow$ **confinement**

Relativistic density functional for quark matter

Expansion around mean fields

$$\mathcal{U} = \underbrace{\mathcal{U}_{MF}}_{0^{th}\ \text{order}} + \underbrace{(\bar{q}q - \langle\bar{q}q\rangle)\Sigma_S}_{1^{st}\ \text{order}} - \underbrace{G_S(\bar{q}q - \langle\bar{q}q\rangle)^2 - G_{PS}(\bar{q}i\vec{\tau}\gamma_5 q)^2}_{2^{nd}\ \text{order}} + \ldots$$

- **Mean-field scalar self-energy**

$$\Sigma_S = \frac{\partial \mathcal{U}_{MF}}{\partial\langle\bar{q}q\rangle}$$

- **Effective medium dependent couplings**

$$G_S = -\frac{1}{2}\frac{\partial^2\mathcal{U}_{MF}}{\partial\langle\bar{q}q\rangle^2}, \quad G_{PS} = -\frac{1}{6}\frac{\partial^2\mathcal{U}_{MF}}{\partial\langle\bar{q}i\vec{\tau}\gamma_5 q\rangle^2}$$

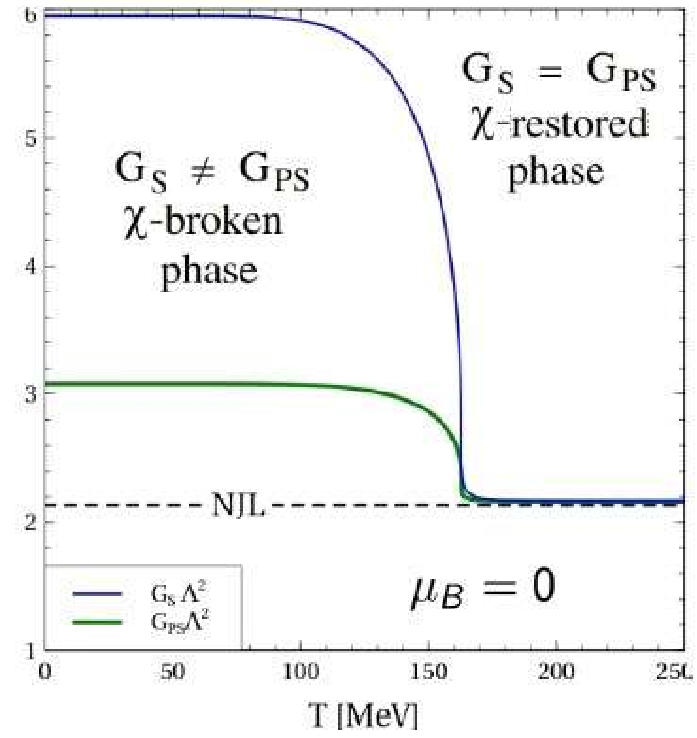

Relativistic density functional for quark matter

Comparison to Nambu—Jona-Lasinio model

$$\mathcal{L} = \overline{q}(i\partial\!\!\!/ - \underbrace{(m + \Sigma_S)}_{\text{effective mass } m^*})q + G_S(\overline{q}q)^2 + G_{PS}(\overline{q}i\vec{\tau}\gamma_5 q)^2 + \cdots + \mathcal{L}_V + \mathcal{L}_D$$

- **Similarities:**
  - current-current interaction
  - (pseudo)scalar, vector, diquark, ... channels
- **Differences:**
  - high m^* at low T, $\mu \Rightarrow$ **"confinement"**

$$\langle\overline{q}q\rangle = \langle\overline{q}q\rangle_0 \;\Rightarrow\; m^* = m - \frac{2G_0}{3\alpha^{2/3}\langle\overline{q}q\rangle_0^{1/3}}$$

$$\Downarrow$$

$$m^* \to \infty \text{ at } \alpha \to 0$$

  - medium dependent couplings:

low T, μ, $\Rightarrow$ $G_S \neq G_{PS}$ $\Rightarrow$ χ-broken
high T, μ, $\Rightarrow$ $G_S = G_{PS}$ $\Rightarrow$ χ-symmetric

T = 0

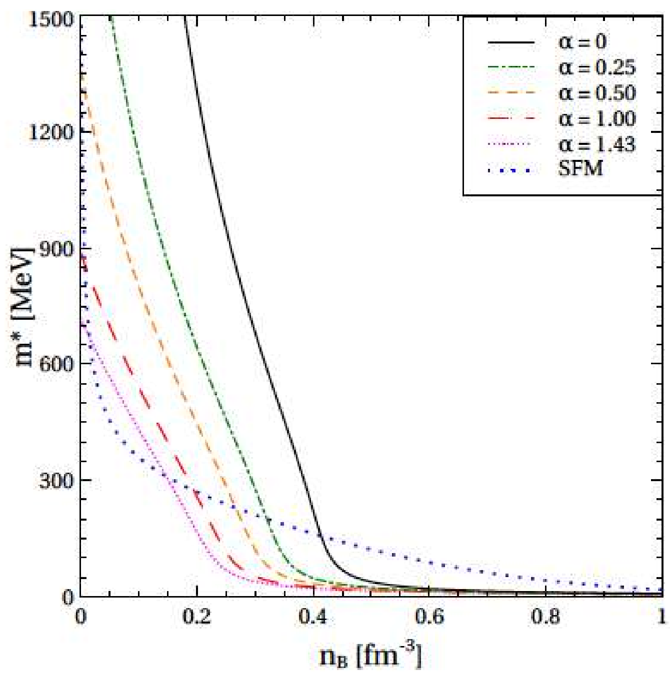

Relativistic density functional for quark matter

Bosonisation by HS-transformation

- **Hubbard-Stratonovich transformation**

$$\exp\left[\int dx\; G(\overline{q}\hat{\Gamma}q)^2\right] = \int[D\phi]\exp\left[-\int dx\left(\frac{\phi^2}{4G}+\phi\overline{q}\hat{\Gamma}q\right)\right]$$

- **Vertexes:** $\hat{\Gamma}_S = 1 \;\Rightarrow$ scalar-isoscalar σ-field
  $\hat{\Gamma}_{PS} = i\gamma^5\vec{\tau} \;\Rightarrow$ pseuscalar-isoscalar $\vec{\pi}$-field
  $\hat{\Gamma}^{\mu}_{V} = \gamma^{\mu} \;\Rightarrow$ vector-isoscalar ω^{μ}-field
  $\hat{\Gamma}^{\mu}_{I} = \gamma^{\mu}\vec{\tau} \;\Rightarrow$ vector-isoscalar $\vec{\rho}^{\mu}$-field
  $\hat{\Gamma}^{A}_{D} = i\gamma^5\lambda_A\tau_2 \;\Rightarrow$ scalar diquark Δ_A-field

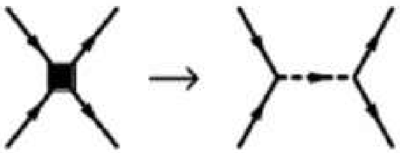

- **Bosonized Lagrangian ($m^* = m + \Sigma_S$ - effective mass, $Q^T = (q\; q^c)/\sqrt{2}$)**

$$\mathcal{L} + q^{+}\hat{\mu}q = \overline{Q}\hat{S}^{-1}Q - \frac{\sigma^2}{4G_S} - \frac{\vec{\pi}^2}{4G_{PS}} + \frac{\omega^2}{4G_V} + \frac{\vec{\rho}^2}{4G_I} - \frac{\Delta_A\Delta_A^*}{4G_D} - \mathcal{U}_{MF} + \langle\overline{q}q\rangle(\Sigma_S+\sigma)$$

$$\hat{S}^{-1} = \begin{pmatrix} \hat{\mathcal{S}}_{+}^{-1} & i\Delta_A\gamma_5\tau_2\lambda_A \\ i\Delta_A^*\gamma_5\tau_2\lambda_A & \hat{\mathcal{S}}_{-}^{-1} \end{pmatrix}, \quad \hat{\mathcal{S}}_{\pm}^{-1} = i\partial\!\!\!/ - m^* - \sigma - i\gamma^5\vec{\pi}\cdot\vec{\tau} \pm \gamma_0\hat{\mu} \pm \omega\!\!\!/ \pm \vec{\rho\!\!\!/}\cdot\vec{\tau}$$

Relativistic density functional for quark matter

Mean field approximation

- **Field equations for σ and $\vec{\pi}$**

$$\begin{cases} \sigma = 2G_S(\langle\overline{q}q\rangle - \overline{q}q) \\ \vec{\pi} = -2G_{PS}\overline{q}i\vec{\tau}\gamma_5 q \end{cases} \Rightarrow \langle\sigma\rangle = \langle\vec{\pi}\rangle = 0 \Rightarrow \sigma, \vec{\pi} - \textbf{beyond MF}$$

comment: $\langle\sigma\rangle = 0$ does not assume χ-symmetry since $\langle\overline{q}q\rangle \neq 0$

- **Thermodynamic potential**

$$\langle\omega_\mu\rangle = \delta_{\mu 0}\omega, \quad \langle\rho^a_\mu\rangle = \delta_{\mu 0}\delta_{a3}\rho, \quad |\langle\Delta_A\rangle| = \delta_{A2}\Delta$$

$$\Downarrow$$

$$\Omega = -\frac{1}{2\beta V} Tr \ln(\beta\hat{S}^{-1}) - \frac{\omega^2}{4G_V} - \frac{\rho^2}{4G_I} + \frac{\Delta^2}{4G_D} + \mathcal{U}_{MF} - \langle\overline{q}q\rangle\Sigma_S$$

- **Vector fields, diquark gap, χ-condensate**

$$\frac{\partial\Omega}{\partial\omega} = 0, \quad \frac{\partial\Omega}{\partial\rho} = 0, \quad \frac{\partial\Omega}{\partial\Delta} = 0, \quad \langle\overline{q}q\rangle = \sum_f \frac{\partial\Omega}{\partial m_f}$$

Relativistic density functional for quark matter

Define the couplings in mesonic channels

- **Mesonic correlations**

$$\mathcal{L} = \ldots + \overline{q}(\sigma + i\gamma_5\vec{\pi}\cdot\vec{\tau} + \not{\omega} + \vec{\not{\rho}}\cdot\tau)q - \frac{\sigma^2}{4G_S} - \frac{\vec{\pi}^2}{4G_{PS}} + \frac{\omega^2}{4G_V} + \frac{\vec{\rho}^2}{4G_I}$$

$$D_i^{-1}(p^2) = \frac{1}{2G_i} -$$ 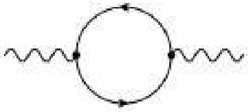 - one-loop mesonic propagator

$$D_i^{-1}(M_i^2) = 0 \;\Rightarrow\; \text{mesonic masses}$$

- **Fierz transformation** - rearrangement of the Dirac, color and flavor indexes

$$\begin{aligned}(\gamma^\mu)_{mn}(\gamma_\mu)_{m'n'} = \mathbf{1}_{mn'}\mathbf{1}_{m'n} + (i\gamma_5)_{mn'}(i\gamma_5)_{mn'} \\ -\frac{1}{2}(\gamma^\mu)_{mn'}(\gamma_\mu)_{m'n} \\ -\frac{1}{2}(\gamma^\mu\gamma_5)_{mn'}(\gamma_\mu\gamma_5)_{m'n}\end{aligned}$$

$$\mathbf{1}_{ij}\mathbf{1}_{kl} = \frac{1}{3}\mathbf{1}_{il}\mathbf{1}_{kj} + \frac{1}{2}(\tau_a)_{il}(\tau_a)_{kj}$$

$$\lambda_\alpha^{ab}\lambda_\alpha^{a'b'} = \frac{16}{9}\mathbf{1}_{ab'}\mathbf{1}_{a'b} - \frac{1}{3}\lambda_\alpha^{ab'}\lambda_\alpha^{a'b}$$

coefficients - proportional to couplings

$$\mathbf{G_S : G_V : G_I : G_D = 1 : 0.5 : 0.5 : 0.75}$$

Relativistic density functional for quark matter

Model setup – parameter fixing with observables

- (Pseudo)scalar interaction channels
  (chiral condensate & π, σ mesons)

m [MeV]	Λ [MeV]	α	$D_0\Lambda^{-2}$
4.2	573	1.43	1.39
M_π [MeV]	F_π [MeV]	M_σ [MeV]	$\langle \bar{l}l \rangle_0^{1/3}$ [MeV]
140	92	980	-267

Pseudocritical temperature

$T_c = 163$ MeV

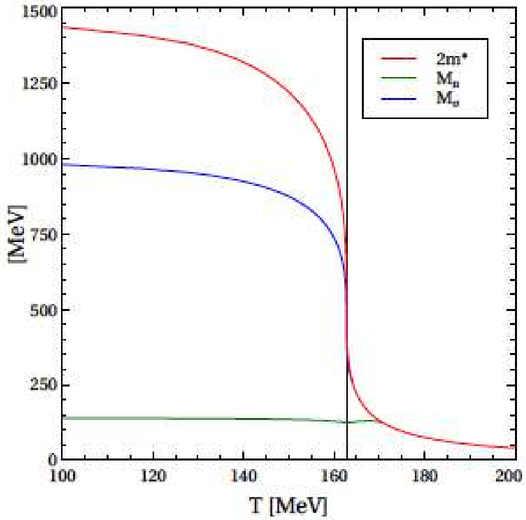

- low T: $2m_{quark} > M_\pi, M_\sigma$
  (stable mesons, confined quarks)
- high T: $2m_{quark} < M_\pi, M_\sigma$
  (unstable mesons, deconfined quarks)

- Vector-isoscalar & vector-isovector channels (ω, ρ mesons)

$$M_\omega = 783 \text{ MeV} \Rightarrow \eta_V \equiv \frac{G_{V0}}{G_{S0}} = 0.452, \quad M_\rho = 775 \text{ MeV} \Rightarrow \eta_I \equiv \frac{G_{I0}}{G_{S0}} = 0.454$$

- Diquark pairing channel (Fierz transformation) $\eta_D \equiv \frac{G_{D0}}{G_{S0}} = 1.5\eta_V = 0.678$

Relativistic density functional for quark matter

Onset of color superconductivity

- **Single quark energy and distribution**

$$E_f^{\pm} = sgn(E_f \mp \mu_f)\sqrt{(E_f \mp \mu_f)^2 + \Delta^2}$$

$$f_f^{\pm} = [\exp(E_f^{\pm}/T) + 1]^{-1}$$

- **Gap equation**

$$\frac{\partial\Omega}{\partial\Delta} = \frac{\Delta}{2G_D} - 2\Delta \sum_{f,a=\pm} \int \frac{d\mathbf{k}}{(2\pi)^3} \frac{1-2f_f^a}{E_f^a} = 0$$

$$\Downarrow$$

two solutions : $\Delta = 0$ **or** $\Delta \neq 0$

- **Two solutions coincide** $\Rightarrow$ **SC onset**

$$\left.\frac{\partial^2\Omega}{\partial\Delta^2}\right|_{\Delta=0} = 0 \quad \Rightarrow \quad \mu_B = \mu_B(G_D)$$

$T = 0$

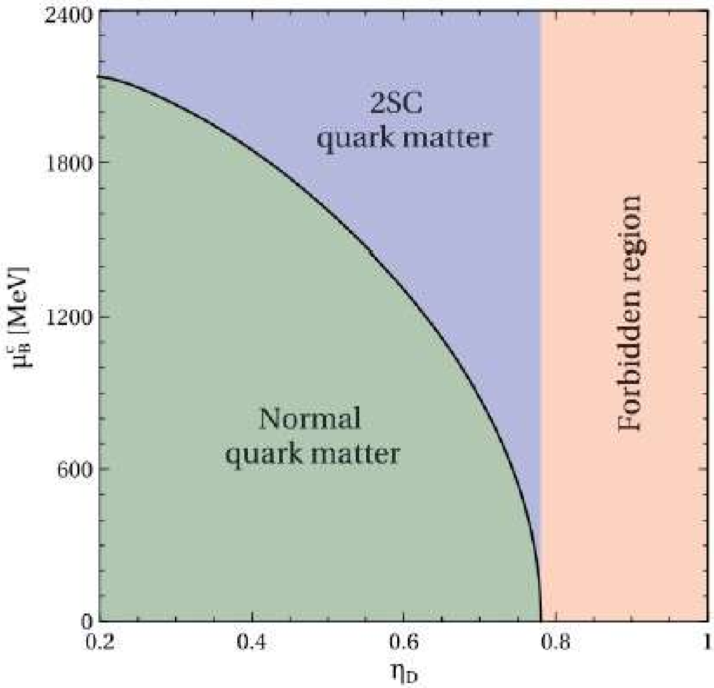

No vacuum superconductivity

$$\Downarrow$$

$$\eta_D \lesssim 0.78$$

(agrees with the Fierz value)

Relativistic density functional for quark matter

Asymptotically conformal EOS for neutron stars

- **Setup:** electric neutrality, β-equilibrium, Maxwell construction with DD2 EoS
- **Scanning over η_V and η_D at $M_{gD} = M_{gV}$**

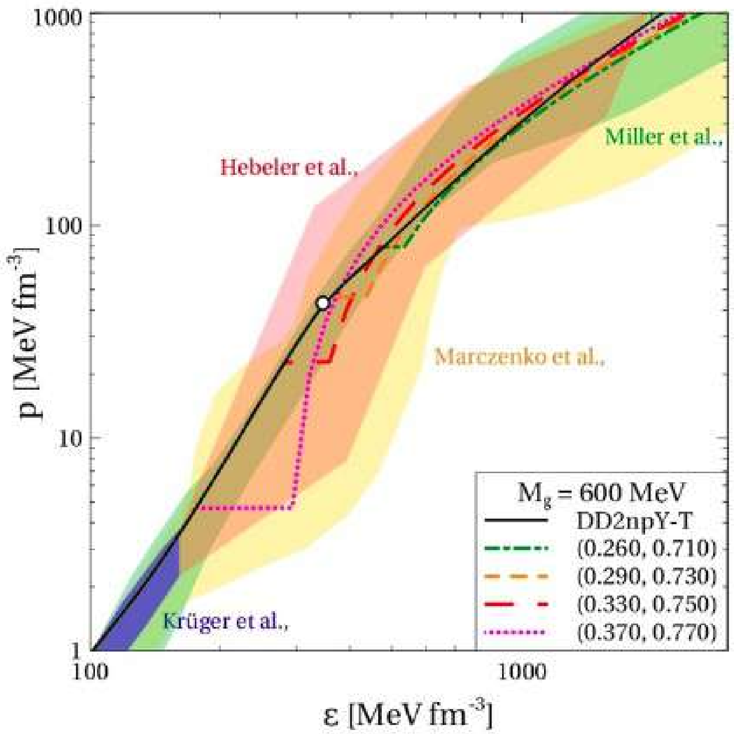

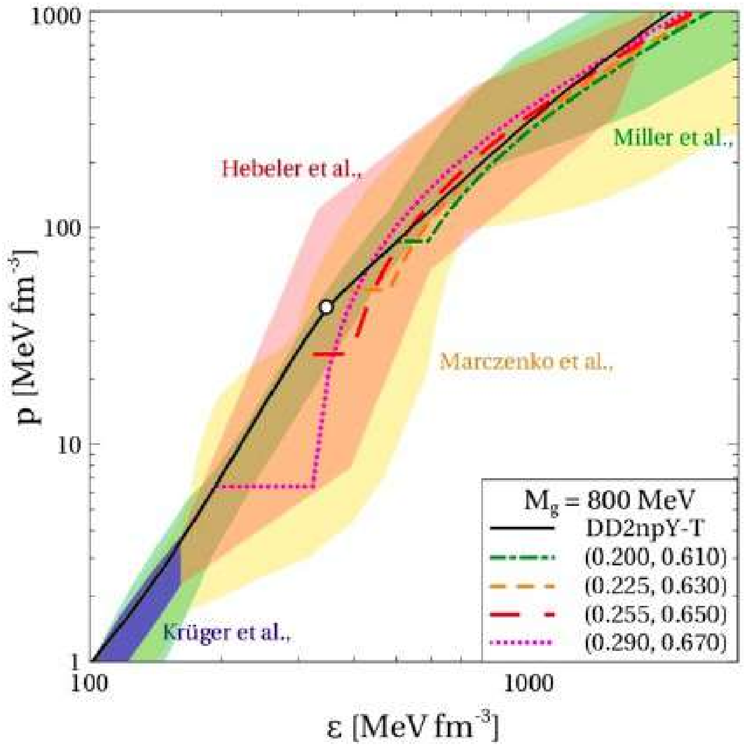

The ω-meson value of η_V and the Fierz value of η_D prefer early deconfinement?

Relativistic density functional for quark matter

Speed of sound

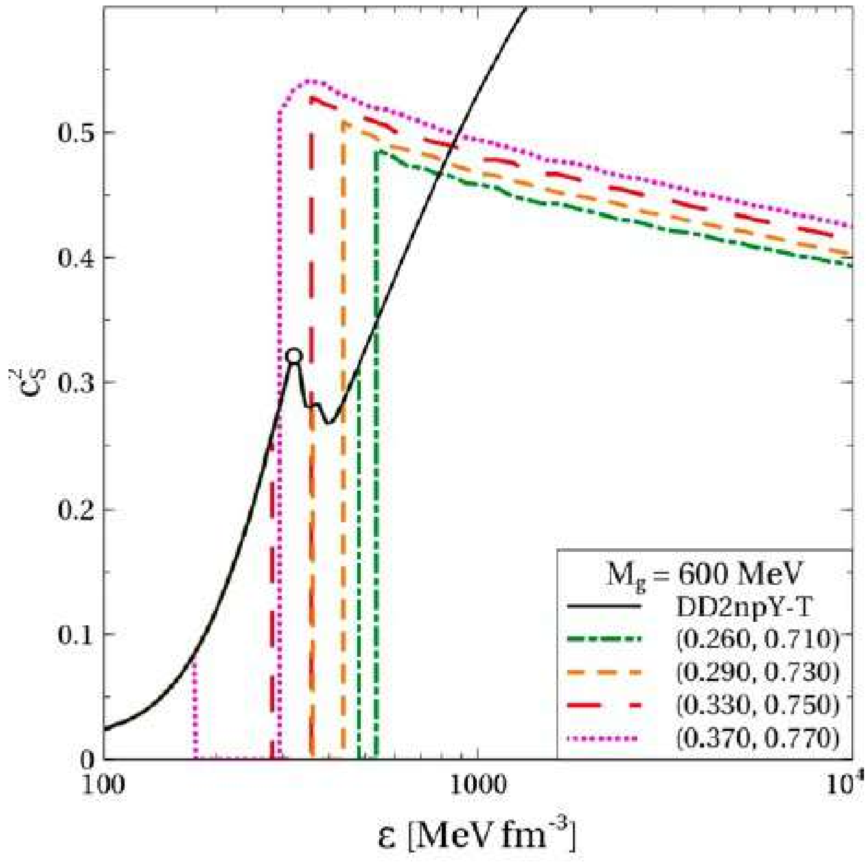

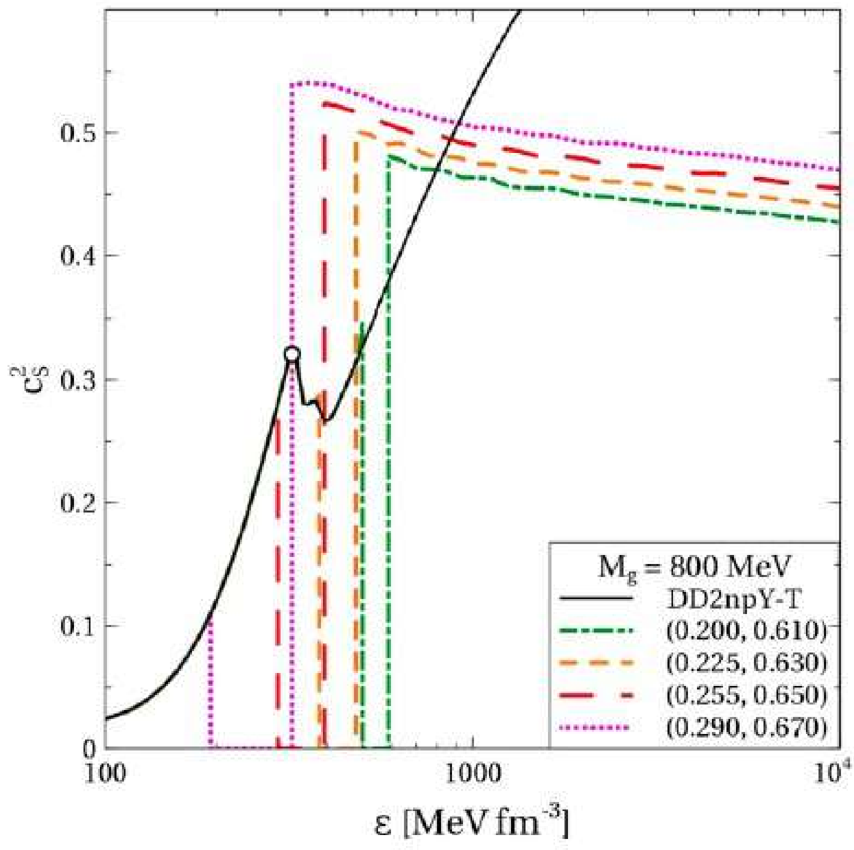

O. Ivanytskyi and D.B., Particles 5 (2022) 514 - 534

Relativistic density functional for quark matter

Mass-radius diagram for hybrid neutron stars

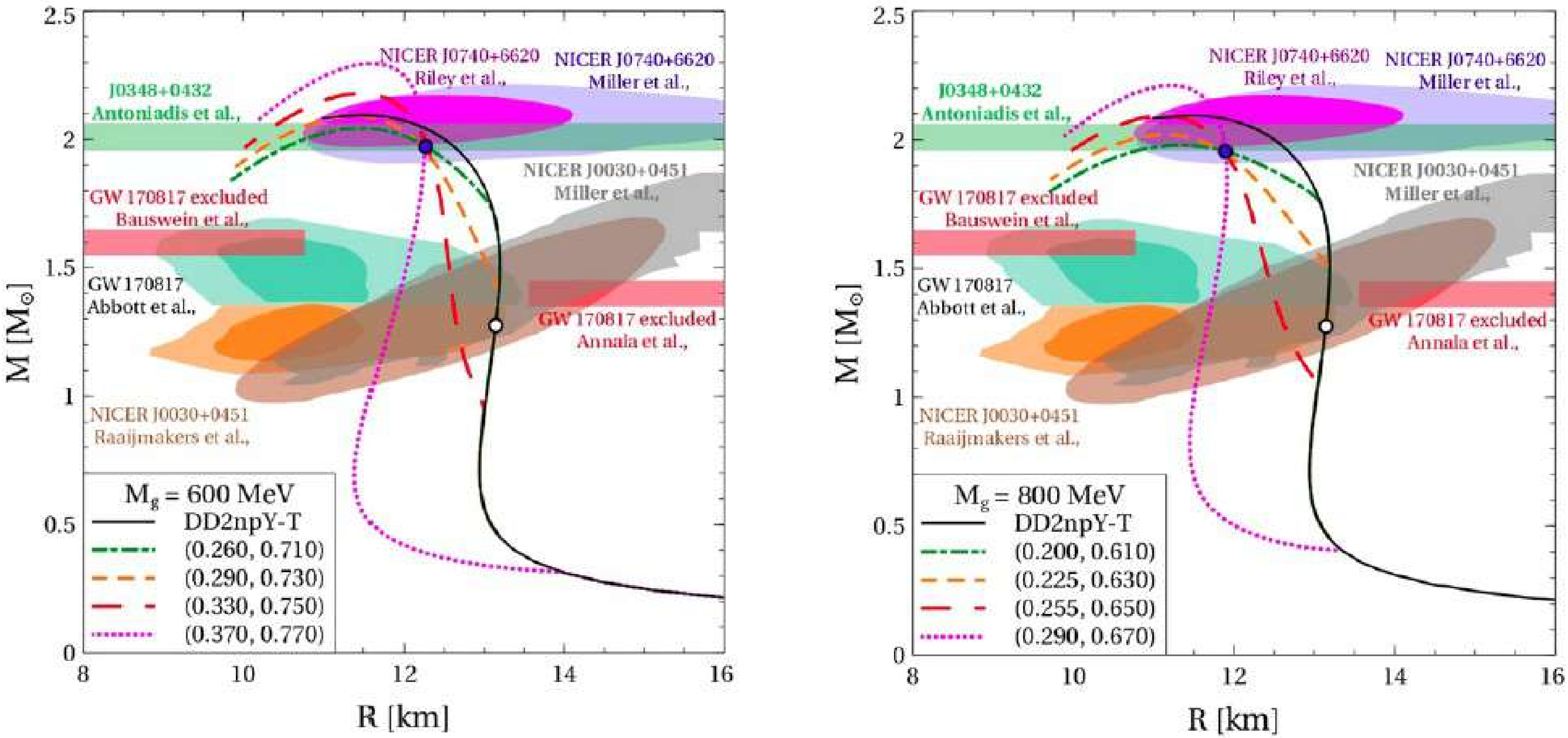

Observational data prefer early deconfinement?

Relativistic density functional for quark matter

Special point (SP) in the mass-radius diagram for hybrid neutron stars

- **Quark EoS**

$$p = \frac{\varepsilon}{3} - \frac{4B}{3}$$

B - bag constant

- **Variation of B**

$\Downarrow$

family of hybrid quark-hadron Eo

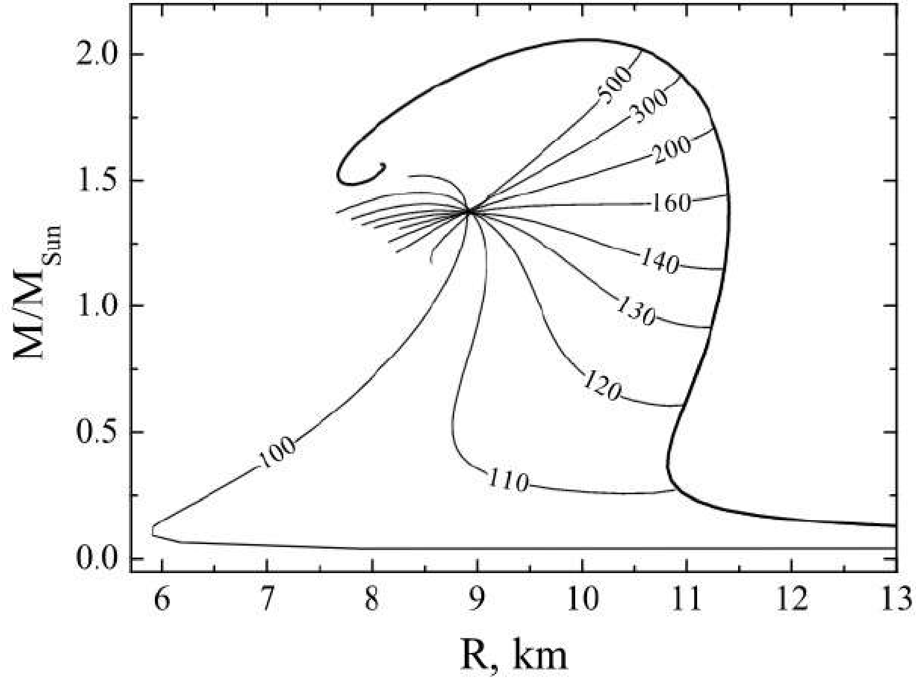

- **Special point** - narrow range of intersection of M-R curves

A. V. Yudin et al., Astron. Lett. 40, 201 (2014)

Relativistic density functional for quark matter

SP in M-R diagram for hybrid neutron stars

- Weak sensitivity to hadron EoS

M. Cierniak and D. Blaschke, Eur. Phys. J. ST 229, 3663 (2020)

- Weak sensitivity to details of quark-to-hadron transition

M. Cierniak and D. Blaschke, Astron. Nachr. 342, 819-825 (2021)

- Sensitivity to quark EoS only

⇓

SP can be used in order to test quark EoS

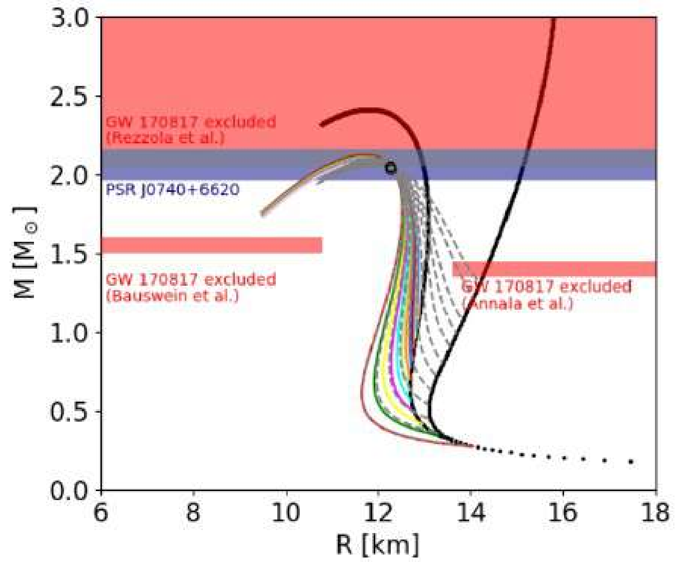

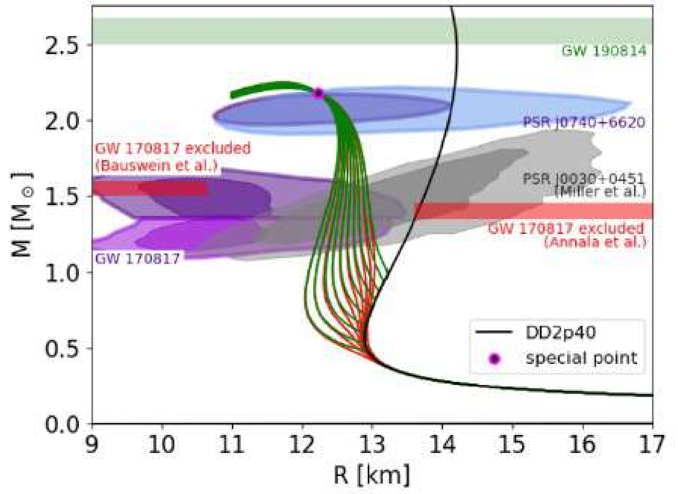

Relativistic density functional for quark matter

Parametrization of the RDF quark matter EoS

- **Phenomenological "confinement"**

  $p \simeq -B$ at small densities

- **Asymptotically conformal**

  $p \propto \mu_B^4$ at high densities

- **Color superconductivity**

  correction $\propto \mu_B^2 \Delta^2$

- **ABPR-like parameterization** $(M_{gluon} = 600 \text{ MeV})$

  $$p = A_4 \mu_B^4 + \Delta^2 \mu_B^2 - B$$

  $A_4, \ \Delta, \ B$ depend on $\eta_V, \ \eta_D$

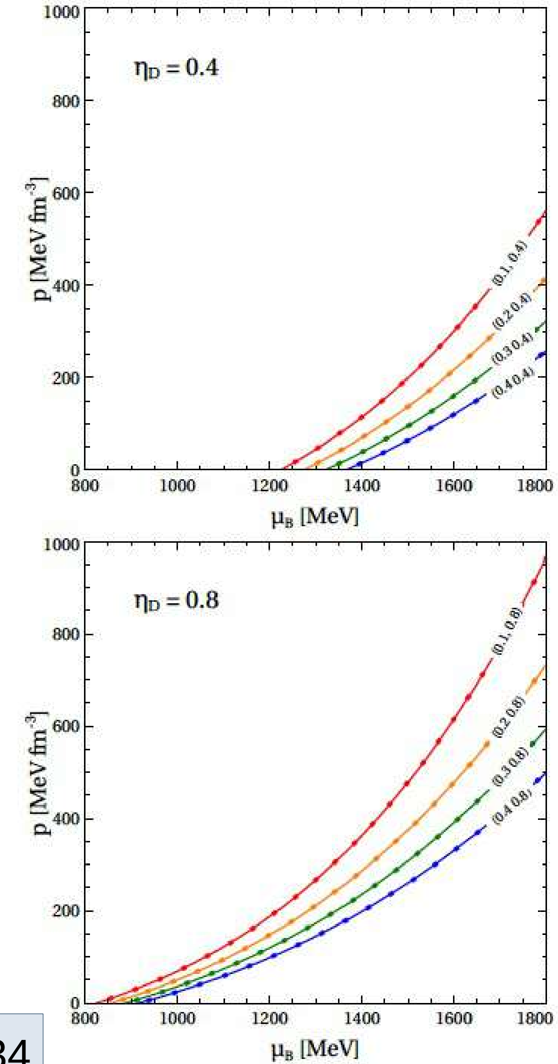

C. Gärtlein et al., arXiv:2301.10765; D.B. et al., PRD107, 063034

Relativistic density functional for quark matter

SP in M-R diagram for hybrid neutron stars

- Variation of η_D at fixed η_V

$\Downarrow$

Special point

- SPs are equidistant
- M_{max} and M_{onset} are anticorrelated

M_{max} – observationally constrained

M_{onset} – controlled by η_V, η_D

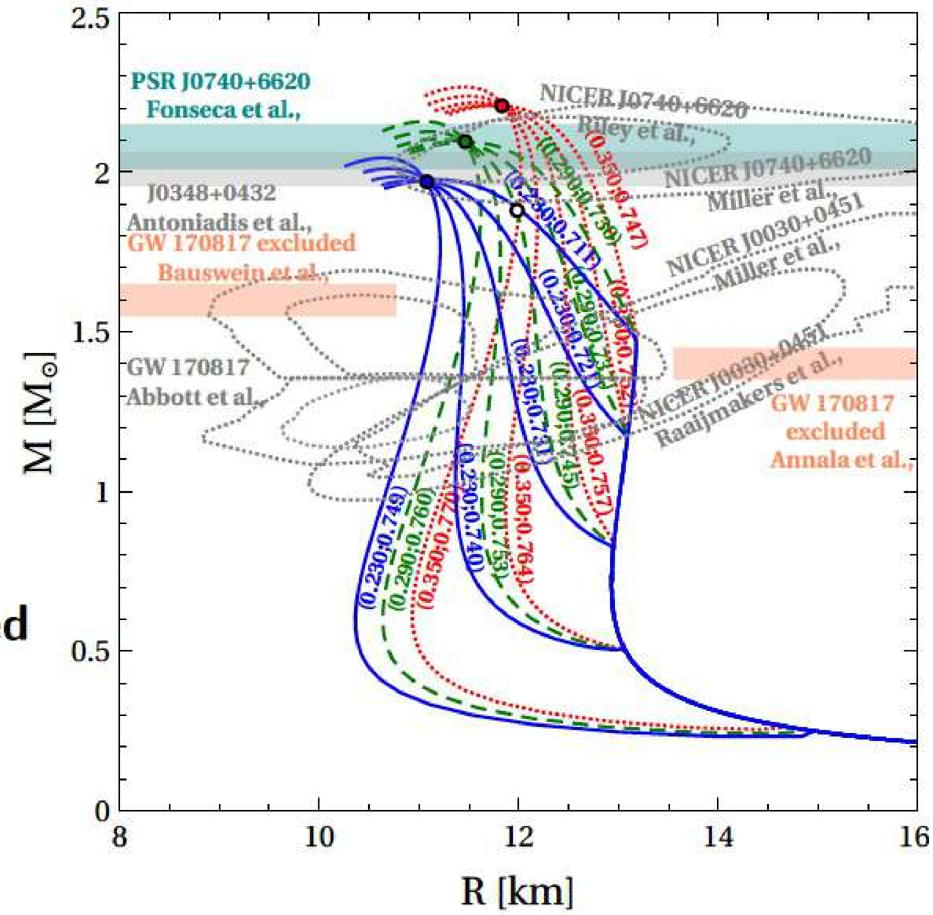

Is it possible to constrain η_V and η_D?

Relativistic density functional for quark matter

SP in M-R diagram for hybrid neutron stars

- **Onset mass**

  M_{onset} is controlled by η_V, η_D

- **Maximum mass**

  $$M_{max} = M_{SP} + \delta \, |M^*_{onset} - M_{onset}|^2$$

  δ depends on η_V and η_D

  $M^*_{onset} = 1.245 \; M_\odot$ - universal

C. Gärtlein et al., 2301.10765 [nucl-th]

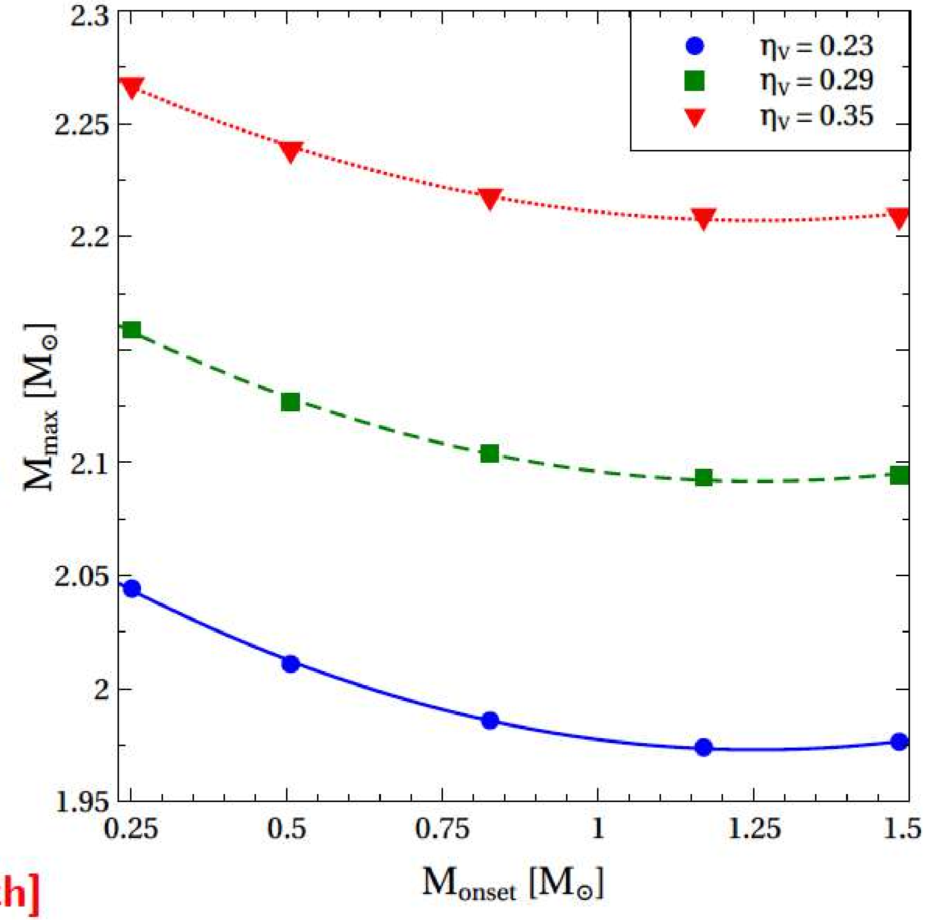

Relativistic density functional for quark matter

SP in M-R diagram for hybrid neutron stars

- No vacuum color-superconductivity

$$\eta_D < 0.78$$

O. Ivanytskyi, D. Blaschke, PRD (2022)

- $M_{max} = 2.08^{+0.07}_{-0.07} M_\odot$

E. Fonseca et al., Astrophys. J. Lett. 915, L12 (2021)

- Not too early deconfinement

$$n_{onset} > n_{saturation}$$

- Stability of the quark branch

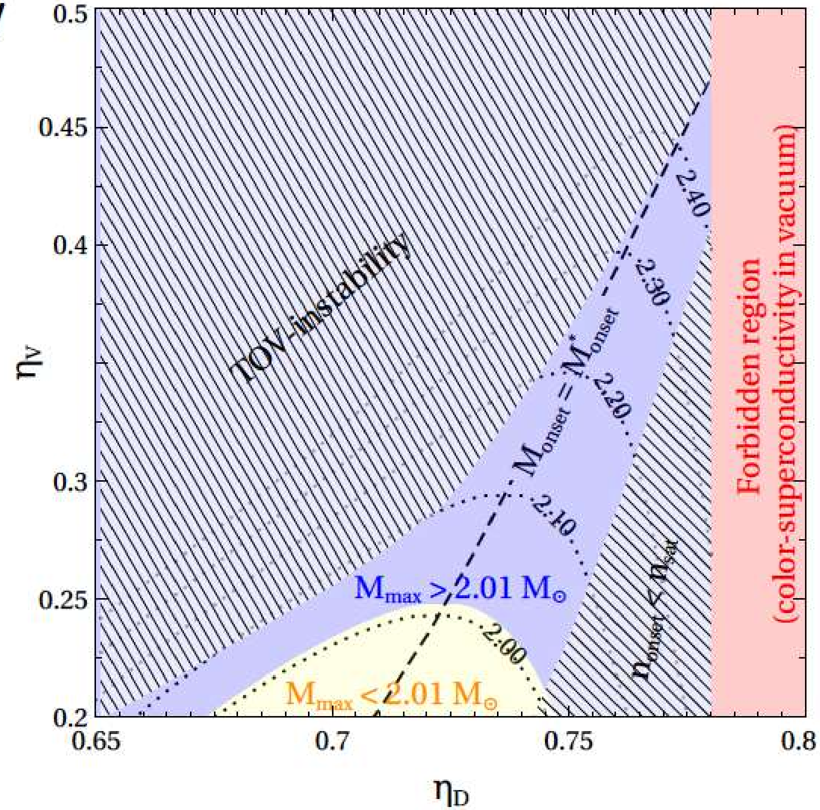

$$M_\omega = 783\ \mathrm{MeV} \Rightarrow \eta_V = 0.452$$

Are the couplings constrained to the small region suggesting $M_{onset} < 0.5 M_\odot$ and $M_{max} > 2.4 M_\odot$?

Relativistic density functional for quark matter

Mass-radius diagram for hybrid neutron stars

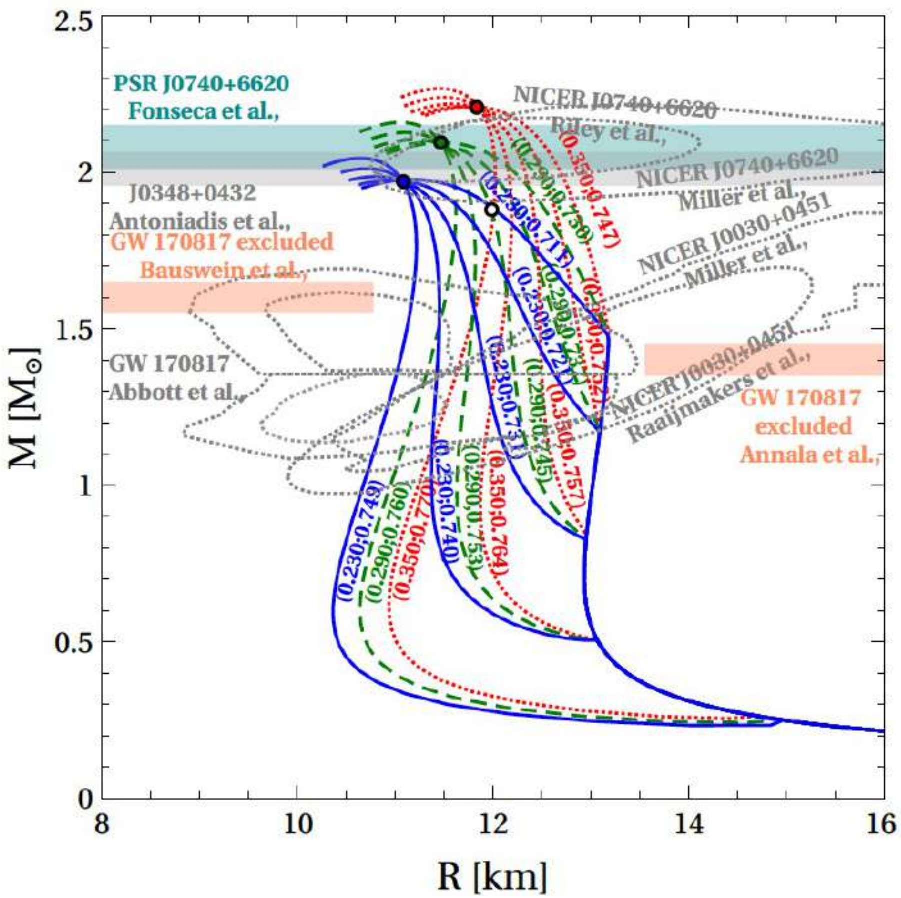

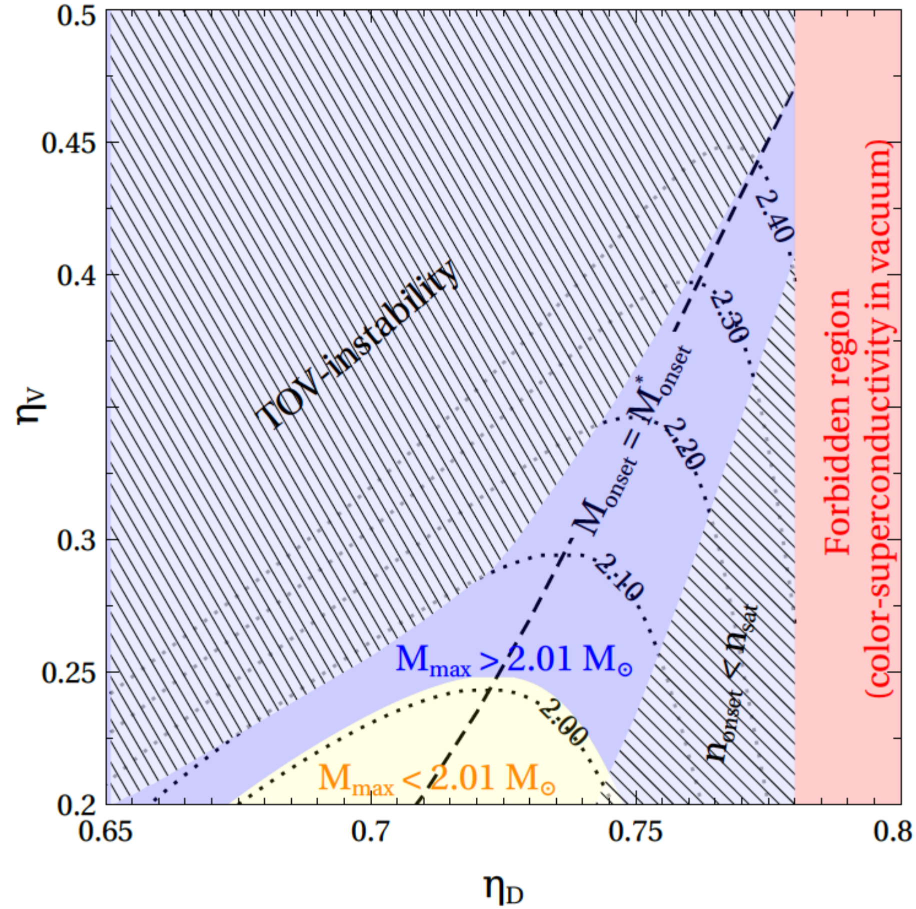

$$M_{max} = M_{SP} + \delta\,|M^*_{onset} - M_{onset}|^{\kappa}$$

$$M_{SP} = k_{M_{SP}}\eta_V + b_{M_{SP}}\ ; \quad \delta = k_\delta \eta_V + b_\delta\ ; \quad M^*_{onset} = 1.254\ M_\odot$$

C. Gärtlein et al., arXiv:2301.10765v2 ; For more details, see talk by **Christoph Gärtlein**

Relativistic density functional for quark matter

Mass-radius diagram for hybrid neutron stars

Compare to:
G. Baym, S. Furusawa, T. Hatsuda, T. Kojo, H. Togashi, ApJ 885, 42 (2019)

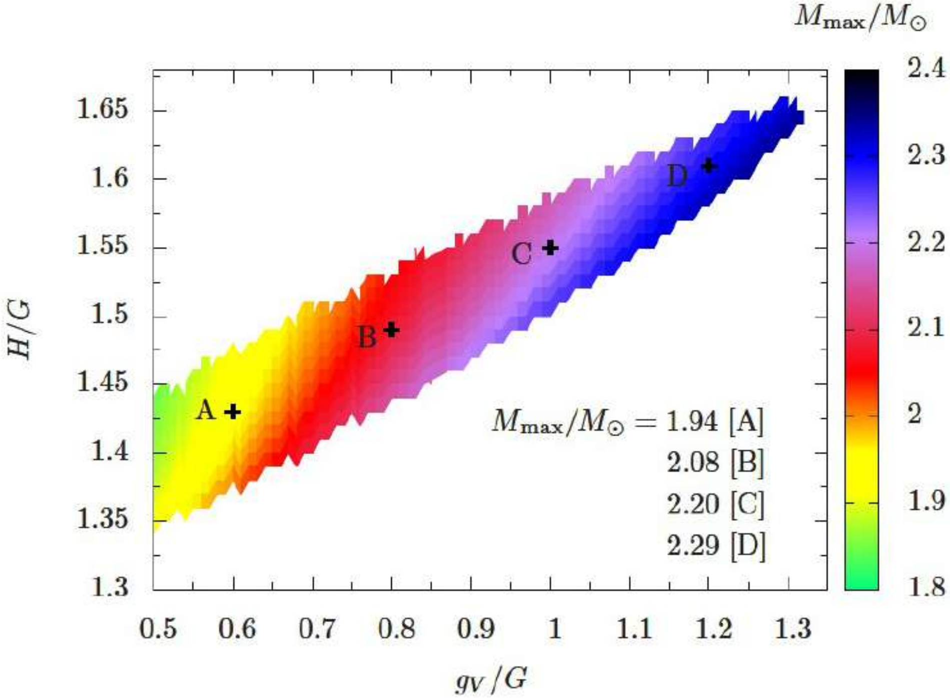

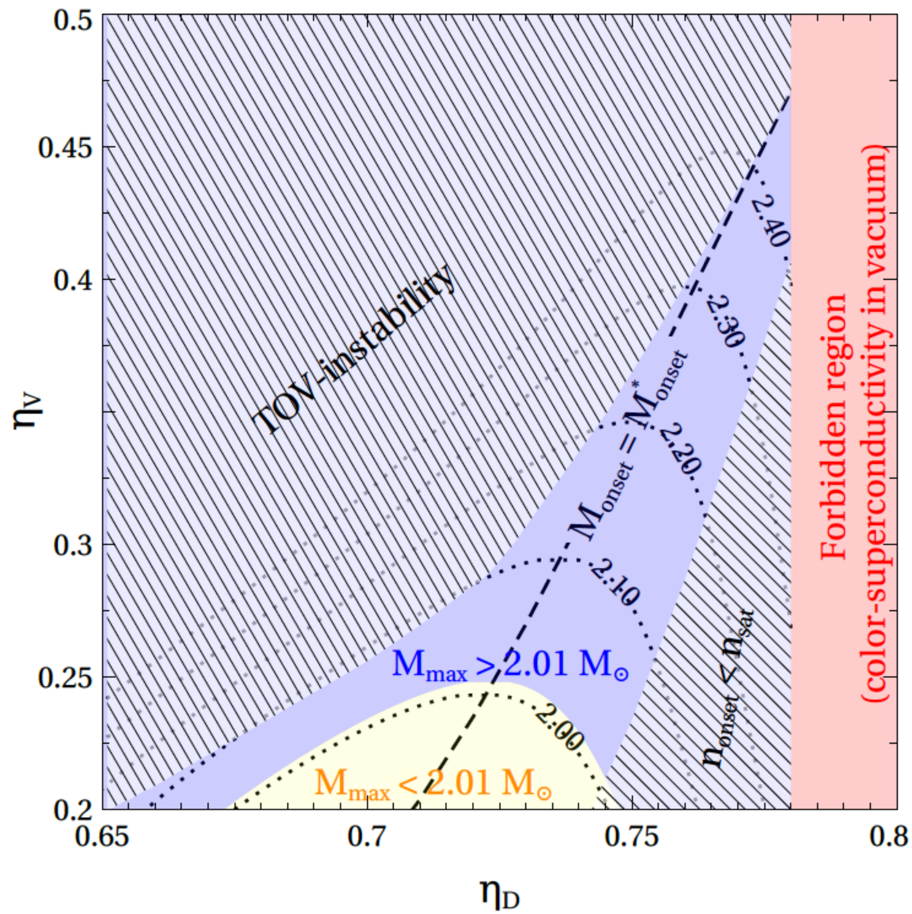

$$M_{max} = M_{SP} + \delta\,|M^*_{onset} - M_{onset}|^\kappa$$

$$M_{SP} = k_{M_{SP}}\eta_V + b_{M_{SP}}\,;\quad \delta = k_\delta \eta_V + b_\delta\,;\quad M^*_{onset} = 1.254\ M_\odot$$

C. Gärtlein et al., arXiv:2301.10765v2 ; For more details, see talk by **Christoph Gärtlein**

Relativistic density functional for quark matter

Phase diagram with two-zone interpolation

- **Normal quark matter**

  2 spin × 2 flavor × 3 color =12

- **2SC quark matter**

  2 spin × 2 flavor × 1 color+1=5

Quark pairing reduces number of quark states

⇓

requires higher T along adiabat

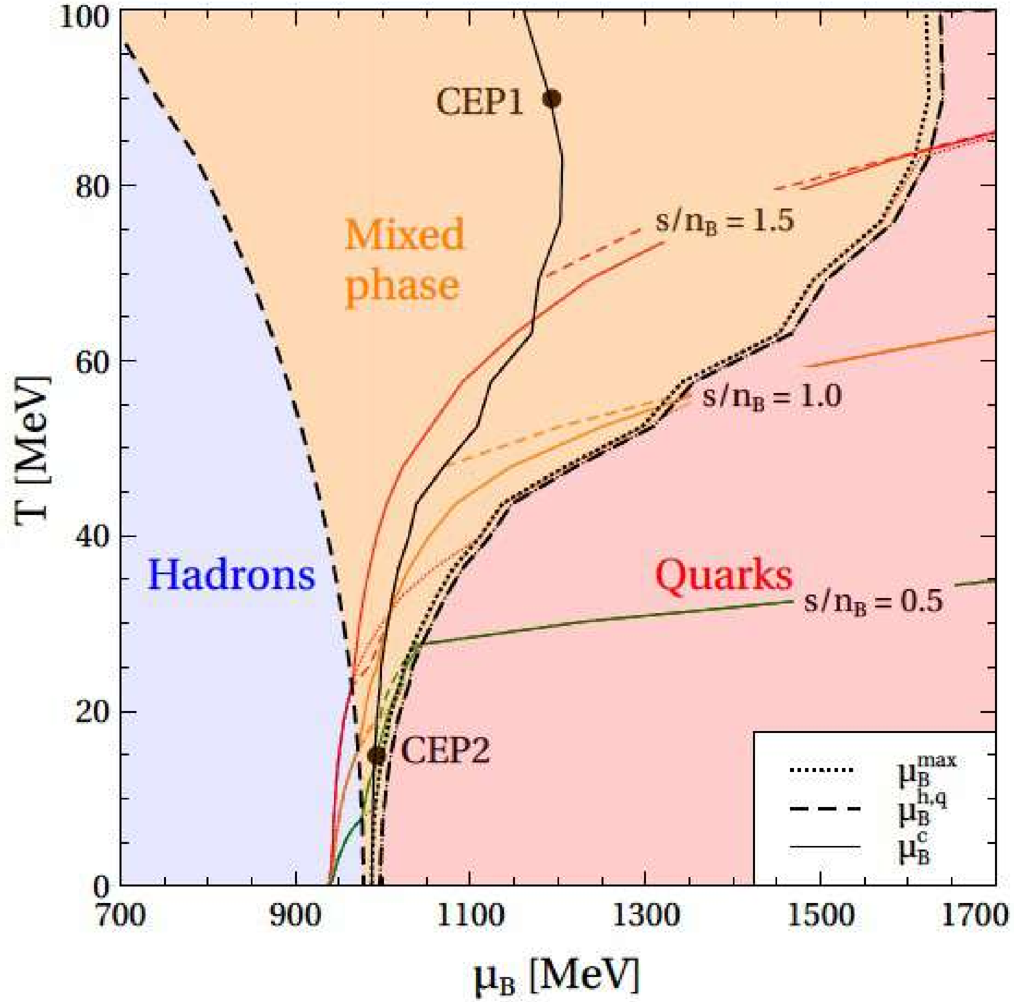

→ **EOS tables are prepared for simulation of supernovae and NS mergers**

Relativistic density functional for quark matter

Phase diagram with two-zone interpolation

- **Normal quark matter**

  2 spin × 2 flavor × 3 color =12

- **2SC quark matter**

  2 spin × 2 flavor × 1 color+1=5

Quark pairing reduces number of quark states

⇓

requires higher T along adiabat

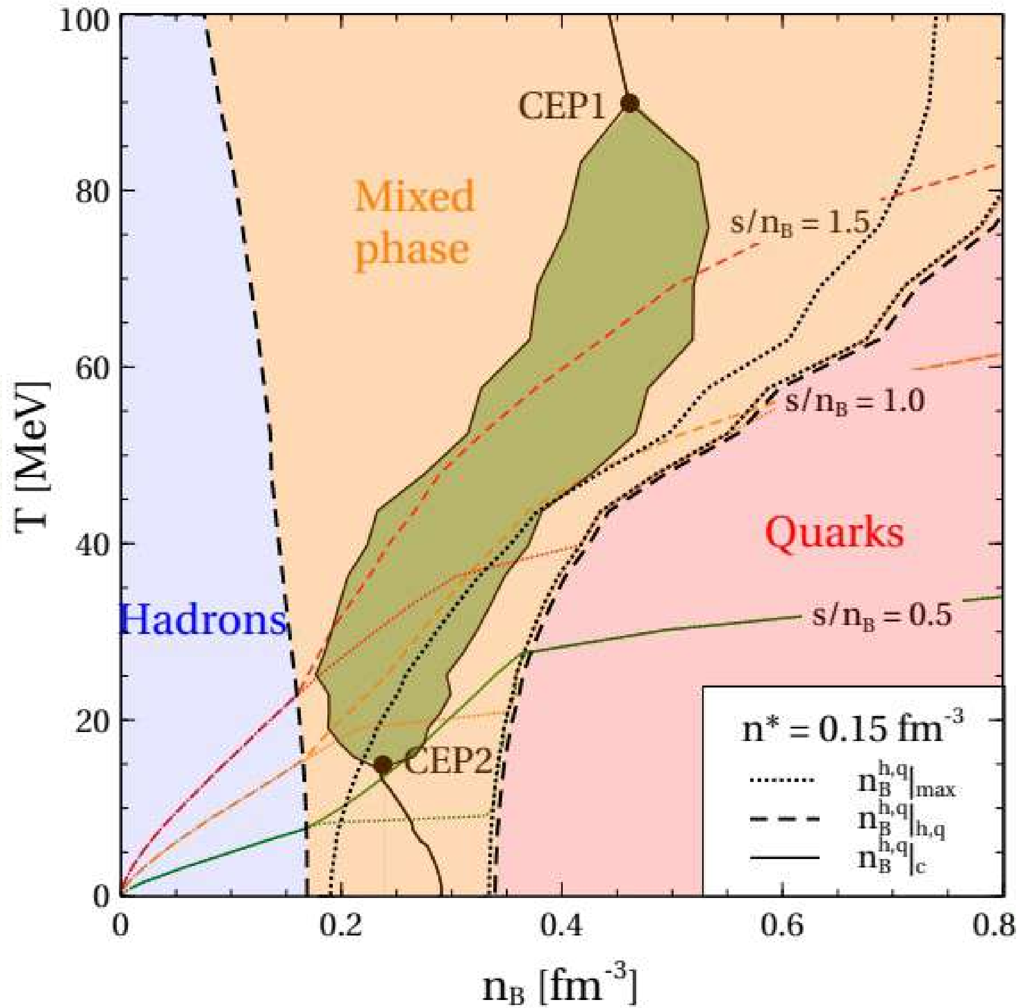

→ **EOS tables are prepared for simulation of supernovae and NS mergers**

Unified EOS for quark-hadron matter

Cluster virial expansion & Beth-Uhlenbeck EoS

Unified approach to quark-nuclear matter

Clustering aspects in the QCD phase diagram

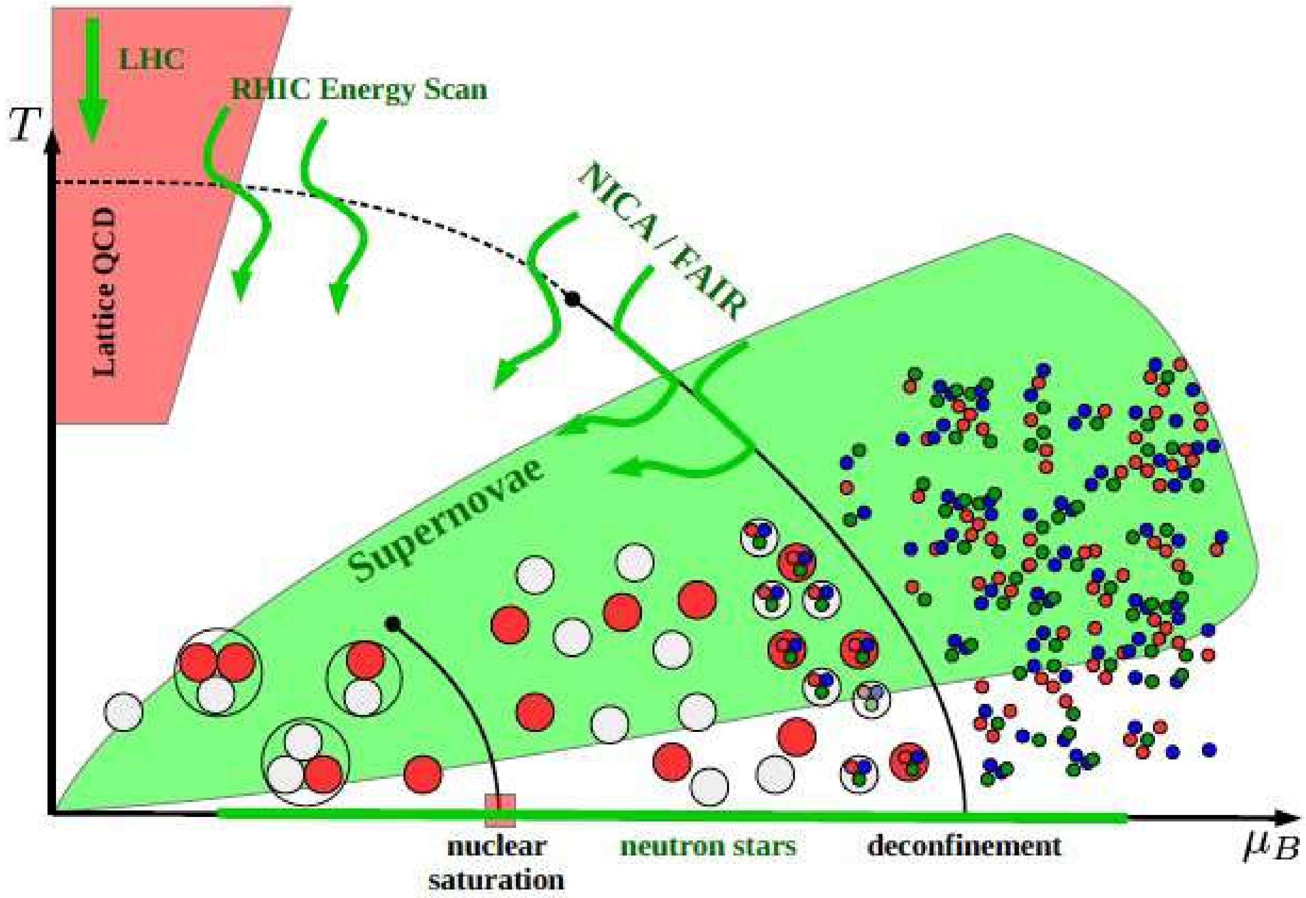

From: N.-U. Bastian, D.B., et al., Universe 4 (2018) 67; arxiv:1804.10178

Unified approach to quark-nuclear matter

Φ-derivable approach to cluster virial expansion

$$\Omega = \sum_{l=1}^{A} \Omega_l = \sum_{l=1}^{A} \left\{ c_l \left[\mathrm{Tr} \ln \left(-G_l^{-1} \right) + \mathrm{Tr} \left(\Sigma_l \; G_l \right) \right] + \sum_{\substack{i,j \\ i+j=l}} \Phi[G_i, G_j, G_{i+j}] \right\} ,$$

$$G_A^{-1} \;\; = \;\; G_A^{(0)^{-1}} - \Sigma_A \; , \; \Sigma_A(1 \ldots A, 1' \ldots A', z_A) = \frac{\delta \Phi}{\delta G_A(1 \ldots A, 1' \ldots A', z_A)}$$

Stationarity of the thermodynamical potential is implied

$$\frac{\delta \Omega}{\delta G_A(1 \ldots A, 1' \ldots A', z_A)} = 0 \; .$$

Cluster virial expansion follows for this $\Phi-$ functional

Figure: The Φ functional for $A-$particle correlations with bipartitions $A = i + j$.

Unified approach to quark-nuclear matter

Green's function and T-matrix, separable approx.

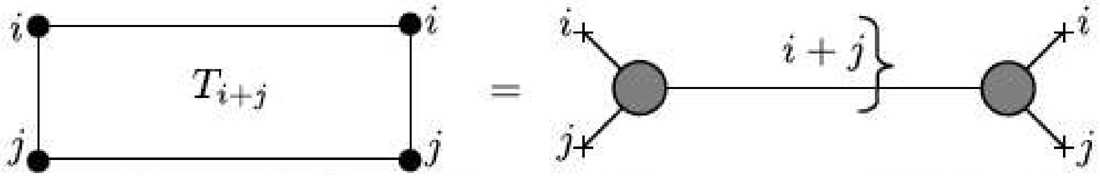

The T_A matrix fulfills the Bethe-Salpeter equation in ladder approximation

$$T_{i+j}(1,2,\ldots,A;1',2',\ldots A';z) = V_{i+j} + V_{i+j}G^{(0)}_{i+j}T_{i+j} \ ,$$

which in the separable approximation for the interaction potential,

$$V_{i+j} = \Gamma_{i+j}(1,2,\ldots,i;i+1,i+2,\ldots,i+j)\Gamma_{i+j}(1',2',\ldots,i';(i+1)',(i+2)',\ldots,(i+j)') \ ,$$

leads to the closed expression for the T_A matrix

$$T_{i+j}(1,2,\ldots,i+j;1',2',\ldots(i+j)';z) = V_{i+j}\left\{1-\Pi_{i+j}\right\}^{-1} \ ,$$

with the generalized polarization function

$$\Pi_{i+j} = \mathrm{Tr}\left\{\Gamma_{i+j}G^{(0)}_i\Gamma_{i+j}G^{(0)}_j\right\}$$

The one-frequency free $i-$particle Green's function is defined by the $(i-1)$-fold Matsubara sum

$$\begin{aligned} G^{(0)}_i(1,2,\ldots,i;\Omega_i) &= \sum\nolimits_{\omega_1\ldots\omega_{i-1}} \frac{1}{\omega_1-E(1)}\frac{1}{\omega_2-E(2)}\cdots\frac{1}{\Omega_i-(\omega_1+\ldots\omega_{i-1})-E(i)} \\ &= \frac{(1-f_1)(1-f_2)\ldots(1-f_i)-(-)^i f_1 f_2\ldots f_i}{\Omega_i-E(1)-E(2)-\ldots E(i)} \ . \end{aligned}$$

Unified approach to quark-nuclear matter

Useful relationships for many-particle functions

$$G^{(0)}_{i+j} = G^{(0)}_{i+j}(1,2,\ldots,i+j;\Omega_{i+j}) \quad = \quad \sum_{\Omega_i} G^{(0)}_i(1,2,\ldots,i;\Omega_i) G^{(0)}_j(i+1,i+2,\ldots,i+j;\Omega_j) \; .$$

Another set of useful relationships follows from the fact that in the ladder approximation both, the full two-cluster ($i+j$ particle) T matrix and the corresponding Greens' function

$$G_{i+j} = G^{(0)}_{i+j}\left\{1 - \Pi_{i+j}\right\}^{-1} \qquad (1)$$

have similar analytic properties determined by the $i+j$ cluster polarization loop integral and are related by the identity

$$T_{i+j} G^{(0)}_{i+j} = V_{i+j} G_{i+j} \; . \qquad (2)$$

which is straightforwardly proven by multiplying Equation for the $T_{i+j}-$ matrix with $G^{(0)}_{i+j}$ and using Equation (1). Since these two equivalent expressions in Equation (2) are at the same time equivalent to the two-cluster irreducible Φ functional these functional relations follow

$$T_{i+j} = \delta\Phi/\delta G^{(0)}_{i+j} \; ,$$
$$V_{i+j} = \delta\Phi/\delta G_{i+j} \; .$$

Unified approach to quark-nuclear matter

Generalized Beth-Uhlenbeck EOS from Φ-deriv.

Consider the partial density of the $A-$particle state defined as

$$n_A(T,\mu) = -\frac{\partial\Omega_A}{\partial\mu} = -\frac{\partial}{\partial\mu} d_A \int \frac{d^3q}{(2\pi)^3}\int\frac{d\omega}{2\pi}\left[\ln\left(-G_A^{-1}\right) + \mathrm{Tr}\left(\Sigma_A\ G_A\right)\right] + \sum_{\substack{i,j\\ i+j=A}} \Phi[G_i, G_j, G_{i+j}] \ .$$

Using spectral representation for $F(\omega)$ and Matsubara summation

$$F(iz_n) = \int_{-\infty}^{\infty}\frac{d\omega}{2\pi}\frac{\mathrm{Im}F(\omega)}{\omega - iz_n}\ , \quad \sum_{z_n}\frac{c_A}{\omega - iz_n} = f_A(\omega) = \frac{1}{\exp[(\omega-\mu)/T] - (-1)^A}$$

with the relation $\partial f_A(\omega)/\partial\mu = -\partial f_A(\omega)/\partial\omega$ we get for Equation (3) now

$$n_A(T,\mu) = -d_A \int \frac{d^3q}{(2\pi)^3}\int \frac{d\omega}{2\pi} f_A(\omega)\frac{\partial}{\partial\omega}\left[\mathrm{Im}\ln\left(-G_A^{-1}\right) + \mathrm{Im}\left(\Sigma_A\ G_A\right)\right] + \sum_{\substack{i,j\\ i+j=A}}\frac{\partial\Phi[G_i,G_j,G_A]}{\partial\mu}\ ,$$

where a partial integration over ω has been performed For two-loop diagrams of the sunset type holds a cancellation[3] which generalize here for cluster states

$$d_A\int\frac{d^3q}{(2\pi)^3}\int\frac{d\omega}{2\pi}f_A(\omega)\frac{\partial}{\partial\omega}\left(\mathrm{Re}\Sigma_A\ \mathrm{Im}G_A\right) - \sum_{\substack{i,j\\ i+j=A}}\frac{\partial\Phi[G_i,G_j,G_A]}{\partial\mu} = 0\ .$$

Using generalized optical theorems we can show that ($G_A = |G_A|\exp(i\delta_A)$)

$$\frac{\partial}{\partial\omega}\left[\mathrm{Im}\ln\left(-G_A^{-1}\right) + \mathrm{Im}\Sigma_A\ \mathrm{Re}G_A\right] = 2\mathrm{Im}\left[G_A\ \mathrm{Im}\Sigma_A\ \frac{\partial}{\partial\omega}G_A^*\ \mathrm{Im}\Sigma_A\right] = -2\sin^2\delta_A\frac{\partial\delta_A}{\partial\omega}\ .$$

The density in the form of a generalized Beth-Uhlenbeck EoS follows

$$n(T,\mu) = \sum_{i=1}^{A} n_i(T,\mu) = \sum_{i=1}^{A} d_i\int\frac{d^3q}{(2\pi)^3}\int\frac{d\omega}{2\pi}f_i(\omega)2\sin^2\delta_i\frac{\partial\delta_i}{\partial\omega}\ .$$

[3] B. Vanderheyden & G. Baym, J. Stat. Phys. (1998), J.-P. Blaizot et al., PRD (2001)

Unified approach to quark-nuclear matter

Example: deuterons in nuclear matter

The $\Phi-$derivable thermodynamical potential for the nucleon-deuteron system reads

$$\Omega = -\mathrm{Tr}\,\{\ln(-G_1)\} - \mathrm{Tr}\{\Sigma_1 G_1\} + \mathrm{Tr}\,\{\ln(-G_2)\} + \mathrm{Tr}\{\Sigma_2 G_2\} + \Phi[G_1, G_2]\ ,$$

where the full propagators obey the Dyson-Schwinger equations

$$G_1^{-1}(1,z) = z - E_1(p_1) - \Sigma_1(1,z);\ \ G_2^{-1}(12,1'2',z) = z - E_1(p_1) - E_2(p_2) - \Sigma_2(12,1'2',z),$$

with selfenergies and Φ functional

$$\Sigma_1(1,1') \ = \ \frac{\delta\Phi}{\delta G_1(1,1')}\ ;\ \ \Sigma_2(12,1'2',z) = \frac{\delta\Phi}{\delta G_2(12,1'2',z)}\ , \Phi =$$

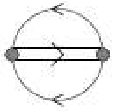

,

fulfilling stationarity of the thermodynamic potential $\partial\Omega/\partial G_1 = \partial\Omega/\partial G_2 = 0$.
For the density we obtain the cluster virial expansion

$$n = -\frac{1}{V}\frac{\partial\Omega}{\partial\mu} = n_{\rm qu}(\mu, T) + 2n_{\rm corr}(\mu, T)\ ,$$

with the correlation density in the generalized Beth-Uhlenbeck form

$$n_{\rm corr} = \int \frac{dE}{2\pi} g(E) 2\sin^2\delta(E)\frac{d\delta(E)}{dE}\ .$$

Unified approach to quark-nuclear matter

Cluster virial expansion for quark-hadron matter

$$\Omega = \sum_{i=Q,M,D,B} c_i \left[\mathrm{Tr}\ln\left(-G_i^{-1}\right) + \mathrm{Tr}\left(\Sigma_i\, G_i\right)\right] + \Phi\left[G_Q, G_M, G_D, G_B\right] ,$$

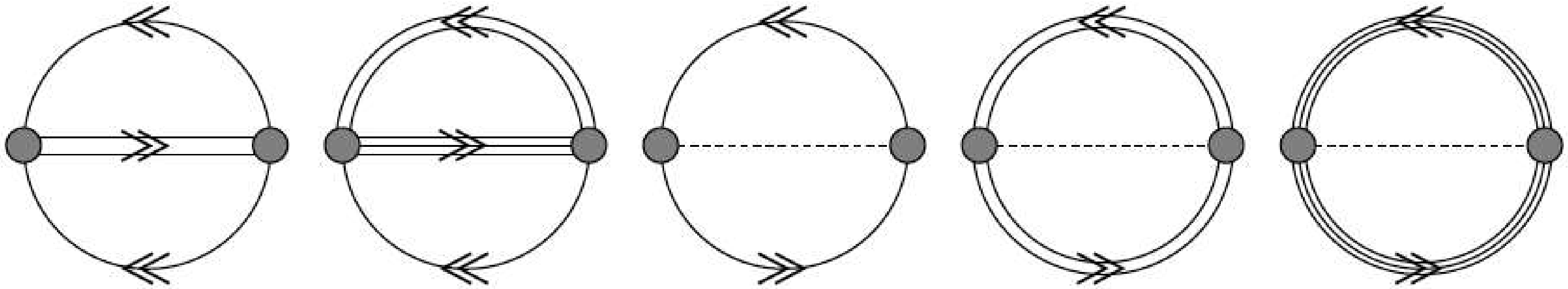

When Φ functional for the system is given by 2-loop diagrams holds

$$n = -\frac{\partial\Omega}{\partial\mu} = \sum_a a\, n_a(T,\mu)$$

$$= \sum_a a\, d_a \int \frac{d\omega}{\pi} \int \frac{d^3q}{(2\pi)^3} \left\{ f_\phi^{(a),+} - \left[f_\phi^{(a),-}\right]^* \right\} 2\sin^2\delta_a(\omega,q) \frac{\partial\delta_a(\omega,q)}{\partial\omega} ,$$

Analogous for the entropy density $s = -\partial\Omega/\partial T$.

Unified approach to quark-nuclear matter

Cluster virial expansion for quark-hadron matter

The cluster decomposition of the thermodynamic potential is given as

$$\Omega_{\rm total}(T,\mu,\phi,\bar\phi) = \Omega_{PNJL}(T,\mu,\phi,\bar\phi) + \Omega_{\rm pert}(T,\mu,\phi,\bar\phi) + \Omega_{MHRG}(T,\mu,\phi,\bar\phi),$$

where the first two terms describe the quark and gluon degrees of freedom via the mean–field thermodynamic potential for quark matter in a gluon background field $\mathcal{U}$

$$\Omega_{PNJL}(T,\mu,\phi,\bar\phi) = \Omega_Q(T,\mu,\phi,\bar\phi) + \mathcal{U}(T,\phi,\bar\phi)$$

with a perturbative correction $\Omega_{\rm pert}(T,\mu,\phi,\bar\phi)$.
The Mott-Hadron-Resonance-Gas (MHRG) part for the multi-quark clusters is

$$\Omega_{MHRG}(T,\mu,\phi,\bar\phi) = \sum_{i=M,B,\ldots} \Omega_i(T,\mu,\phi,\bar\phi),$$

where the multi–quark states are described by the GBU formula:

$$\begin{aligned} n &= -\frac{\partial\Omega}{\partial\mu} = \sum_a a\, n_a(T,\mu) \\ &= \sum_a a\, d_a \int \frac{d\omega}{\pi} \int \frac{d^3q}{(2\pi)^3} \left\{ f_\phi^{(a),+} - \left[f_\phi^{(a),-} \right]^* \right\} 2\sin^2\delta_a(\omega,q) \frac{\partial\delta_a(\omega,q)}{\partial\omega} , \end{aligned}$$

where d_i is the degeneracy factor, a is the number of valence quarks in the cluster an $f_\phi^{(a),+}$, $\left[f_\phi^{(a),-}\right]^*$ are the Polyakov-loop modified distribution functions.
Analogous for the entropy density $s = -\partial\Omega/\partial T$.

Unified approach to quark-nuclear matter

Polyakov-loop modified distribution functions

For multiquark clusters with net number a of valence quarks holds

$$f_\phi^{(a),\pm} \stackrel{(a\ \mathrm{even})}{=} \frac{(\phi - 2\bar{\phi} y_a^\pm) y_a^\pm + y_a^{\pm 3}}{1 - 3(\phi - \bar{\phi} y_a^\pm) y_a^\pm - y_a^{\pm 3}} ,$$

$$f_\phi^{(a),\pm} \stackrel{(a\ \mathrm{odd})}{=} \frac{(\bar{\phi} + 2\phi y_a^\pm) y_a^\pm + y_a^{\pm 3}}{1 + 3(\bar{\phi} + \phi y_a^\pm) y_a^\pm + y_a^{\pm 3}} ,$$

where $y_a^\pm = e^{-(E_p \mp a\mu)/T}$ and $E_p = \sqrt{\vec{p}^2 + M^2}$.
It is instructive to consider the two limits $\phi = \bar{\phi} = 1$ (deconfinement)

$$f_{\phi=1}^{(a=0,2,4,\dots),\pm} = \frac{y_a^\pm}{1 - y_a^\pm} , \quad f_{\phi=1}^{(a=1,3,5,\dots),\pm} = \frac{y_a^\pm}{1 + y_a^\pm} ,$$

and $\phi = \bar{\phi} = 0$ (confinement),

$$f_{\phi=0}^{(a=0,2,4,\dots),\pm} = \frac{y_a^{\pm 3}}{1 - y_a^{\pm 3}} , \quad f_{\phi=0}^{(a=1,3,5,\dots),\pm} = \frac{y_a^{\pm 3}}{1 + y_a^{\pm 3}} .$$

Unified approach to quark-hadron matter

Inputs: mass spectrum & phase shifts (models)

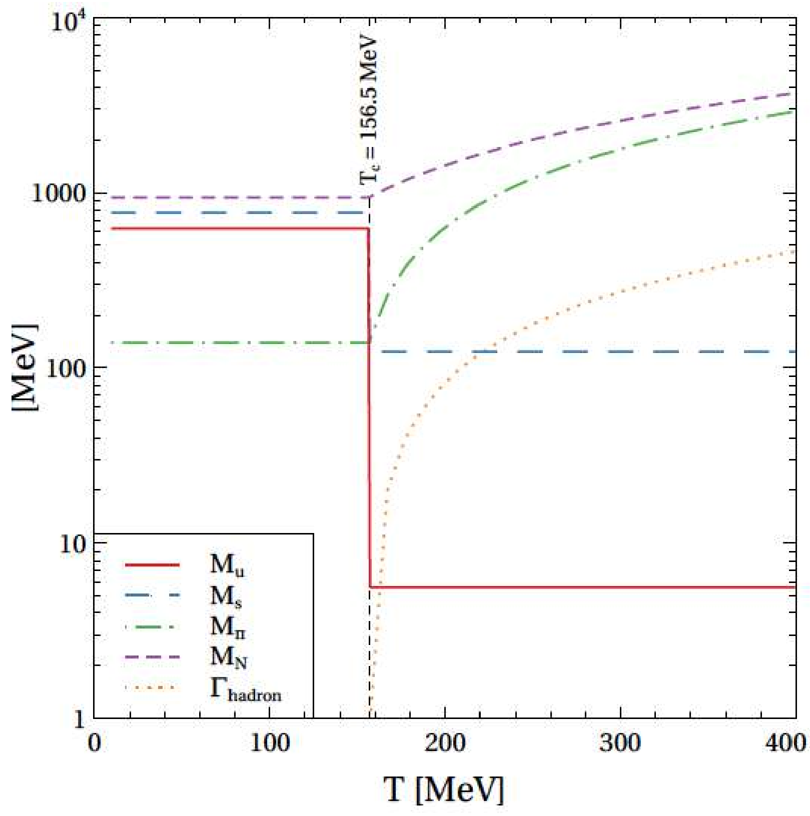

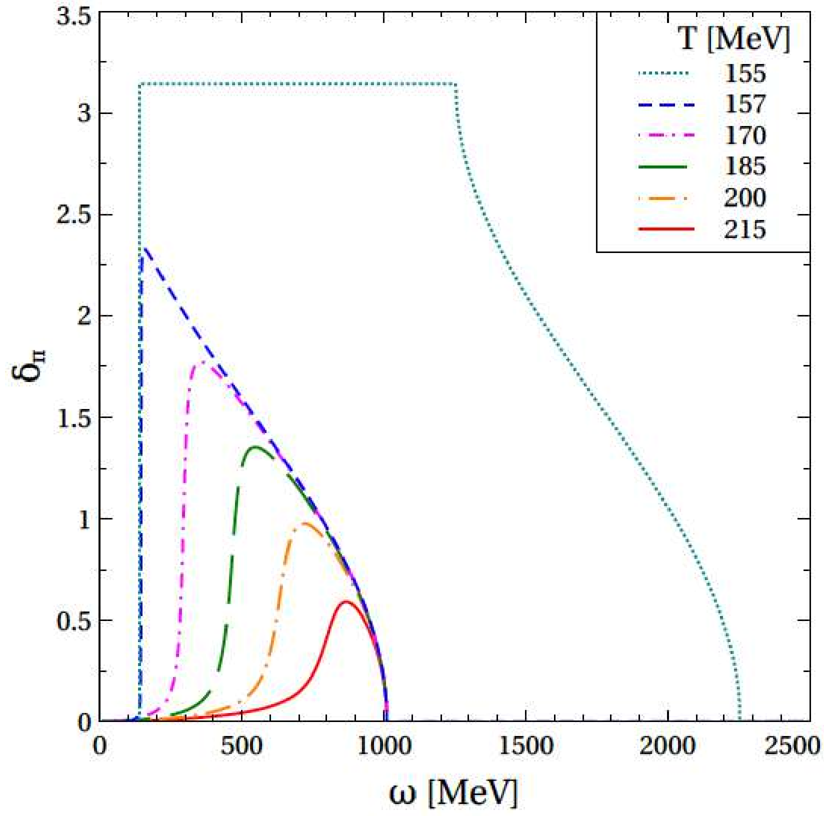

D.B., M. Ciernak, O. Ivanytskyi and G. Röpke, arXiv:2308.07950

Unified approach to quark-hadron matter

CASUS
CENTER FOR ADVANCED SYSTEMS UNDERSTANDING

Inputs: mass spectrum & phase shifts (models)

Mesons:

PDG mesons	d_i	M_{PDG} [MeV]	M_i [MeV]	$M^{<}_{th,i}$ [MeV]	$M^{>}_{th,i}$ [MeV]
π^+/π^0	3	140	140	1254	11.2
K^+/K^0	4	494	494	1397	129.6
η	1	548	878	1349	90.1
ρ^+/ρ^0	9	775	783	1254	11.2
ω	9	783	783	1254	11.2
K^{*+}/K^{*0}	12	895	806*)	2651	140.8
η'	1	960	878	1349	90.1
a_0	3	980	1095*)	2508	22.4
f_0	1	980	1095*)	2508	22.4
ϕ	3	1020	1069	1540	248
...					
$\pi_2(1880)$	15	1895	1095*)	2508	22.4
$f_2(1950)$	5	1944	1095*)	2508	22.4
$a_4(2040)$	27	1996	1095*)	2508	22.4
$f_2(2010)$	5	2011	1095*)	2508	22.4
$f_4(2050)$	9	2018	1095*)	2508	22.4
$K_4^*(2045)$	36	2045	1238*)	2651	140.8
$\phi(2170)$	3	2175	1381*)	2794	259.2
$f_2(2300)$	5	2297	1095*)	2508	22.4
$f_2(2340)$	5	2339	1095*)	2508	22.4

Baryons:

PDG baryons	d_i	M_{PDG} [MeV]	M_i [MeV]	$M^{<}_{th,i}$ [MeV]	$M^{>}_{th,i}$ [MeV]
n/p	4	939	939	1881	16.8
Λ	2	1116	1082	2024	135.2
Σ	6	1193	1082	2024	135.2
Δ	16	1232	1251**)	3135	28
Ξ^0	2	1315	1225	2167	253.6
Ξ^-	2	1322	1225	2167	253.6
$\Sigma(1385)$	6	1385	1394**)	3278	146.4
$\Lambda(1405)$	2	1405	1394**)	3278	146.4
$N(1440)$	4	1440	1251**)	3135	28
...					
$N(2195)$	36	2220	1251**)	3135	28
$\Sigma(2250)$	6	2250	1394**)	3278	146.4
$\Omega^-(2250)$	2	2252	1680**)	3564	383.2
$N(2250)$	20	2275	1251**)	3135	28
$\Lambda(2350)$	10	2350	1394**)	3278	146.4
$\Delta(2420)$	48	2420	1251**)	3135	28
$N(2600)$	24	2600	1251**)	3135	28

… and colored clusters !

D.B., M. Ciernak, O. Ivanytskyi and G. Röpke, arXiv:2308.07950

Unified approach to quark-hadron matter

Results for Mott-Hadron Resonance Gas (MHRG)

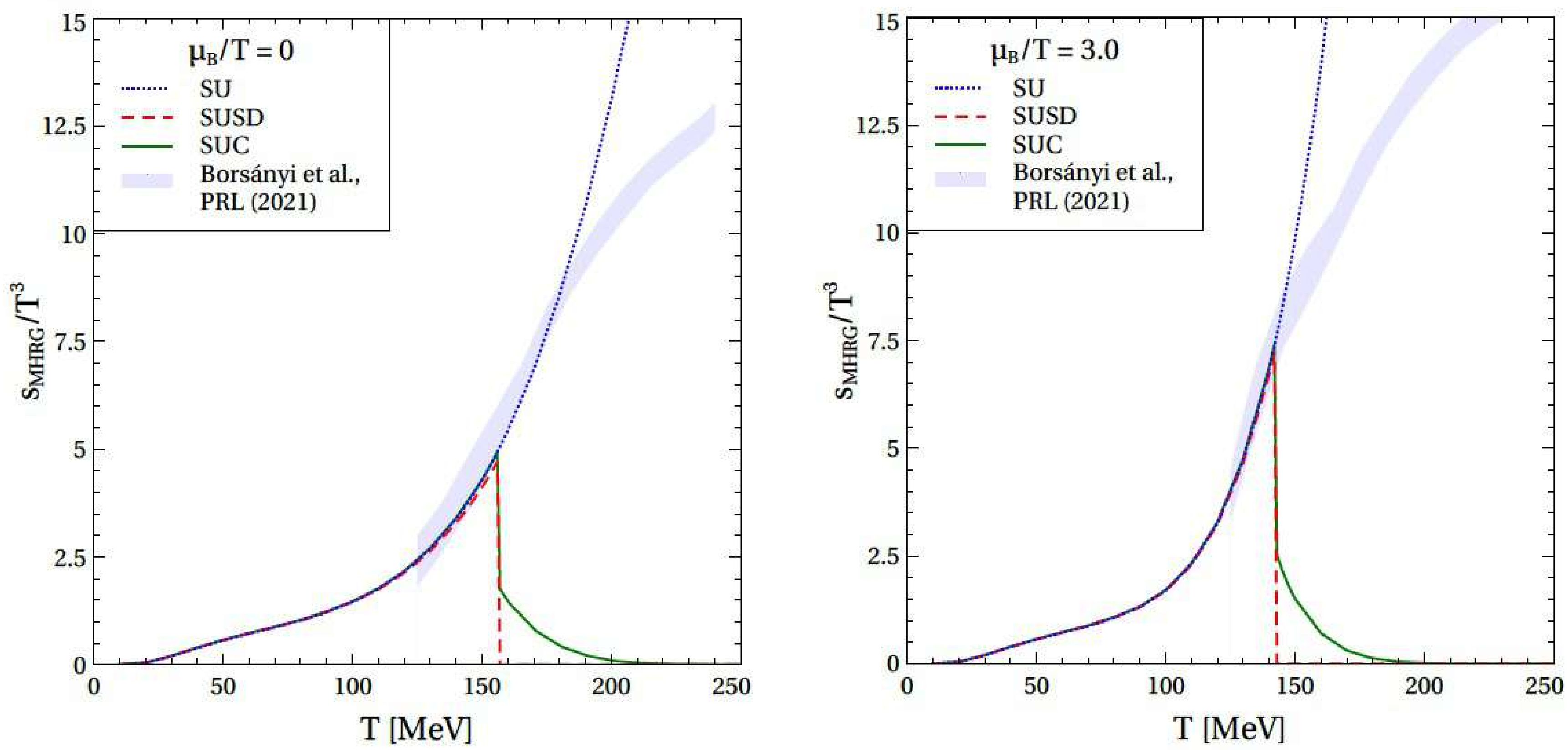

D.B., M. Ciernak, O. Ivanytskyi and G. Röpke, arXiv:2308.07950

Unified approach to quark-hadron matter

Entropy for MHRG: role of the sin^2-term

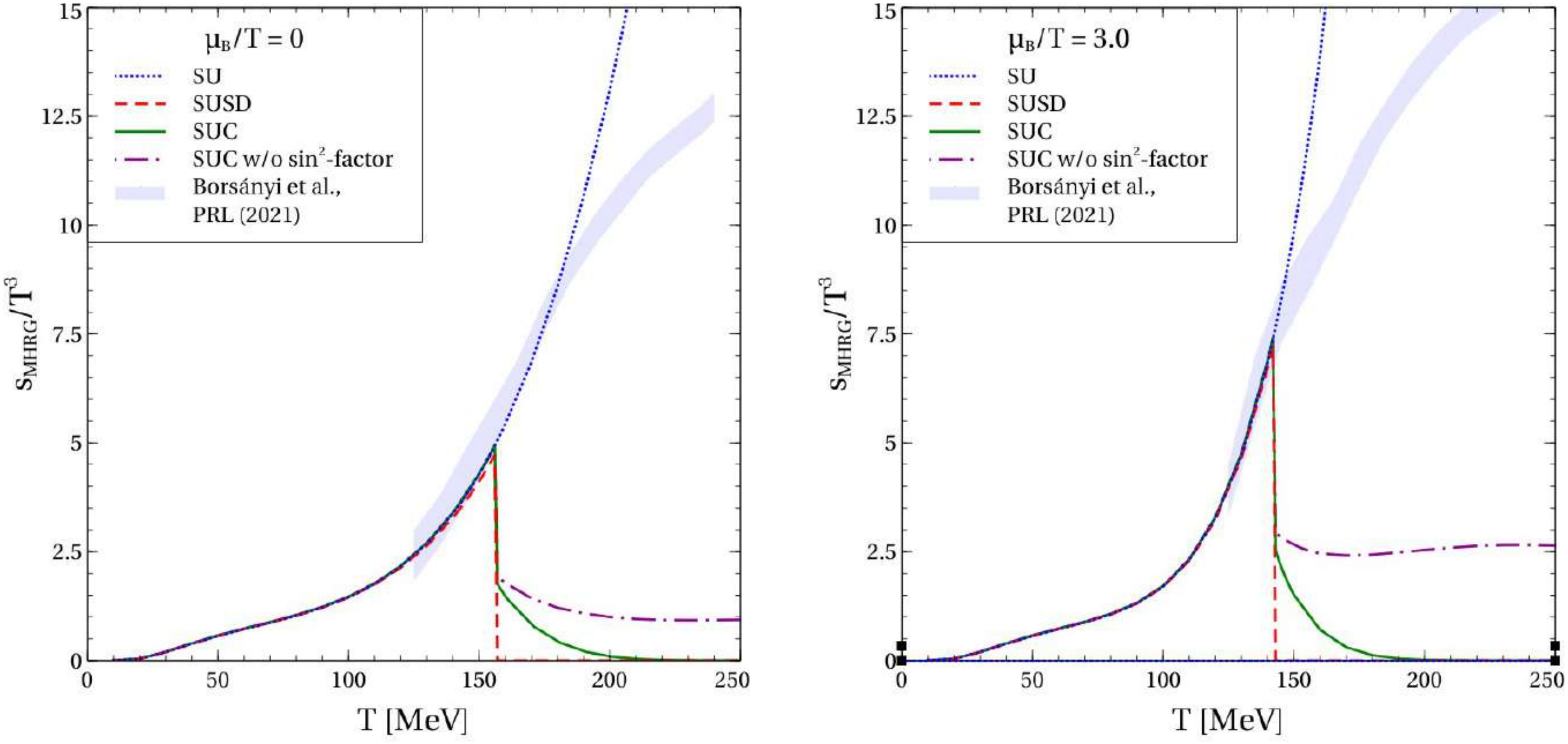

D.B., M. Ciernak, O. Ivanytskyi and G. Röpke, arXiv:2308.07950

Unified approach to quark-hadron matter

Results for the entropy density

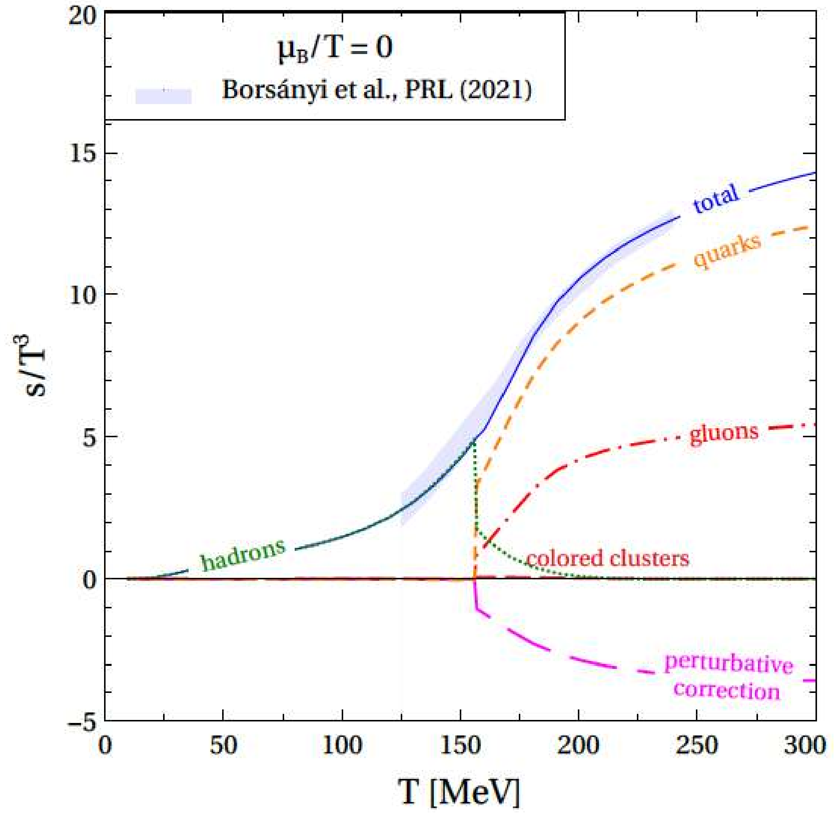

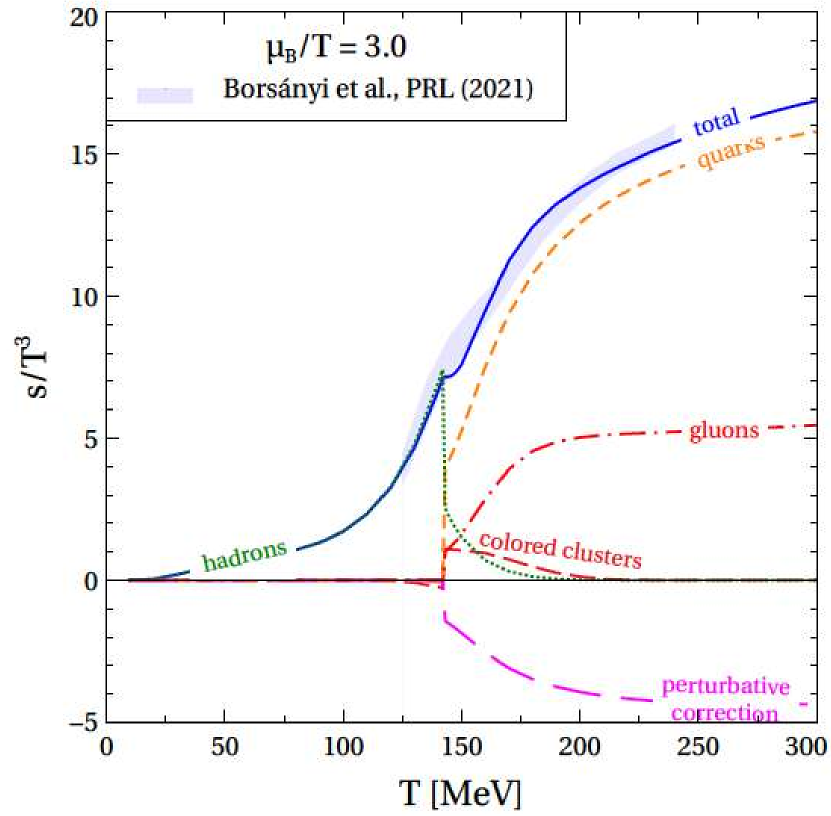

D.B., M. Ciernak, O. Ivanytskyi and G. Röpke, arXiv:2308.07950

Unified approach to quark-hadron matter

Results for the entropy density & composition

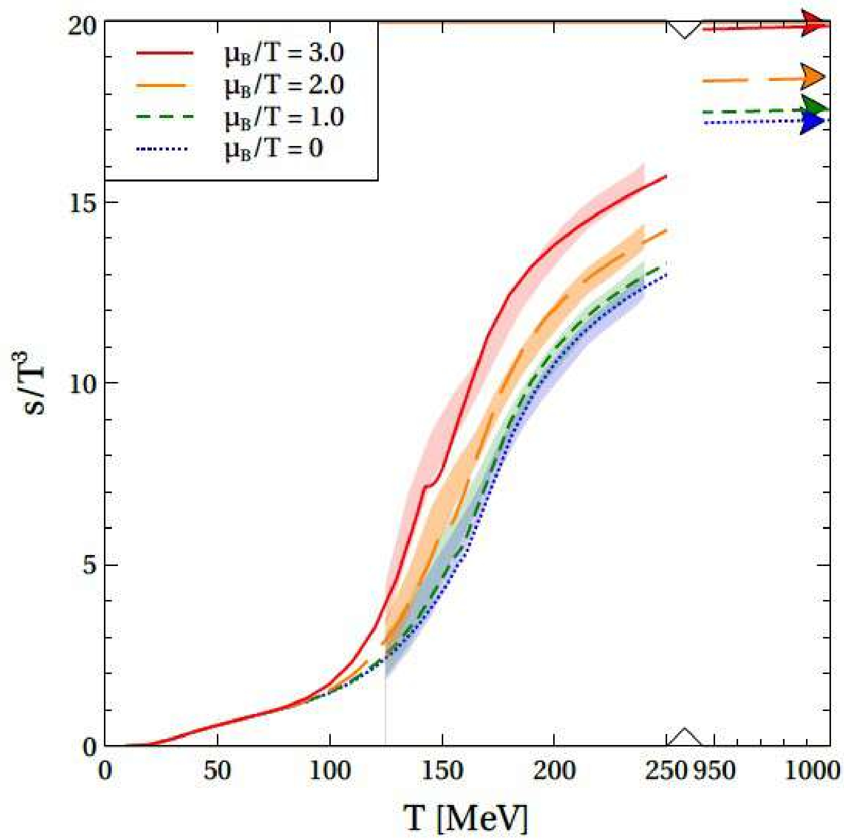

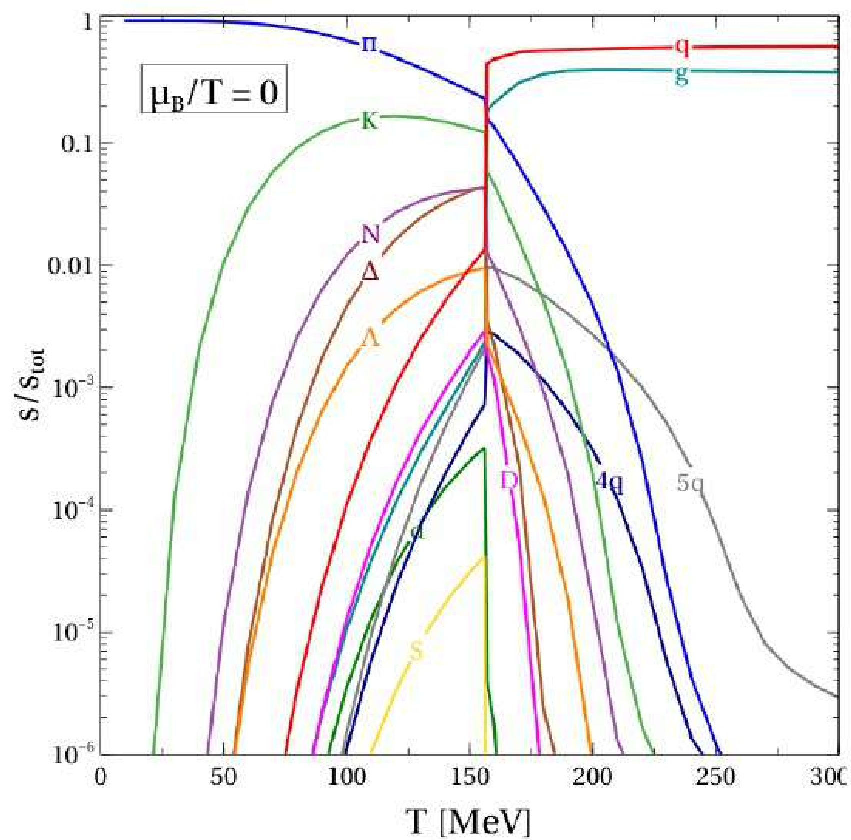

D.B., M. Ciernak, O. Ivanytskyi and G. Röpke, arXiv:2308.07950

Conclusion

Density functional methods solve obstacles in neutron star astrophysics

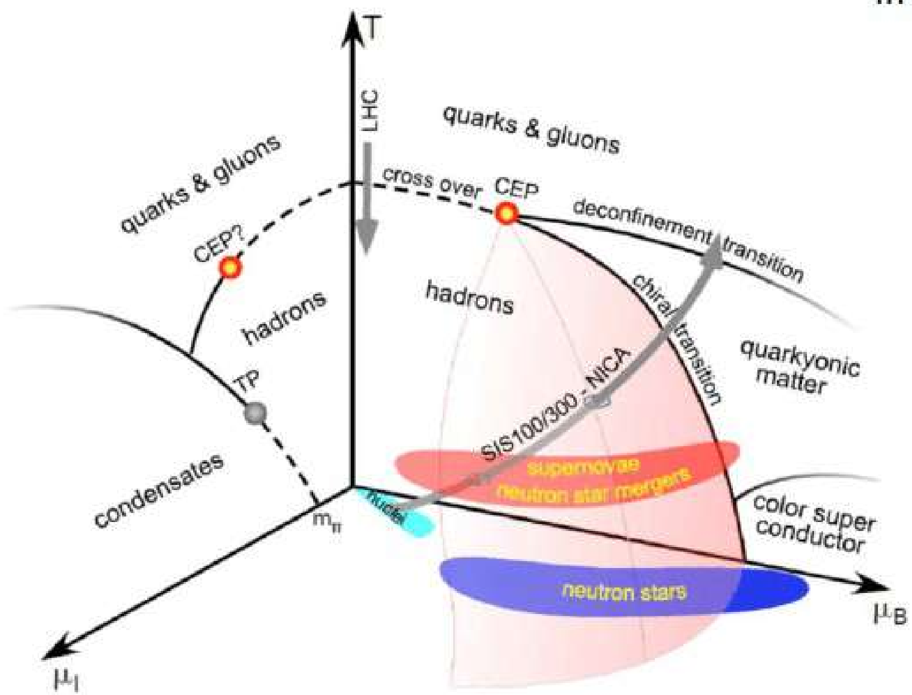

From: NuPECC Long Range Plan 2017

Prominent contributions to deconfinement in modern multimessenger Astrophysics:

- Quark deconfinement transition triggers the supernova explosion of a very massive ($M = 50M_\odot$) blue supergiant progenitor star
  T. Fischer et al., Nature Astron. 2 (2018) 960
- Unambiguous signal of a strong phase transition in the postmerger GW from a binary NS merger predicted
  A. Bauswein et al., Phys. Rev. Lett. 122 (2019) 061102
- Strong deconfinement phase transition in NS can be detected by observing the mass twin star phenomenon
  D. B. et al., Universe 6 (2020) 81

Thanks to my collaborators:

T. Fischer, G. Röpke, A. Bauswein, O. Ivanytskyi,
N. Bastian, M. Cierniak, U. Shukla, S. Liebing, K. Maslov,
A. Ayriyan,
H. Grigorian,
D.N. Voskresensky,
M. Kaltenborn,
G. Grunfeld,
D. Alvarez-Castillo,
B. Dönigus, ...

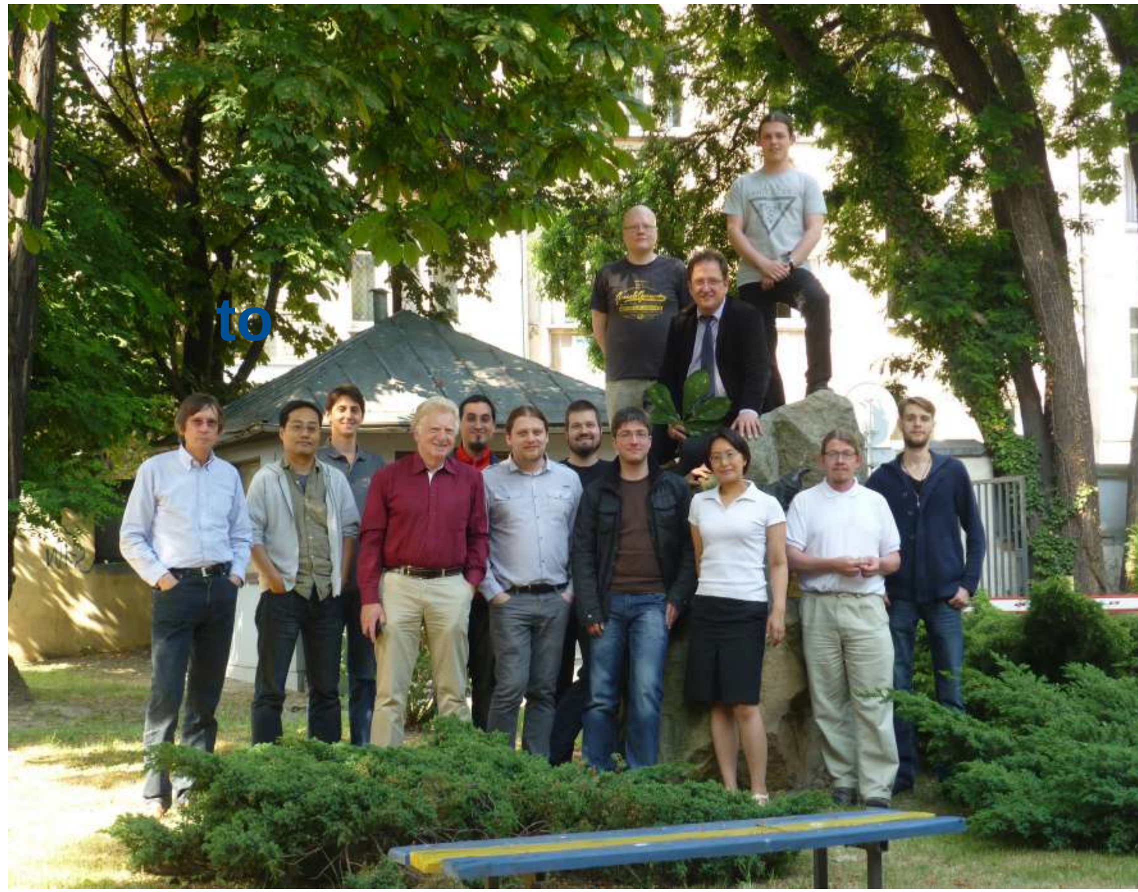

Wroclaw Group ...

WHERE IS WROCLAW IN EUROPE ?

WHERE IS WROCLAW IN EUROPE ?

WHERE IS WROCLAW IN EUROPE ?

WHERE IS WROCLAW IN EUROPE ?

WHERE IS WROCLAW IN EUROPE ?

Understanding complex systems with data

CASUS pushes the frontier of data-driven complex systems science

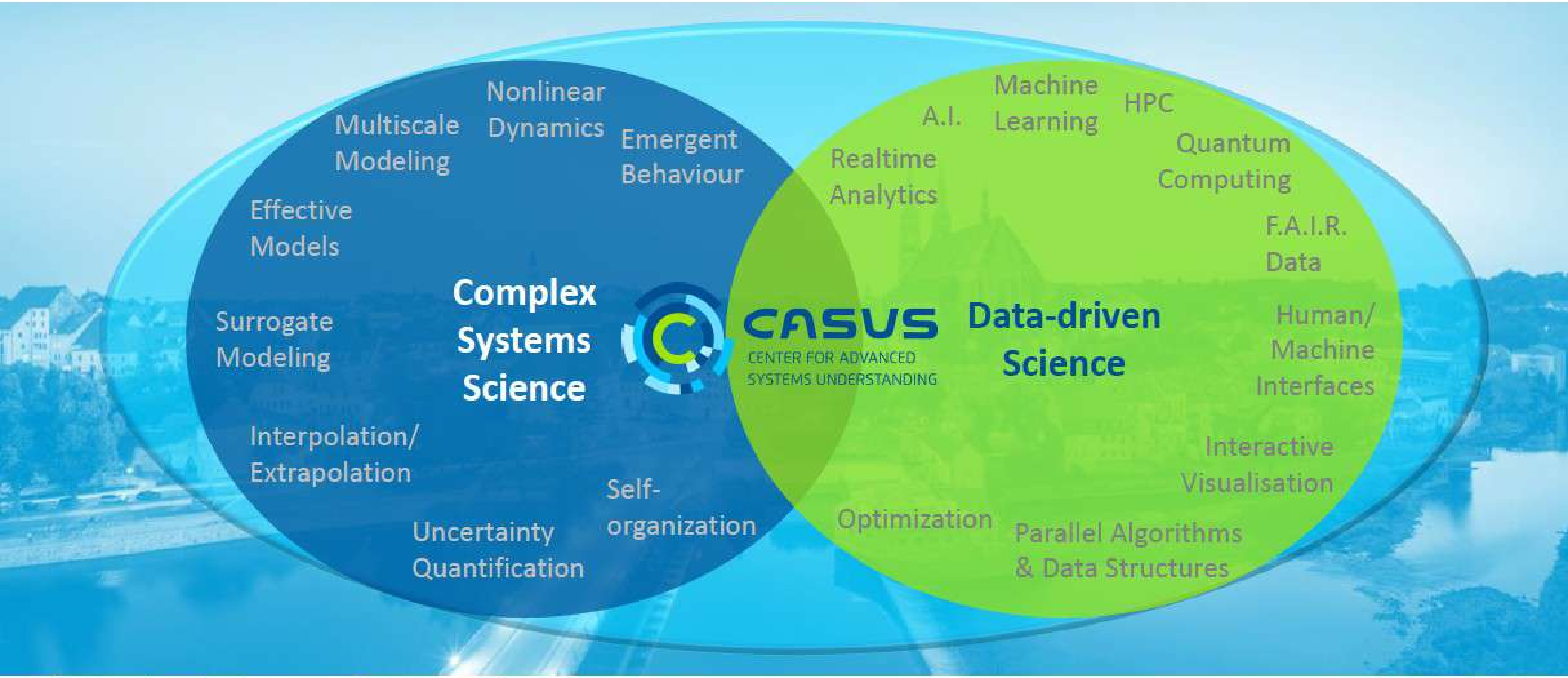

70 people, 20 countries, the brightest minds

CASUS
CENTER FOR ADVANCED SYSTEMS UNDERSTANDING

Prof. Dr. Justin Calabrese
Ecological Data Science

Smithsonian

Dr. Ricardo Martinez-Garcia
Dynamics of Complex Living Systems

PRINCETON UNIVERSITY

Dr. Attila Cangi
Matter under Extreme Conditions

Sandia National Laboratories

Dr. Michael Hecht
Mathematical Foundations of Complex System Science

MAX PLANCK INSTITUTE OF MOLECULAR CELL BIOLOGY AND GENETICS

Dr. Artur Yakimovich
Machine Learning for Infection and Disease

Roche
UCL

Dr. Weronika Schlechte-Welnicz
SCULTETUS Center

CRTD
Center for Regenerative Therapies TU Dresden

Excellence recognized

ERC Starting Grant
Dr. Tobias Dornheim

CASUS/UWr joint Professor
Prof. Dr. David Blaschke

Professor University of Arizona (Faculty)
Dr. Jesse Alston

CASUS CENTER FOR ADVANCED SYSTEMS UNDERSTANDING

COLLEGE OF AGRICULTURE & LIFE SCIENCES
Natural Resources & the Environment

Fullbright scholarship
Dr. Debanjan Konar

FULBRIGHT

CASUS

CENTER FOR ADVANCED SYSTEMS UNDERSTANDING

www.casus.science

HZDR HELMHOLTZ ZENTRUM DRESDEN ROSSENDORF

TECHNISCHE UNIVERSITÄT DRESDEN

CBG Max Planck Institute of Molecular Cell Biology and Genetics

HELMHOLTZ CENTRE FOR ENVIRONMENTAL RESEARCH – UFZ

Uniwersytet Wrocławski

SPONSORED BY THE

Federal Ministry of Education and Research

STAATSMINISTERIUM FÜR WISSENSCHAFT UND KUNST

Freistaat SACHSEN

Outlook: The German Centre for Astrophysics (DZA)

CASUS
CENTER FOR ADVANCED SYSTEMS UNDERSTANDING

Research Technology Digitization

„Science Creating Prospects for the Region!“

DZA

Scientific Commission: 13. July 2022
Structural and Transfer-Commission: 30. August 2022
Final decision (Approval): 29. September 2022

Why in Saxony? Lusatia is a unique region for Astrophysics, Technology and Digitization

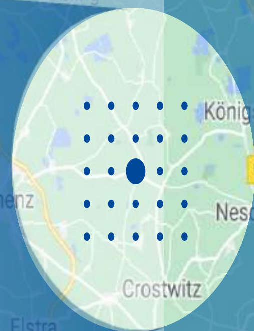

Location for the Low Seismic Lab

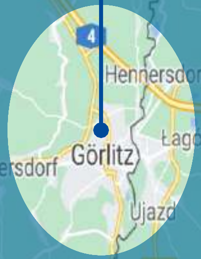

TECHNISCHE UNIVERSITÄT DRESDEN

DZA

A center for astrophysics with advanced data intensive computing and technology development.

Thank you for the invitation to Zakopane and excellent organization!